SPECTROSCOPIC STUDIES OF SOME HAEMOGLOBIN DERIVATIVES.

by

K. Gray, B.Sc.,

being a thesis submitted in the University of Keele in partial fulfilment of the requirements for the award of the Degree of Doctor of Philosophy.

January, 1974.

THE ARTICLE 'BIOCHEMICAL AND BIOPHYSICAL RESEARCH COMMUNICATIONS, 1972, VOL.48, NO.4, PP.1019-1024' NOT SCANNED AT REQUEST OF THE UNIVERSITY. SEE ORIGINAL FOR CONTENT.

ACKNOWLEDGEMENTS

The author is very grateful for the kind assistance of the following individuals:

Professor D.J.E. Ingram for the provision of research laboratory facilities within the Department of Physics.

Dr. E.F. Slade for supervising the work for this thesis with the right blend of advice, encouragement and enthusiasm.

Mr. H. Wardell, Mr. G. Dudley, and the Technical Staff of the Department of Physics and the University Workshop for the manufacture of microwave and cryogenic equipment.

Members of the Department of Physics for their occasional assistance over three years.

Mr. K. Topley for assistance with the photographic reproductions in this thesis.

Mrs. K. Gray for her encouragement over three years and for reading the proofs.

ABSTRACT

This thesis describes a study of the magnetic and optical properties of human haemoglobin and certain of its derivatives. The techniques of electron spin resonance spectroscopy and optical spectrophotometry at low temperatures are used.

An introduction to the theory and techniques of electron spin resonance is given and the properties of transition metal ions are discussed. The general properties of haemproteins are described; there is particular reference to optical and magnetic studies.

The preparation of solutions of various haemoglobin derivatives from fresh human red cells is described. Room temperature studies of various derivatives are described; the results of cryogenic optical absorption measurements are reported.

Electron spin resonance studies of haemoglobin hydrate, fluoride and formate solutions are reported in Chapter 4; the theoretical simulation of the spectra is described and values of g_x, g_y, g_z and the linewidth are obtained. Reference is made to aspects of experimentation at 70 GHz microwave frequency. Consideration is given to the incorporation of an anisotropic linewidth. The Hamiltonian parameters 2D and E are obtained from measurements at 35 GHz and 70 GHz.

The angular variation in g value in the ab, ac, bc planes at 70 GHz is presented in Chapter 5 for deoxyhaemoglobin single crystals treated with an oxidising agent giving ferric ions, and the G tensor is calculated. A negative result is noted for untreated deoxyhaemoglobin at 70 GHz. By obtaining g_x and g_y from ab plane studies at 35 GHz, the Hamiltonian parameters 2D and E were calculated. The linewidth variation is discussed.

A part of the results presented in Chapter 3 has been pub-

lished (with E.F. Slade) in Biochemical and Biophysical Research Communications and a reprint of this paper is bound with this thesis.

INTRODUCTION

1. This thesis is chiefly concerned with the application of electron spin resonance and optical absorption techniques to the study of certain derivatives of the protein haemoglobin, which contains ferric ions. These ions are located centrally in four approximately planar parts of the protein molecule, known as haem groups. The biologically important mechanism of reversible oxygenation takes place at these four groups.

It is therefore of some interest to find out details of the electronic orbitals involved in the chemical binding at these haem iron atoms. Because there is some evidence that oxygenation may be a cooperative mechanism between haems, it is also important to determine the relative positions of the haem planes in the molecule.

2. The presence of an ion having some total angular momentum vector $\overline{J}$ in an experimental magnetic field H gives rise to a number of energy levels corresponding to different spatial orientations of the angular momentum vector. These levels, which are known as Zeeman levels, have energies $g\beta M_J H$ where M_J is the magnetic quantum number. It is the function of electron paramagnetic resonance spectroscopy to examine direct transitions of electrons between these Zeeman levels by making use of microwave or millimetre wave electromagnetic radiation. In practice, the frequency of this radiation is held constant and the magnetic field permitted to vary; whenever the separation of energy levels is equal to the microwave quantum, a paramagnetic absorption line is observed.

However, the paramagnetic ion is not generally free but is

in constant interaction with its containing lattice. These interactions modify the energy levels of the free ion. In certain cases large Zeeman splittings may be produced which call for the use of quanta of higher frequency to observe the absorption lines.

By studying the dependence of the absorption spectrum upon the magnetic field, information may be obtained about the electronic structure and lattice interactions of ions. Examination of the angular dependence of the EPR spectrum enables the orientation of the haem planes in the protein molecule to be found.

3. Optical spectrophotometry is a technique which involves the measurement of optical absorption coefficients for protein solutions of known concentration and is complementary to electron paramagnetic resonance in this work. The latter method may generally only be used at cryogenic temperatures whereas optical absorption spectra may be studied at room temperatures as well as low temperatures.

Typical optical absorption lines occur for the various protein derivatives studied. The spectra are not only associated principally with the metal ion (influenced by the presence of ligands) but also with electronic transitions between metal and ligand ions, which are known as charge transfer spectra. The absorption intensities of these spectral lines depend upon the spin state of the metal ion. For example, ferric ions may exist in the $S = \frac{1}{2}$ or $S = 5/2$ spin states. There is reason to suppose that some proteins exist as thermal equilibrium mixtures of these states; observation of the optical absorption spectra over a wide range of temperature yields interesting information to support this proposal. Certain derivatives give anomalous results. However, it may also be true that shifts in a chemical equilibrium between two species of ligand having differing spin states could yield

a similar result.

4. In this thesis, electron paramagnetic resonance is introduced in Chapter One and the biological significance of haemoglobin is explained in the second chapter. Chapter Three is concerned with optical absorption studies. In Chapters Four and Five, EPR data are used to obtain information about the electronic state of the ions and the relative orientations of the haems in the protein molecules.

CHAPTER ONE

ELECTRON PARAMAGNETIC RESONANCE

1.1. Introduction.

Electron paramagnetic resonance absorption occurs when a suitable quantum of energy is used to raise an electron from a lower to a higher Zeeman energy level; relaxation processes permit such electrons to lose energy and those return to a lower level. Unless this occurred, no further energy absorption would take place after a certain time. The conditions for resonance will be derived in outline for an isolated paramagnetic ion and related to the physical processes involved by reference to the Bloch classical theory. This account will be extended by means of the Crystal Field theory to transition metal ions in solids. Mention will be made of the method of detecting the resonance.

1.2. The free paramagnetic ion.

Since the electron has both spin and charge it necessarily possesses a magnetic moment $\bar{\mu}_e$ which is proportional to the magnitude of the spin

$$\bar{\mu}_e = -g\beta\bar{S} \qquad (1)$$

In a free ion where Russell-Saunders coupling is obeyed, then

$$\bar{\mu}_e = -g\beta\bar{J} \qquad (2)$$

where $\bar{J} = \bar{L} + \bar{S}$ and g is the Lande splitting factor. If the ion is situated in a steady magnetic field $\bar{B}$ then the magnetic moment interacts with energy

$$E = -\bar{\mu}_J \cdot \bar{B} \qquad (3)$$

or from (2)

$$E = g\beta\bar{B} \cdot \bar{J} \qquad (4)$$

and if the magnetic field is aligned along the z axis then this becomes

$$E = g\beta B M_J \qquad (5)$$

The allowed values of energy are eigenvalues of an operator H such that

$$H\Psi = E\Psi \qquad (6)$$

where Ψ is a wave function. The required values of E are given by inserting $M_J = J, J - 1, \ldots, -J$ in (5).

This means that the $(2J + 1)$-fold degeneracy of the magnetic interaction energy is lifted by the magnetic field; the splitting between the levels produced is field dependent and is referred to as the Zeeman effect. In the special case of a single free electron there are $(2J + 1) = 2$ possible orientations of the total angular momentum vector in the magnetic field i.e., parallel or antiparallel to the field.

Electron paramagnetic resonance is concerned with the inducing of transitions between Zeeman levels. For populations N_1 , N_2 in upper and lower levels with identical statistical weights, at thermal equilibrium the ratio N_1/N_2 is given by Maxwell-Boltzman statistics as

$$N_1/N_2 = \exp(-\Delta E/kT) \qquad (7)$$

where k is Boltzman's constant. It will be possible to induce transitions between these levels separated by the energy gap ΔE if radiation of frequency ν is applied, provided that the selection rule $M_J = \pm 1$ applies, then

$$h\nu = \Delta E = g\beta B \qquad (8)$$

It is necessary to observe the effect of applying an oscillating magnetic field to the spin system of the form

$$B' = B_o \sin\omega t$$

It is a result of applying time dependent perturbation theory to a two level system that the transition probability is

given by

$$P_{12} = \frac{2\pi}{\hbar} \langle 2 | B' | 1 \rangle^2 \delta(E_2 - E_1 - h\nu) \quad (9)$$

where $\langle 2|B'|1\rangle$ is the matrix element which couples the two states. If ω_{12} is set equal to $(E_2 - E_1)/\hbar\nu$ this becomes

$$P_{12} = \frac{g^2 \beta^2 B^2}{\mu} \langle 2 | J_x | 1 \rangle^2 \frac{\sin^2(\omega_{21} - \omega)}{(\omega_{21} - \omega)^2} \quad (10)$$

for the transition probability to be non-zero two conditions must be simultaneously satiafied; the matrix element must be non-zero which is true only if the selection rule $M_J = M_J \pm 1$ is obeyed and the applied radiation must have an angular frequency equal to ω_{21}: this relationship yields an absorption line of the form of a Dirac delta function. The rate of absorption of radiation depends upon the populations of the two levels involved.

1.2.2. The Phenomenological approach to Absorption.

The model proposed to explain early relaxation experiments relies upon a classical analogy between a spinning magnetic top and a spinning electron (Bloch, 1946). However, it has been shown to correlate well with quantum mechanical results.

If a spinning top is situated in a static magnetic field then the torque on the top is given by

$$\bar{L} = d/dt(\bar{J}\hbar) \quad (11)$$

where the top has a total angular momentum $\bar{J}\hbar$.

But the torque is also given by

$$\bar{L} = \bar{B} \times \bar{\mu} \quad (12)$$

where the magnetic moment is $\bar{\mu} = -\gamma \bar{J} \hbar$.

and so

$$d/dt(\bar{\mu}) = \gamma \bar{B} \times \bar{\mu} \qquad (13)$$

Thus one may refer to the angular momentum vector $\bar{J}$ or the magnetic moment precessing in the magnetic field. A solution for the precessional motion is found by solving (13) to give

$$\omega_o = \gamma B \qquad (14)$$

However it is not enough to consider one isolated spin; one assumes that there exists a total magnetisation vector $\bar{M}$ for an assembly of spins where

$$\bar{M} = \sum \bar{\mu}_i \qquad (15)$$

and this leads to an equation similar to (13)

$$d\bar{M}/dt = \gamma \bar{B} \times \bar{M} \qquad (16)$$

which has the same solution for angular frequency.

To describe the macroscopic behaviour of the assembly of spins, Bloch introduced two relaxation times T_1 and T_2 by which the assembly may reach thermodynamic equilibrium. T_1 is referred to as the spin lattice relaxation time and is a measure of the time taken by a paramagnetic ion to give up its energy to the crystal lattice. It is thought that there are two significant interactions. First, thermal lattice vibrations modulate the electric fields due to the electrons and nuclei and these act on the spins via the spin-orbit coupling (Kronig, 1939). Second, in crystals where ions of large spin S are close to each other, modulation of the dipole-dipole interaction by the lattice vibrations may provide a relaxation mechanism (Waller, 1932). The values of T_1 arising from these two processes are rather different.

T_2 is called the spin-spin relaxation time. In the case of the classical precessing top, one may imagine a collision to occur between tops such that the precession is momentarily interrupted; the top will then resume its precessional motion with a new random phase with respect to the driving angular frequency. No information about phase is communicated across the collision. In the case of electron spins, coupling occurs because the magnetic fields of one spin are experienced by another spin. Random activities of individual spins will be communicated to other spins and these interactions may be regarded as collisions. The spin-spin relaxation time may be regarded as the average time interval between dephasings of a precessing spin.

Bloch showed that the complex magnetic susceptibility $\chi(\omega)$ changes sharply at resonance in both its real and imaginary parts. It may be shown that only the imaginary part is responsible for power absorption from the microwave magnetic field. The real part of the susceptibility corresponds to a change of phase, that is, dispersion.

The rate of energy absorption is given by

$$W = \tfrac{1}{2}\omega\chi'' B_1^2 \qquad (17)$$

where the imaginary part of the susceptibility is given by

$$\chi'' = \omega\chi_o f(\omega) \qquad (18)$$

where $f(\omega)$ is a line width function and χ_o is the static magnetic susceptibility (Abragam, 1970)

1.2.3. Detecting the resonance.

The detection of the electron paramagnetic resonance is essentially the measurement of changes in the complex magnetic susceptibility of the sample; by making use of a suitable microwave circuit this may be reduced experimentally to observing changes in the power absorbed by the paramagnetic sample in a microwave cavity. Dispersion may also be observed.

The microwave spectrometer employed in these investigations was of the reflection type. The spectrometer is shown schematically in Fig. 1.1; power from the signal klystron is fed into one port of a microwave magic tee and is divided between the two side ports which are connected to the sample cavity and a matching circuit containing an attentuator and an adjustable short or a slide screw tuner. The microwave detector, which is connected to the fourth port of the tee, receives ideally no microwave power when there is no resonance. This is brought about by matching the two side ports so that the signal power is divided equally between them: no power is transmitted to the detector since the reflected waves are mixed in antiphase at the fourth port. When resonance occurs the reflection coefficient of the microwave cavity arm changes and an output appears at the fourth port of the tee which communicates with the crystal. In practice, it is necessary to unbalance the magic tee slightly in order to bias the crystal diode; this bias current through the diode should be adjusted to optimise the signal to noise ratio. (Torrey, 1948). The 70 Ghz spectrometer in use has been described elsewhere (Slade, 1968/9) and reference is made to experimental details in Chapter 4. In recent years considerable effort has been expended in devising suitable detectors for the millimetre wavelengths, both by extending conventional microwave detectors

and by designing infrared detectors which will operate successfully far into the far infrared. A table of useful millimetre wave detectors is shown in Fig. 1.2.

The mean power absorbed by the paramagnetic sample per unit volume is given by (17). The Q factor of the resonant cavity containing the sample is

$$Q = \frac{\omega \cdot \text{Energy stored}}{\text{Average power dissipated}} = \frac{\frac{1}{2}\omega \int_{V_c} B_1^2 \, dV_c}{P_1 + \frac{1}{2}\omega \int_{V_s} B_1^2 \chi'' \, dV_s} \qquad (19)$$

where P_1 is the power dissipated in the cavity in the absence of resonance, and V_c and V_s are the volumes of the cavity and sample respectively. If the paramagnetic losses are small in comparison with P_1 then (Poole, 1967)

$$Q = Q_o \left(1 - \frac{\int_{V_s} B_1^2 \chi'' \, dV_s \, Q_o}{\int_{V_c} B_1^2 \, dV_c} \right) = Q_o \left(1 - \chi'' \eta Q_o \right) \qquad (20)$$

where Q_o is the Q factor of the cavity alone and η is a filling factor which depends upon the field distribution in the cavity and sample. The change in Q factor brought about by resonance is thus

$$\Delta Q = Q_o^2 \chi'' \eta \qquad (21)$$

and this may be related to the change in microwave voltage at the crystal detector. Assuming a linear detection characteristic of the form

$$dV/dI = r$$

the voltage change is given by (Feher, 1957, Wilmshurst, 1962)

$$\Delta V = \chi'' \eta Q_o \left(\frac{P_0}{2}\right)^{\frac{1}{2}} r^{\frac{1}{2}} \qquad (22)$$

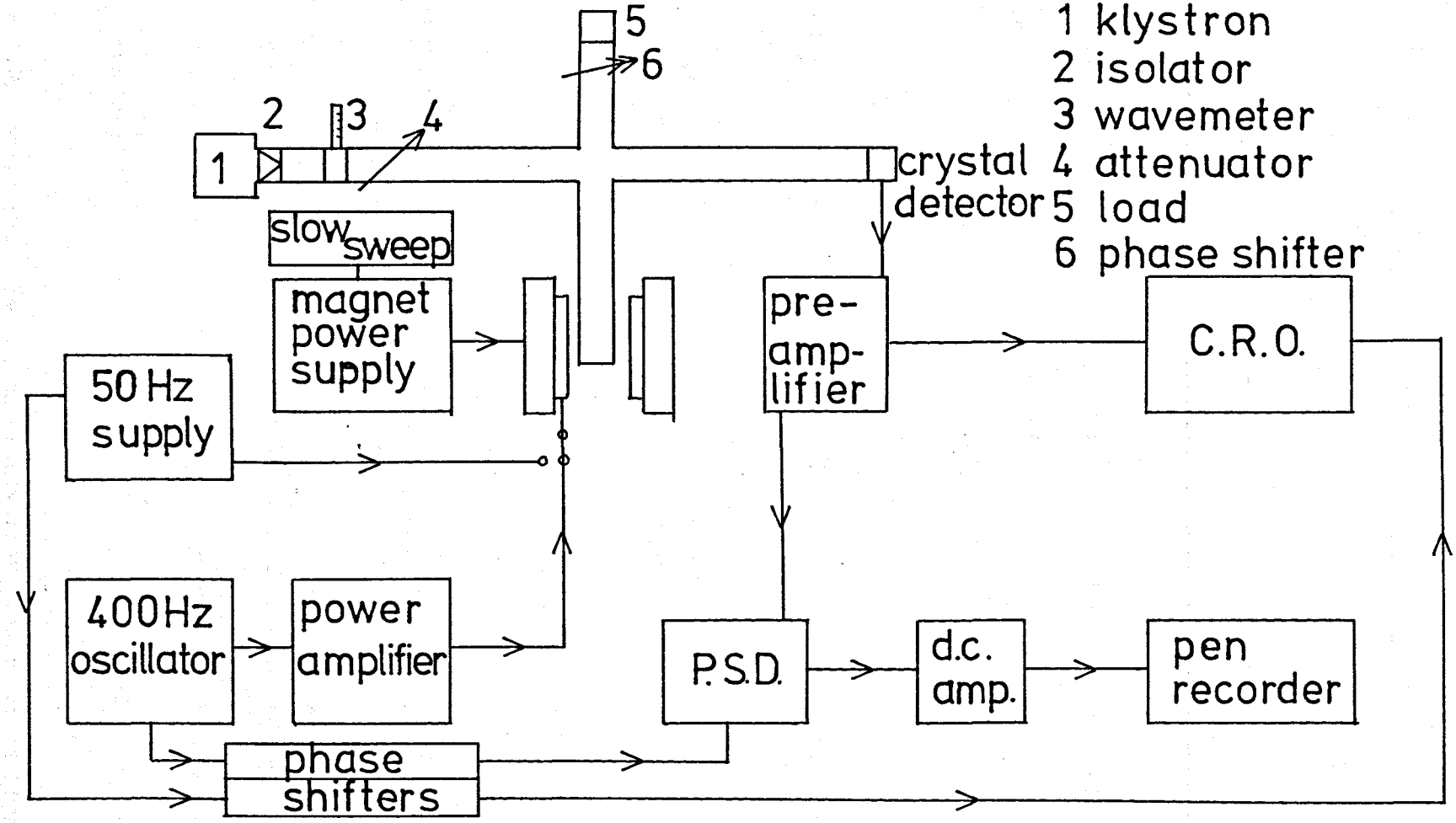

E.P.R. REFLEXION SPECTROMETER.

Fig. 1.1

Fig. 1.2

Microwave and millimetre wavelength detectors.

Detector	Operating temperature ^{o}K	NEP, 1 Hz, watts	Responsivity volts/watt	Response time, seconds.
Golay cell	300	3×10^{-10}	10^{5}	0.015
Carbon bolometer	2.1	10^{-11}	2×10^{-4}	0.010
Ge bolometer	2.15	10^{-13}	4.5×10^{3}	2×10^{-4}
Superconducting bolometer	3.7	3×10^{-12}		1.25
Ideal photo-conductive detector	1.5	1.8×10^{-14}	(Wavelength 1 mm)	
InSb wideband detector with magnetic field (1 mm wavelength)	1.5	5.0×10^{-12}	10^{3}	2×10^{-7}
InSb without magnetic field	4	10^{-12}	(Wavelengths 0.5 to 8 mm)	3×10^{-7}
Ge cyclotron resonance detector (mms wavelengths)	4	2.0×10^{-12}	10^{6}	5×10^{-9}
Pyroelectric detectors, $BaTiO_3$, TGS	300	3.0×10^{-9}		10^{-6}
Point contact diodes	300	2.5×10^{-11}	p-Si f_{co} 75 GHz n-Ge 460 GHz n-Ga-As 1600 GHz GaAs Schottky 350 GHz	
Josephson junction In-In, wavelength 2 mm.	4.2	5.0×10^{-13}		10^{-8}

N.B. N.E.P. represents the Noise Equivalent Power in a bandwidth of 1 Hz.

where P_o is the microwave power injected to the microwave bridge. The use of a three port circulator would improve the voltage change but it has been suggested that bridge balance is then more difficult to maintain over long periods (Buckmaster, 1967) and circulators are not readily available at millimetre wave frequencies.

In order to calculate the minimum detectable susceptibility it is necessary to compare the signal voltage at the amplifier input after the detector with the noise voltage. The r.m.s. noise voltage across the detector load resistor R is

$$V_n = \left(F\,k\,T\,df\,R\,(1 + t)\right)^{\frac{1}{2}} \qquad (23)$$

where F is the receiver noise figure, df the pass band, and t includes the effect of 1/f crystal noise. If this is equated to the signal voltage, an expression may be obtained for the minimum detectable susceptibility χ''_{min}

$$\chi''_{min} = \frac{1}{\pi\eta\,Q_o}\left(\frac{F\,k\,T\,df\,(1 + t)}{2\,P_o}\right)^{\frac{1}{2}} \qquad (24)$$

If this is interpreted in terms of the minimum detectable number of spins, at 10 GHz microwave frequency, $N_{min} \approx 10^{12}$ spins per unit milliTesla linewidth for practical values of parameters in (24).

1.4. Paramagnetism in transition metal ions.

The paramagnetism arises from incomplete filling of inner orbital shells of electrons. A free iron atom possesses 26 electrons; 18 occupy closed shells and the remainder are in the orbitals $(3d)^6\,(4s)^2$. The reason why electrons do not fill

the 3d shell before the 4s is because in the central field approximation both shells have approximately the same energy. When the iron atom is ionised, the incomplete shells are $(3d)^5$ and $(3d)^6$ in the ferric and ferrous ions respectively.

The electronic energy levels of the free ion depend upon a number of interactions which form the terms of a general Hamiltonian

$$H = \sum \left(\frac{\bar{P}_i^2}{2m}\right) - \left(\frac{Ze^2}{r_i}\right) + \left(\frac{e^2}{r_{ij}}\right) + \lambda_{ij}\,\bar{l}_i.\bar{s}_j + H_N \qquad (25)$$

in the absence of an external magnetic field. The first term represents the total electron kinetic energy of the ion. The second and third terms represent the coulomb energies of the electrons in the electrostatic field of the nucleus and in each other's fields. These first three terms are dominant in magnitude and result in the configurations of the free ion.

The expression $\lambda_{ij}\bar{l}_i\bar{s}_j$ takes into account the spin-orbit coupling and is summed over all pairs of electrons; the spin-orbit effect is the magnetic coupling between electron spin $\bar{s}_i$ and orbital angular momentum $\bar{l}_j$. This term causes splitting into multiplets. The hyperfine interaction between the electron and the nucleus of the ion is shown in the fifth term; both the magnetic dipole moment and the nuclear quadrupole moment may participate.

1.5. The paramagnetic ion in the crystal lattice.

When, as is usually the case, the paramagnetic ion is situated at a normal lattice site in a crystal, surrounded by diamagnetic ions and widely separated from other paramagnetic ions, the energy levels of the free ion are modified. The assumption may be made that the effect of the surrounding ions is to set up an electrostatic field at the ion under consideration. Unpaired electrons in the incomplete shells of the paramagnetic ion experience this field and their usual orbital motions are thereby modified. We represent this interaction by an additional term in the general Hamiltonian, V_{ce}, and this method of estimating the modifying effect of the crystal on the properties of the ion is called the crystalline electric field approximation. In some cases the energy term due to the crystalline electric field exceeds the spin-orbit term in the Hamiltonian and hence it is necessary to distinguish between three cases.

1.6. The Crystal Field.

When the crystal field term is smaller than the spin-orbit interaction, free ion calculations on the Hamiltonian are valid, to a first approximation, and the crystal field is classed as weak. Ions of the second and third transition series of elements satisfy this criterion since their paramagnetic electrons are situated deep in the shell structure of the ion and are consequently well screened from the crystal field by the outer diamagnetic shells.

When the crystal field energy is greater than the electrostatic potential energy between pairs of electrons, the crystal field is referred to as strong. This means that the

torques exerted on the orbital motions of the electrons are determined by the lattice site symmetry, rather than only by the correlative interactions of the electrons. However, the physical picture in this case shows that ligands can no longer be represented by point electrostatic charges and that covalency is present: this means that the simple crystal field model is inadequate to describe the situation and it becomes necessary to examine other models in this context.

In the iron transition series, the crystal field energy is usually greater than the spin-orbit interaction but less than the coulombic interaction of the electrons. The intermediate to strong field is of most importance in considering the iron ion in haemoglobin and myoglobin.

If it is assumed that the crystalline electric field is due to a point charge approximation, where each ion contributing to the overall field is replaced by a single point charge, then Laplace's equation is satisfied

$$\nabla^2 V_{ce} = 0 \qquad (26)$$

and the electric potential can be expanded as a series sum of spherical harmonics

$$V_{ce} = \sum_{k=0}^{\infty} \sum_{q=-k}^{k} B^q_k (r)^k \; Y^q_k(\theta, \phi) = \sum_{k=0}^{\infty} \sum_{q=-k}^{k} V^q_k \qquad (27)$$

where $Y^q_k(\theta,\phi)$ is a function of angle in the crystal and of linear dimension. If this expression is used to calculate V_{ce} for the model of simple octahedral symmetry where single equal point charges are located at $x = \pm a$, $y = \pm a$, $z = \pm a$, orthogonality rules of the spherical harmonic functions and the symmetry rules of the site in question

considerably simplify (27) to yield

$$V_{oct} = \frac{7\pi^{\frac{1}{2}}e}{2} \frac{r^4}{a^5} \left[Y^0_4 + \left(\frac{5}{14}\right)^{\frac{1}{2}} (Y^4_4 + Y^{-4}_4) \right] \qquad (28)$$

Because of the centre of symmetry in the octahedral arrangement of ions, only even powers of electron coordinates occur and hence only even spherical harmonics are present (k = 0,2,4...). If the symmetry is lower, for example, tetrahedral, then odd values of k occur. Detailed accounts of computations of spherical harmonics may be found tabulated under different symmetries (Bleaney, 1953, Hutchings, 1964, Low, 1960).

It is possible to express V_{oct} in Cartesian coordinates as

$$V_{oct} = \frac{35 e^2}{4 a^2} \left(x^4 + y^4 + z^4 - \frac{3}{5} r^4 \right) \qquad (29)$$

Having found the crystalline potential it may be used in the Hamiltonian, in a place appropriate to the field strength, to find the energy levels of the paramagnetic ion. To do this it is necessary to calculate the matrix elements of the potential; an especially useful method has been found (Stevens, 1952). It is possible to form operators from each term in the expansion for V_{ce} by replacing the coordinates x,y,z by the angular momentum operators L_x, L_y, L_z; because the angular momentum operators are noncommutative it is essential to replace expressions of the form (xy) by $\frac{1}{2}(L_xL_y + L_yL_x)$. It has been shown that the matrix elements formed by these operators are proportional to the matrix elements of the original potential functions. These equivalent operators have been extensively listed (Stevens, 1952, Low, 1960). In the example of the iron group in octahedral symmetry, an equivalent operator is formed from (29) as

$$H_{oct} = eDB\langle r^4\rangle(0.05(35L_z^4-30L(L+1)L_z^2 + 25L_z^2 - 6L(L+1) + 3L^2(L+1)^2) + 0.125(L_+^4 + L_-^4)) \quad (30)$$

From the viewpoint of group theory, which provides a more powerful method of treating the crystal field, the addition of the non-spherically symmetric crystal field potential to the spherically symmetric Hamiltonian produces a new Hamiltonian which is no longer invariant under three dimensional rotation. Consequently, the d orbitals of the free ion are no longer eigenfunctions of the Hamiltonian. It is thus necessary to construct combinations of the d orbitals which reflect the lowered symmetry of the ion in the lattice. This operation is achieved either by the operator equivalent method or, with identical results, from group theory.

One may see intuitively from the conventional three dimensional representation of the d orbitals in Fig. 1.4 that the effects of each ligand charge will be different from orbital to orbital. The $d_{x^2-y^2}$ orbital lies along the x and y axes; an electron in such an orbital will have a maximum probability density along the Cartesian axes but an electron in a d_{xy} orbital has a maximum probability density along directions making angles of 45^o with the x and y axes. Consequently, an electron in the $d_{x^2-y^2}$ orbital will experience a greater electrostatic repulsion from a negatively charged ligand on the axis than that experienced by an electron in the d_{xy} orbital. This is the same as saying that the energy of the d_{xy} orbital is reduced relative to that of the $d_{x^2-y^2}$ orbital. Parallel arguments may be applied to the d_{xz} and d_{yz} orbitals. It is not at once obvious how the energy of the d_{z^2} orbital is related to that of the other

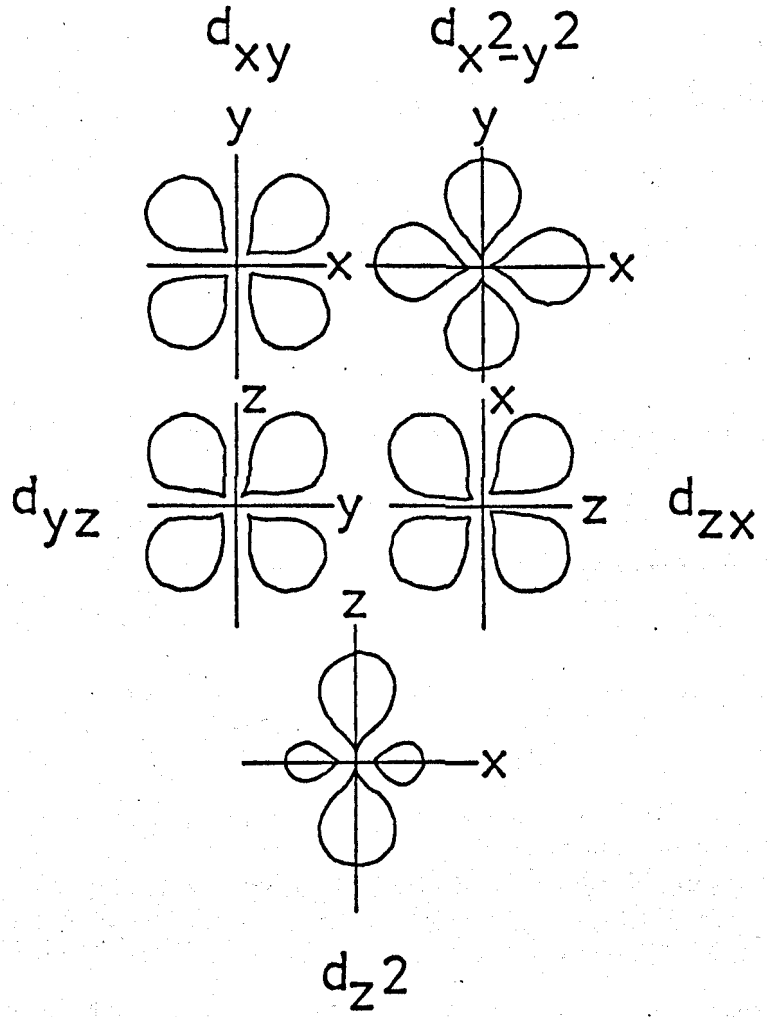

THE d ORBITALS

Fig. 1.4

four orbital and how it reacts to the crystal field. It is, in fact, degenerate with the $d_{x^2-y^2}$ orbital; with reservations (Orgel, 1966) one may see that the d_{z^2} orbital may be expressed as the sum of the $d_{z^2-x^2}$ and the $d_{z^2-y^2}$ orbitals, the sum being equivalent to the $d_{x^2-y^2}$ orbital.

The overall result of the cubic field is to lift the degeneracy of the free ion d orbitals in part; the orbitals are separated into a triply degenerate set of orbitals, referred to as the t_{2g} orbitals - because they belong to the so-called t_{2g} representation of the octahedral symmetry group under which a cubic ligand field is invariant - and a doubly degenerate pair of orbitals called the e_g orbitals. In Fig. 2.6 it may be observed that these two kinds of energy levels are separated by an energy difference Δ which is a measure of the potential of the crystal field; clearly the value of the ligand field splitting is determined by the actual ligands for any given paramagnetic ion.

Because the t_{2g} orbitals are lower in energy than the e_g orbitals, they are preferentially occupied by electrons. However, two other effects tend to promote electrons to higher orbitals; electrons which are occupying the same orbitals, for example, electrons in the d_{xy} and d_{yz} orbitals, have a larger electrostatic repulsion than electrons in dissimilar orbitals and electrons also possess an exchange energy which favours high spin states. To achieve the high spin states, the exclusion principle requires electrons to be distributed in separate orbitals. The relative magnitudes of the interorbital splitting and the two pairing energies determine the electron distribution between the t_{2g} and e_g orbitals.

When the ligand field splitting is very much less than the

Fig. 1.5

Ferrous ion, Fe(++).

S = 0	$(t_{2g})^6$
S = 1	$(t_{2g})^5(e_g)^1$
S = 2	$(t_{2g})^4(e_g)^2$
S = 2	$(t_{2g})^3(e_g)^3$
S = 1	$(t_{2g})^2(e_g)^4$

Ferric ion, Fe(+++).

S = $\frac{1}{2}$	$(t_{2g})^5$
S = 3/2	$(t_{2g})^4(e_g)^1$
S = 5/2	$(t_{2g})^3(e_g)^2$
S = 3/2	$(t_{2g})^2(e_g)^3$
S = $\frac{1}{2}$	$(t_{2g})^1(e_g)^4$

pairing energies, the electrons are distributed to give the maximum spin; in the converse case, the electrons fill the lower t_{2g} orbitals. The actual occupation of the orbitals for ferric and ferrous iron is detailed in the table in Fig. 1.5.

The equations for the term energies arising out of these possible configurations have been solved (Tanabe, 1954); diagrams have also been produced which show how the term energies depend upon the ligand field as it is gradually applied from zero in the case of the free ion (Orgel, 1955). In this latter case, the individual energies are derived experimentally from the atomic spectra of particular ions. The Orgel diagram for octahedral complexes of Mn^{++}, a d^5 ion, is shown in Fig. 1.6 where it may be seen that the ground state is $^6A_{1g}$.

The abscissa is expressed usually as the ratio Δ/B, where B is a Racah parameter; Racah parameters express values of integrals of radial and angular functions used to compute interelectron energies (Racah, 1942, 1952). However, in this diagram, B is assumed independent of the coordinated ligands and the energies are plotted as functions of the ligand field splitting only.

The diagram shows that as the ligand field strength increases, the symmetry and spin of the ground state changes. At lower values of ligand field, the ground state is $^6A_{1g}$ with a total spin of $S = 5/2$. At the mean pairing energy, π, the $^2T_2$ term becomes lower in energy than the $^6A_{1g}$ and the ground state assumes a total spin $S = \frac{1}{2}$.

Using the free ion values of the Racah parameters, the energy where the changeover occurs has been calculated to be $27900\ cm^{-1}$ (Tanabe, 1954).

Strictly interpreted, the locality where the change

TERM DIAGRAM FOR d^5 CONFIGURATION.

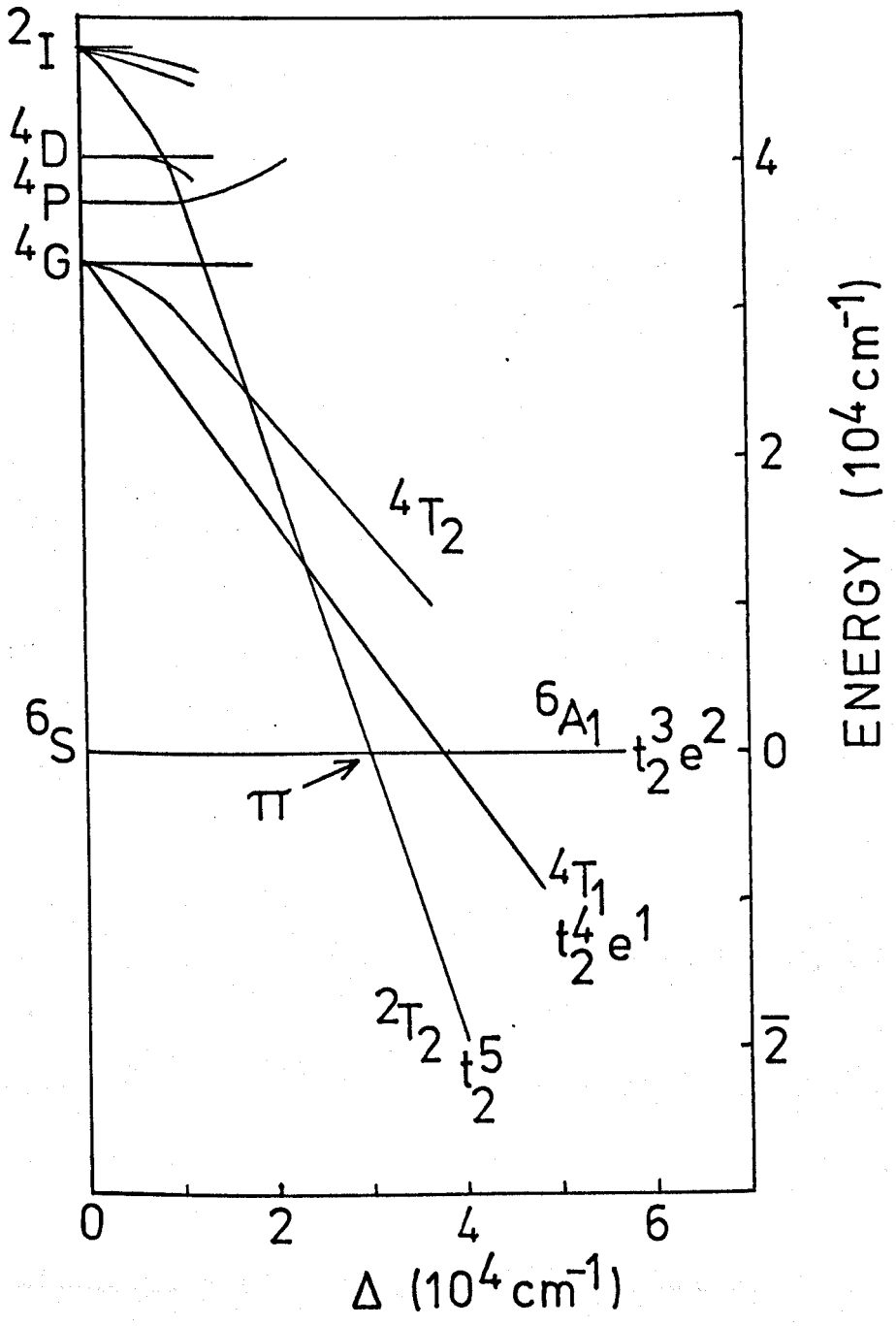

Fig. 1.6

of ground state occurs does not correspond to states in equilibrium, that is, there is no crossover point. If the total molecular energy of the ligated ion is expressed as a function of the metal-ligand bond length, for various ligands, the actual change of ground state never corresponds to a situation where the minima of the potential energy curves for $^6A_{1g}$ and $^2T_{2g}$ are coincident; the equating of the ligand field energy with the mean pairing energy is thus an approximation (Ewald, 1963).

These diagrams and other results (Griffith, 1956, 1964) led to the belief that S = 3/2 is never a stable ground state; in view of the values of magnetic susceptibility obtained for certain haemoglobin complexes (Pauling, 1940) which suggested an intermediate spin state, it was proposed that some haemoglobin complexes were equilibrium mixtures of spin states (George, 1961). This would mean that their particular values of ligand field energy were within kT of the change over in ground state.

In the case of a large axial component in the ligand field $^4T_{1g}$ (S = 3/2), which is never the ground term, is split into two components. The latter of these, $^4A_{2g}$, will always lie only a little way above the ground term for some range of the ligand field energy (Griffith, 1964). If rhombic symmetry obtains then the $^4T_1$ is split into three (Kotani, 1964).

Although the crystal field theory is very useful, in certain cases it is inadequate. This is especially true for strong field complexes.

1.7. Molecular orbital and Ligand Field Theories.

The molecular orbital theory was initially developed to explain the electronic properties of covalent organic compounds. Orbitals are postulated in this model which fulfil the same

functions for a molecule as do the s,p,d orbitals of an atom; the electronic structure of the molecule is then described by filling these molecular orbitals with two electrons each in order of ascending energy. The molecular orbitals are constructed of linear combinations of the atomic orbitals. If two orbitals are able to form delocalised molecular orbitals, two such orbitals are always formed; one is always more stable and the other less stable than the original atomic orbitals. The former are called antibonding or π orbitals; the latter are bonding or σ orbitals. The degree of covalency is represented by the electrons situated in the bonding orbitals. Molecular orbital theory is quite successful in classifying four different kinds of ferric haemoglobin complex: these are

(a) essentially ionic complexes such as haemoglobin fluoride with only six σ bonds;

(b) ionic complexes with a somewhat stronger bond perpendicular to the haem plane. $HbOH^-$ appears to lie in this group with a π bond to the OH^- ion.

(c) complexes with strong bonding of the two perpendicular ligands; haemoglobin azide may be one of these.

(d) essentially covalent complexes such as haemoglobin cyanide, with six σ and twelve π bonds.

All haemoglobin complexes differ only in the number of π bonds; admixture coefficients have been defined which control the combination of ligand orbitals with the d orbitals of the metal ion (Van Vleck, 1935).

The Ligand Field Theory is a development of the crystal field theory; the latter is quantitatively inadequate because it is not a good description to replace the ligands by point charges. The charge distribution of the ligands and the magnetic electrons of the central ion are often imprecisely known, the

exact ligand position may be conjectural, and the wavefunctions of electrons on the central ion and the ligands often overlap.

Ligand field theory is a hybrid approach to the problem in which the ligand field splittings are recognised to result from a number of individual contributions, such as purely electrostatic effects, and the bonding and antibonding orbitals. This has the advantage that the energies of the electronic levels of complexes may be calculated in terms of ligand field energy; they may then be adjusted to fit experimental results using appropriate values of the Racah parameters (Sutton, 1968).

1.8. Orbital angular momentum in intermediate and strong crystal fields.

In intermediate and strong crystal fields with octahedral symmetry, the Russell-Saunders coupling is broken down, and the angular momentum vector $\overline{L}$ then precesses about the crystal field. There are (2L+1) allowed orientations but if the energy separations are large then only the lowest level will be populated: this means L_z is never greater than unity. However, S state ions such as Mn^{++} and Fe^{3+} ($^6S_{5/2}$) are a rather special case in that the 3d shell is exactly half filled with electrons and there is thus no orbital angular momentum to be quenched.

Since there can be no spin-orbit coupling in the ground term ^6S, spin-orbit coupling with excited states must be invoked in order to explain observed angular momentum contributions. The selection rules for this configurational interaction are $\Delta L = 0, \pm 1$ and $\Delta J = 0$ and they limit the choice of excited state to $^4P_{5/2}$ and it has been derived that (Judd, 1963, Weissbluth, 1967)

$$|^6S>' = |^6S> - \frac{(5)^{\frac{1}{2}}\zeta}{7(B+C)} |^4P>$$

where ζ is the one electron spin-orbit coupling factor; in this case the ground state is lowered by 23 cm^{-1}.

In the case of ions with odd numbers of electrons - as is the case with Fe^{3+} - then Kramers' theorem states that two-fold degeneracy always remains unlifted by the crystalline electric field. Kramers' theorem depends upon the invariance of the Hamiltonian under time reversal, a symmetry operation which reverses the spins and momenta of all electrons. When eigenstates of an n electron system are operated upon by this symmetry operator, degenerate states result if n is odd (Carrington, 1967). When a magnetic field is applied, the Hamiltonian is no longer invariant and the degeneracy is lifted.

1.9 The Spin Hamiltonian.

The Zeeman energy levels and other important properties of a paramagnetic ion in a crystal are usually formalised into a quantum mechanical spin Hamiltonian; the numerical constants in this expression summarise all the data of the experimentally observed EPR spectra. Previously we have noted that the energy levels of the paramagnetic ion in a crystalline electric field can be determined from the free ion Hamiltonian by incorporating the crystal field interaction energy. If the ground state is obtained from the total electron kinetic energy of the ion and the electrostatic interactions of the electrons and the crystal field energy, since in the iron transition series the latter is often greater than the spin-orbit interaction, then the spin-orbit and magnetic interactions in a magnetic field may be added as a perturbation on the degenerate spin state associated with the

orbital ground state

$$H' = \lambda(\bar{L}.\bar{S}) + \beta \bar{B} . (\bar{L} + 2\bar{S})$$

If the orbital states arising out of the crystal field splitting are labelled as $|0\rangle$, $|1\rangle$, $|2\rangle$, ..., $|n\rangle$, commencing from the ground state, then the first order energy shift in the ground state is given by

$$\langle 0 | \lambda \bar{L} . \bar{S} + \beta (\bar{L} + 2\bar{S}) . \bar{B} | 0 \rangle = 2\beta \bar{S} . \bar{B}$$

since complete orbital quenching means $\langle 0 | \bar{L} | 0 \rangle = 0$.

However, experimental g values inform us that angular momentum is reintroduced; in practice, the second order term in spin-orbit coupling may be as large as that in first order. The second order contribution is given by

$$\sum_{n \neq 0} \frac{-|\langle 0 | \lambda \bar{L} . \bar{S} + \beta (\bar{L} + 2\bar{S}) . \bar{B} | n \rangle|^2}{E_n - E_o}$$

The numerator in the latter sum term may be expanded to

$$\langle 0 | \lambda L . S + \beta (L + 2S).B | n \rangle \langle n | \lambda L.S + \beta(L + 2S).B | 0 \rangle$$

Allowing the variables (i,j) to represent Cartesian coordinates (x,y,z), the second order contribution in spin orbit coupling may then be written

$$\sum_{i,j} \lambda^2 \langle 0 | L_i | n \rangle \langle n | L_j | 0 \rangle S_i S_j + \langle 0 | \bar{S} | n \rangle + 2 \sum_{i,j} \lambda\beta \langle 0 | L_i | n \rangle \langle n | L_j | 0 \rangle S_i B_j$$

where the terms in $B_i B_j$ have been omitted as they lead to a displacement of all levels by an equal amount. Adding the first and second order contributions in spin-orbit coupling we obtain

$$H_S = 2\beta \bar{B} . \bar{S} - \sum_{i,j} \Lambda_{ij} (2\beta\lambda B_i S_j + \lambda^2 S_i S_j)$$

where

$$\Lambda_{i,j} = \sum_{n \neq 0} \frac{\langle 0 | L_i | n \rangle \langle n | L_j | 0 \rangle}{E_n - E_o}$$

By inserting a delta function such that

$$\delta_{ij} = 1 \quad \text{if} \quad i = j$$

$$\delta_{ij} = 0 \quad \text{if} \quad i \neq j$$

the following is obtained

$$H_s = \sum_{i,j} (2(\delta_{ij} - \lambda \Lambda_{ij}) \beta B_i . S_j + \lambda^2 \Lambda_{ij} S_i S_j)$$

Using tensors this may be written

$$H_s = \beta \bar{B} . \bar{g} . \bar{S} + \bar{S} . \bar{D} . \bar{S}$$

where $g_{ii} = 2(1 - \lambda \Lambda_{ii})$.

This Hamiltonian is clearly expressed in terms of spin operators only and the resulting energy levels are eigenstates of this Spin Hamiltonian operator. (Abragam, 1951). The spin Hamiltonian always reflects the symmetry of the paramagnetic site. A suitable choice of axes, for example, x,y,z, to be the principal tensor axes, may reduce the complexity of the mathematics. The Zeeman term $\beta . \bar{B} . \bar{g} . \bar{S}$ may be written under the latter assumption as

$$\beta .(g_x B_x S_x + g_y B_y S_y + g_z B_z S_z)$$

since $\bar{g}$ is then diagonal so $g_x = g_{xx}$ and $g_{ij} = 0$.

In the case of cubic symmetry there is no difference between x,y and z and so

$$\Lambda_x = \Lambda_y = \Lambda_z = \Lambda$$

thus

$$H_S = g \beta \bar{B} . \bar{S} + \lambda^2 \Lambda (S_x^2 + S_y^2 + S_z^2)$$

and no zero field splitting ob tains; there may however be zero field shifts. Upon lowering the symmetry to the axial case

$$\Lambda_x = \Lambda_y = \Lambda_{\perp}$$
$$\Lambda_z = \Lambda_{\parallel}$$

whence

$$H_S = g_{\parallel} \beta B_z . S_z + g_{\perp} \beta (B_x S_x + B_y S_y) + \lambda^2 (\Lambda_{\parallel} S_z^2 + \Lambda_{\perp} (S_x^2 + S_y^2))$$

Since $S_x^2 + S_y^2 = S^2 - S_z^2$ then

$$\lambda^2 (\Lambda_{\parallel} S_z^2 + \Lambda_{\perp} (S_x^2 + S_y^2)) = D (S_z^2 - \tfrac{1}{3} S (S + 1))$$

Omitting the constant terms this becomes

$$H_S = g_{\parallel} \beta B_z S_z + g_{\perp} \beta (B_x S_x + B_y S_y) + D S_z^2$$

In the presence of a rhombic distortion, $\Lambda_x \neq \Lambda_y \neq \Lambda_z$, and an additional term must be added representing splittings by crystal field components with symmetry lower than axial. A general form of the spin Hamiltonian for an axial field with rhombic distortion may be written as

$$H_S = \beta .(g_x B_x S_x + g_y B_y S_y + g_z B_z S_z) + D (S_z^2 - \tfrac{1}{3} S(S+1)) + E (S_x^2 - S_y^2)$$

Further terms may be added to take nuclear interactions into

account. It may be seen that the spin Hamiltonian enables description of the ground states of paramagnetic ions to be achieved in terms of only a few parameters; the number of Zeeman levels between which transitions are observed determines a fictitious or effective spin angular momentum S', such that (2S' + 1) equals the experimentally observed number of levels. The effective spin angular momentum S' is associated with a magnetic dipole moment $-g_{eff}\,\beta\,S'$; this effective g value will generally be anistropic and have values in the principal directions g_x, g_y and g_z. Thus in any direction with direction cosines l, m, n with the principal directions,

$$g = (l^2 g_x^2 + m^2 g_y^2 + n^2 g_z^2)^{\frac{1}{2}}$$

and in axial symmetry when $g_x = g_y = g_\perp$ and $g_z = g_{11}$

$$g^2 = g_{11}^2 \cos^2\theta + g_\perp^2 \sin^2\theta$$

and the resulting energy levels are shown in Fig. 1.8. Since the matrix of $2\beta B_z S_z$ is diagonal, each level is an eigenstate of S_z only; this means that the eigenstates are not mixed by the magnetic field and the selection rule $\Delta M_S = \pm 1$ operates. This permits transitions between the substates of the lowest doublet separated by $2\beta B_z$

$$\text{whence} \quad g_z = 2$$

In the case of haemproteins, the allowed transitions between $|-3/2>$ and $|-\tfrac{1}{2}>$ have not been observed.

Only off diagonal matrix elements occur if the magnetic field is directed in the x or y directions; to first order, the $|\pm 3/2>$ and $|\pm 5/2>$ doublets are unsplit and the energy splitting in $|\pm\tfrac{1}{2}>$ is given by diagonalising

$$\begin{bmatrix} 0 & 3\beta B_x \\ 3\beta B_x & 0 \end{bmatrix}$$

or

$$\begin{bmatrix} 0 & -3i\beta B_y \\ 3i\beta B_y & 0 \end{bmatrix}$$

to give $6\beta B_h$ and hence $g_h = g_x = g_y = 6$ is observed. In the second order, the energies of the doublets are modified by mixing via B_x and B_y to be (Weissbluth, 1967)

$$E = 0 \pm 3\beta B_h - 4\beta^2 B_h^2/D,$$
$$2D \pm 11/4 \cdot \beta^2 B_h^2/D$$
$$6D \pm 5/4 \cdot \beta^2 B_h^2/D$$

The secular determinant may be solved to obtain the eigenvalue energies of a given Hamiltonian. If the DS_z^2 term is much larger than the magnetic field interaction, the latter can be treated as a perturbation on the zero field Hamiltonian. Using third order perturbation theory, the value of g_{eff} for the lowest doublets may be found (Kirkpatrick, 1964). Otherwise, the diagonalisation may be achieved numerically using a computer. (Pontin, 1968).

1.10. The ferric ion, $^6S_{5/2}$.

The ferric ion will have an orbital singlet ground state which will thus have only $(2S + 1)$-fold spin degeneracy. A first order interaction with the crystal field will not lift this degeneracy. A splitting can be obtained by assuming spin-orbit coupling and going to a high order of perturbation theory (Van Vleck, 1934) but it has been shown that the experimentally observed splitting is too large to be explained on this basis. (Abragam, 1951). In the latter work, it has been assumed that the spherical charge cloud of an S state ion is in fact slightly distorted. The eigenvalue energies will then be dependent upon

spin orientation because the inter-dipole energies will be related to the axes of symmetry of the distorted spherical cloud.

The observed EPR spectrum may usually be fitted to a spin Hamiltonian of the form

$$H_S = g\beta B.S + D(S_z^2 - \tfrac{1}{3}S(S+1)) + E(S_x^2 - S_y^2) + 1/6 \cdot a \cdot (S_x^4 + S_y^4 + S_z^4) + cS_z^4$$

where the additional term involves a fifth order interaction (Watanabe, 1957, Pryce, 1950).

To calculate the g values observed during interaction with a magnetic field $\overline{B}$ it is necessary to compute the matrix elements of $2\beta\,\overline{B}.\overline{S}$ within the substates of the ground state $^6A_1$. Assuming a magnetic field applied along the z axis (the fourfold axis of symmetry perpendicular to the haem plane in haemoglobin) the nonvanishing matrix elements are all along the diagonal, and the energies of the components of $^6A_1$ are

$$\begin{aligned} E &= 0 \pm \beta B_{11} \\ &= 2D \pm 3\beta B_{11} \\ &= 6D \pm 5\beta B_{11} \end{aligned}$$

where $B_{11} = B_z$.

The fundamentals of electron spin resonance as required in this work have been outlined; some general experimental techniques have been briefly discussed. In the next chapter, the properties of the haemproteins will be described and some results previously obtained by electron spin resonance in other work noted.

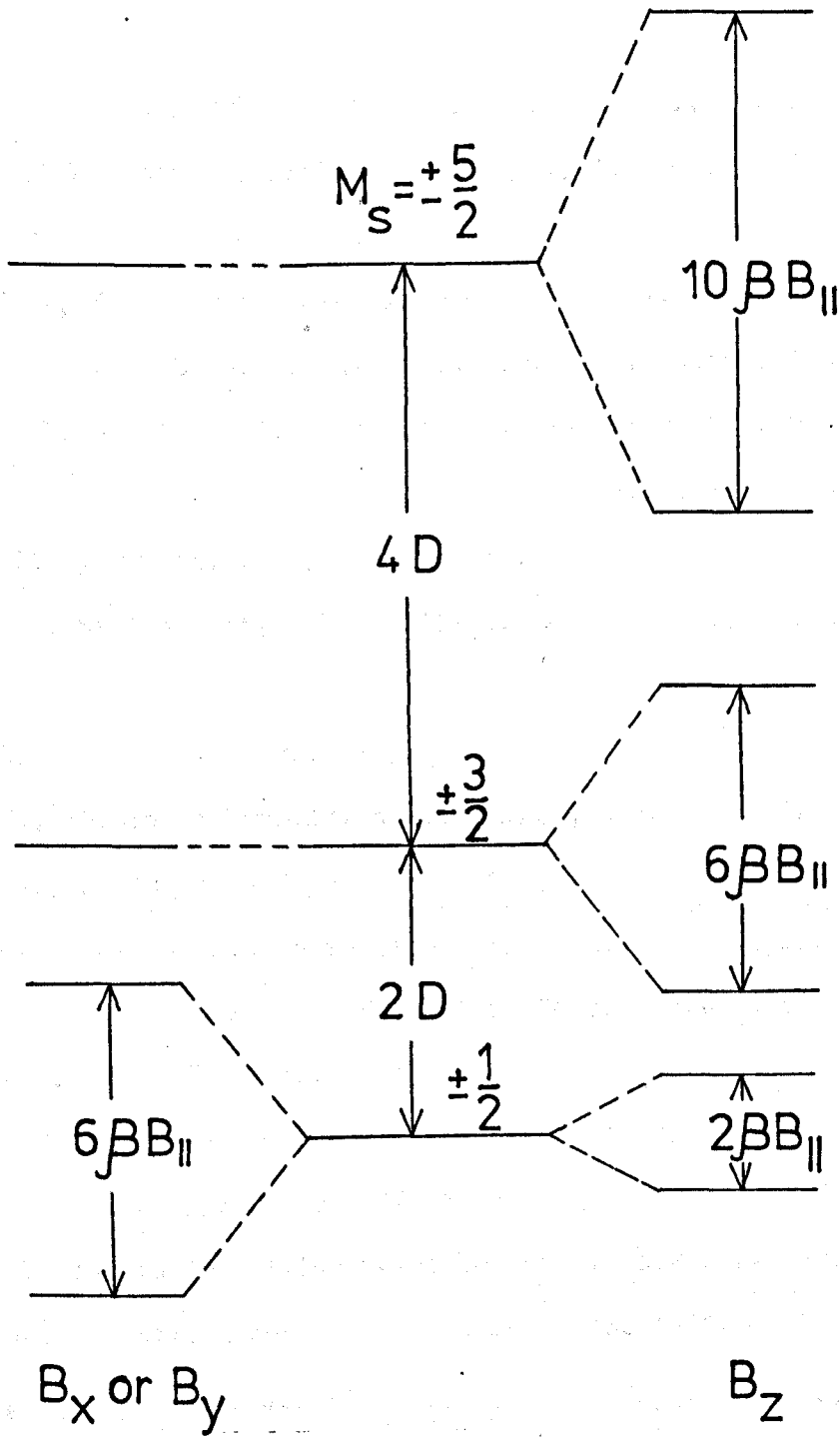

SPLITTING OF $^6A_1$ IN A STATIC MAGNETIC FIELD

Fig. 1.8

1.11. References.

Abragam, A., B. Bleaney, EPR of transition ions, OUP., 1970.

Bleaney, B., K.W.H. Stevens, Repts. Prog. Phys., 16, 108, 1953.

Bloch, F., Phys. Rev., 70, 460, 1946.

Buckmaster, H.A., J.C. Dering, Can. J. Phys., 45, 107, 1967.

Carrington, A., A.D. McLachlan, Intro. to Mag. Res., Harper, 1967.

Ewald, A.H., R.L. Martin, I.G. Gross, A.H. White, Proc. Roy. Soc., A280, 235, 1964.

Feher, G., Bell Sysy Tech. J., 36, 449, 1957.

George, P., J.S. Beetlestone, J.S. Griffith, Haematin Enzymes, p.105, Pergamon, 1961.

Griffith, J.S., Proc. Roy. Soc., A235, 23, 1956.

Griffith, J.S., Theory of Transition Metal Ions, C.U.P., 1964.

Hutchings, M.T., Solid State Physics, 16, 227, 1964.

Judd, B.R., Operator Techniques in Atomic Spectra, McGraw-Hill, 1963.

Kirkpatrick, E.S., K.A. Muller, R.S. Rubins, Phys. Rev., 135, 86, 1964.

Kotani, M., Adv. in Chem. Phys., 7, 159, 1964.

Low, W., Adv. Solid State Physics,,13, Suppl. 2, 1960.

Orgel, L.G., J. Chem. Phys., 23, 1004, 1955.

Orgel, L.G., Intro. to Transition Metal Ion Chem., p.23, 2nd Ed., 1966.

Pake, G.E., Paramagnetic Resonance, p.60, Benjamin, 1962.

Pontin, R.G., E.F. Slade, D.J.E. Ingram, J. Phys. C, 2, 1146, 1969.

Poole, C.P., Electron Spin Resonance, Wiley, 1966.

Schoffa, G., Adv. in Chem. Phys., 7, 182, 1964.

Racah, G., Phys. Rev., 85, 381, 1952; 61, 186, 1942.

Slade, E.F., D.J.E. Ingram, Proc. Roy. Soc., A312, 85, 1969.

Stevens, K.W.H., Proc. Phys. Soc., A65, 209, 1952.

Sutton, D., Electronic Spectra of Trans. Metal Ion Complexes, p. 116, McGraw-Hill, 1968.

Tanabe, Y., S. Sugano, J. Phys. Soc. Japan, 9, 753, 1954.

Torrey, H.C., A.C. Whitmer, Crystal Rectifiers, McGraw-Hill, 1948.

Van Vleck, J.H., J. Chem. Phys., 3, 807, 1935.

Waller, I., Z. Phys., 79, 370, 1932.

Weissbluth, M., Struct. Bond., 2, 1, 1967.

Wilmshurst, T.H., W.A. Gambling, D.J.E. Ingram, J. Elec. Contr., 13,339,1962.

CHAPTER TWO

PROPERTIES OF THE HAEMPROTEINS

2.1. Introduction.

Proteins form an important group of large molecules found in living systems; they perform many varied functions and exhibit different chemical activities. Some proteins are present in tissue as scaffolding but many are enzymes. An enzyme catalyses a physiologically important chemical reaction by participation in the reaction; some enzymes display considerable specificity and may only enhance one reaction; others catalyse many reactions.

The respiratory proteins are usually of a globular shape and are constructed from amino acids linked by peptide bonds to form long polypeptide chains. Apart from the end to end bonds, there may be crosslinkages which serve to stabilise the three dimensional shape of the protein molecule. The protein amino acids are colourless, water soluble, and contain at least one free amino group and a free carboxyl group thus

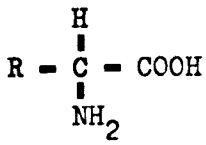

where R is a hydrogen atom or organic radical. The synthesis of peptides from amino acids involves the reaction of the amino group of one acid with the carboxyl group of another acid; this reaction is impossible to accomplish directly since these groups do not readily react. It is therefore essential to incorporate intermediate stages involving more reactive radicals and the simultaneous protection of other reactive groups where bonding is not desired. The overall result is the formation of a so-called

peptide bond by the elimination of a water molecule, the bond being depicted thus.

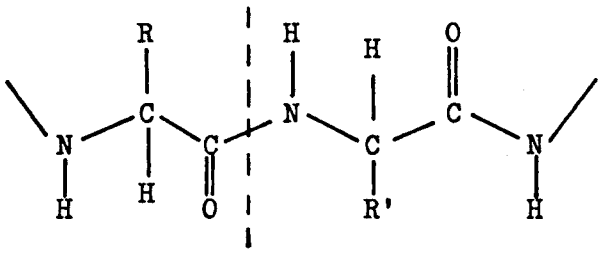

The actual bond lengths and angles have been determined (Corey, 1955) by x-ray diffraction studies of single crystals of amino acids. General rules have been formulated for the structure of certain synthetic polypeptides, resulting in a model known as the alpha helix (Pauling, 1951) which formed a most satisfactory basis for the structures of amino acids and polypeptides. The sequential ordering of amino acids is called the primary structure; the three dimensional helix is referred to as the secondary structure.

As will be later remarked, the properties of a given protein are heavily dependent upon the variety and sequence of the amino acids in its constituent polypeptide chains. Protein synthesis demands the assembly of amino acids in specific sequences. The materials necessary to this ordering process are found in the cells in which the process occurs. These are the nucleic acids and the ribosomes.

The nucleic acids are long chain molecules of two kinds: in ribonucleic acid (RNA) the backbone of the chain is comprised of alternate sugar rings and phosphate rings. In deoxyribonucleic acid (DNA) there are alternate phosphate groups and deoxygenated sugar rings. A double helical structure was proposed for DNA and it was pointed out that this structure provided a mechanism for the replication of genetic material (Watson, 1953, Crick, 1953). The DNA helices present in the chromosomes of a cell might control the production of replicas of itself by

separation of the two strands of DNA forming the double helix, the separated strands facilitating in some way the formation of complementary partners.

The ribosomes are aggregates of ribonucleoproteins present in the cytoplasm of the cell. The internal structure of these aggregates is chiefly unknown since they have proved difficult to crystallize and thus are not readily amenable to study by x-ray diffraction.

The precise manner in which the polypeptide chain of the protein is constructed is still to be determined in detail but the general principles are known. They involve the presentation of suitable amino acids by transfer RNA and the provision of sequencing information by messenger RNA which is probably prepared by DNA replication.

It is believed that the primary structure, that is, the proper sequencing of amino acids, is sufficient to ensure that the helical chain folds into the most stable three dimensional conformation: this latter is called the tertiary structure (Berg, 1961, Anfinsen, 1961).

2.2. Respiratory proteins.

The proteins involved in the respiratory process of various animal species may be divided into two classes: haem and nonhaem proteins. The haem proteins contain a metal ion located in a planar ring system; in nonhaem proteins this is not the case.

The haem proteins include myoglobin, haemoglobin, chlorocruorin, and the cytochromes. Chlorophylls, which enable the absorption of light energy by plants, are magnesium haem complexes. Nonhaem proteins include haemerythrin, haemovanadium and haemocyanin.

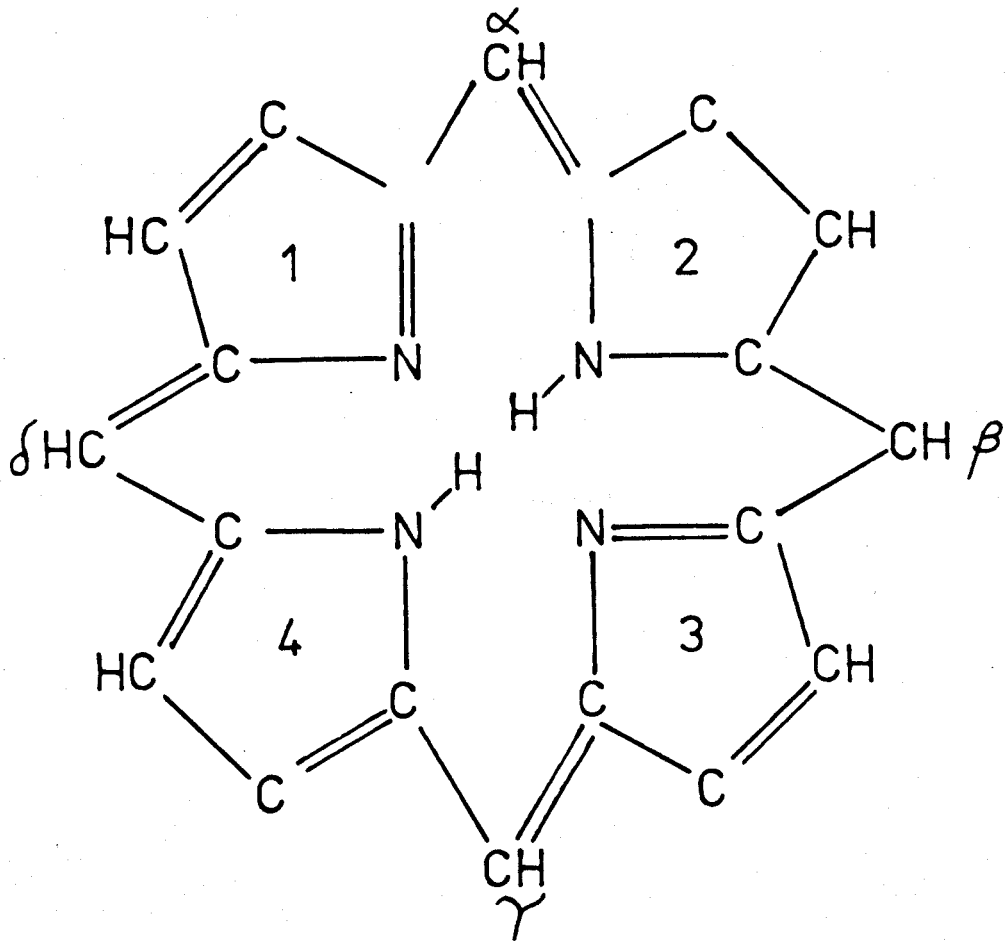

PORPHIN

Fig. 2.1

2.2.1. Nonhaem proteins.

Haemerythrin, a ferrous iron protein, is found in Brachiopoda. The ferrous ion is attached to the protein polypeptide chain; the molecular weight is species dependent and varies between 66000 and 107000 (Ghiretti, 1962, Klotz, 1935).

Haemocyanin, which contains two univalent copper ions per molecule, is found in various forms of ocean life. This protein comprises the largest single biological molecular entity known: the molecular weight is approximately 9×10^6. It is known that this protein can bind one molecule of oxygen reversibly and it is thought that an oxygen bridge is formed between the copper ions (Ghiretti, 1934). It is not known whether the copper ions are equivalently bound; it is suspected that during oxygenation there is no substitution for another ligand but that the coordination number of the copper ions increases, although this number is unknown (Jorgensen, 1966).

Haemovanadium is found in the blood corpuscles of many members of the small marine species Rotifera. A labile oxygen adduct is formed by this protein but its physiological function is not clear (Burton, 1966, Kovalskii, 1964).

2.2.2. Haemproteins.

In order to discuss the haemproteins in detail it will be first necessary to outline the chemistry of porphyrins and their attachment to the folded polypeptide chain.

2.2.2.1. Porphyrins.

The macrocyclic ring system, known as haem, is derived from protoporphyrin IX which is itself a derivative of porphin which

is shown in Fig. 2.1; the formula indicates that porphin is comprised of four pyrrole rings (1 - 4) and is planar. Porphyrins occur naturally by substitution at the periphery of the molecule.

Porphyrins form complexes with divalent metal ions by substitution of the central hydrogen atoms attached to the four nitrogens; these new derivatives may be represented by a number of conventional formulae differing only in the number of saturated and unsaturated bonds. Protoporphyrin IX, whose structural formula is given in Fig. 2.2, forms a stable resonance hybrid with a divalent ferrous ion centrally coordinated.

Trivalent metal complexes may also be prepared; haemin, the ferric analogue of haem, appears on the oxidation of ferrous haem. Haemin possesses the same cyclic structure as haem but there is an unbalanced positive charge on the metal ion. This results in the ligation of another charged ion, commonly the chloride, which neutralizes this excess charge. Both haem and haemin contain sixfold coordinated metal ions; various small molecules coordinate along an axis perpendicular to the porphyrin plane and these include water, carbon monoxide, and the cyanide radical (Walter, 1952, Gibson, 1963, Keilin, 1949).

The relationship of haem to its derivatives and the haemproteins is shown in Fig. 2.3.

2.2.2.2. Haemproteins.

With the exception of the chlorophylls, which contain magnesium, the important haemproteins are compounds containing iron in the ferrous or ferric states. Cytochromes, of which about twenty three occur naturally, assist in the transfer of electrons to molecular oxygen in physiological oxidation processes; although they are closely related to haemoglobin, they do not form oxygen

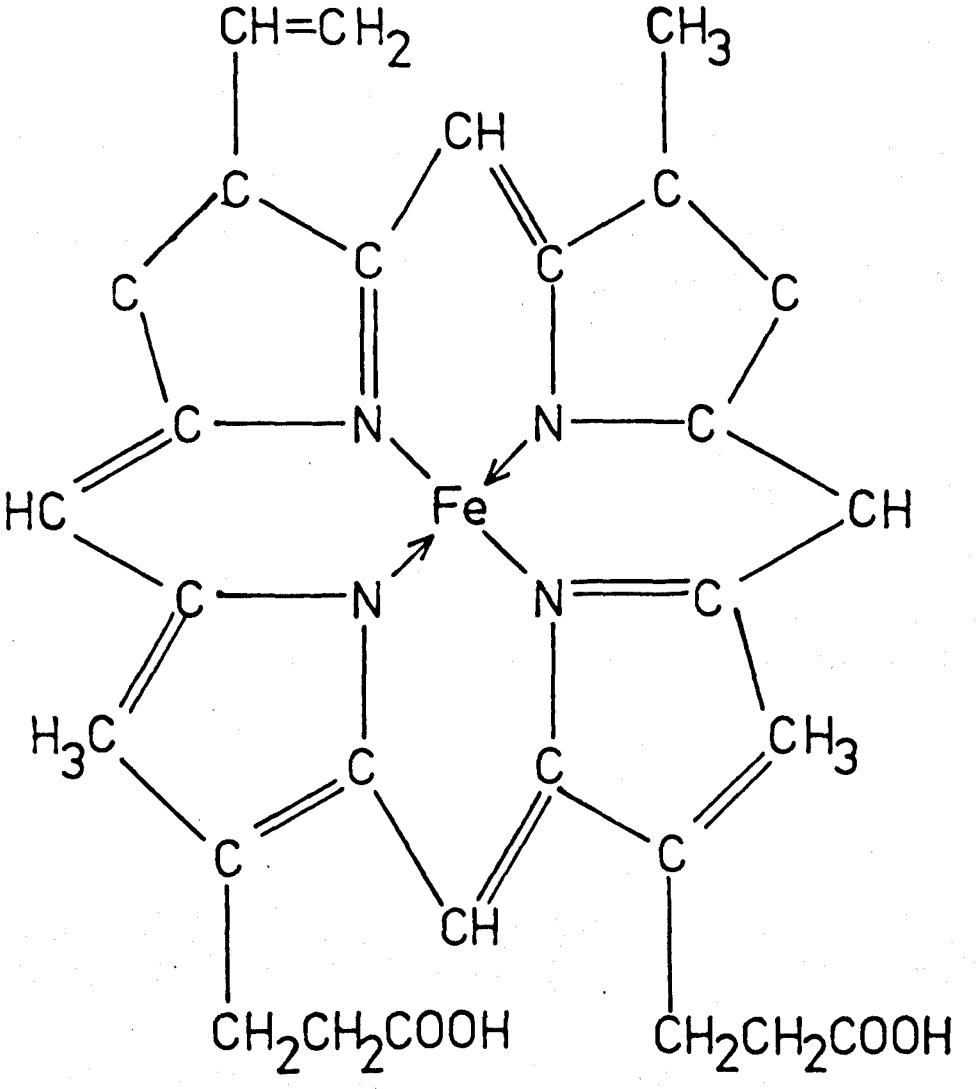

FERROUS PROTOPORPHYRIN IX

(HAEM)

Fig. 2.2

adducts even when containing ferrous iron.

2.2.2.3. Haemoglobin and myoglobin.

These two proteins are intimately concerned with the respiratory process in mammals; haemoglobin, which is the larger molecule, transports oxygen from the lungs to the tissues and myoglobin acts as an oxygen store in the tissues. At times of exceptional and immediate oxygen demand, myoglobin liberates oxygen. Myoglobin contains one haem group per molecule and has a molecular weight of about 16000; oxymyoglobin has a molecule of oxygen attached at the ferrous ion of the haem. Reduced myoglobin (deoxyMb) has no ligand and is five-coordinated.. When the central metal ion is oxidised to the ferric valence state it can no longer bind oxygen but is able to take up other ligands, e.g. fluoride or azide; ferric myoglobin is frequently referred to as metmyoglobin.

The x-ray crystallographic studies of Kendrew and his coworkers on sperm whale metmyoglobin have determined the spatial architecture to a resolution of 1.4 Å, enabling the positions of individual atoms (except hydrogen) to be found. (Kendrew, 1958, 1960, 1963). These investigations, facilitated by empirical modifications to the method of isomorphous replacement (Robertson, 1936, Green, 1954), showed that the polypeptide chain was folded to yield the tertiary globular structure called globin. Earlier results at 2 Å resolution indicated that the electron density along the folded polypeptide chain was consistent with the hypothesised alpha helical model; about 70% of the chain is helical. The globin structure is very compact and contains almost no internal liquid; the molecule interior is largely hydrophobic.

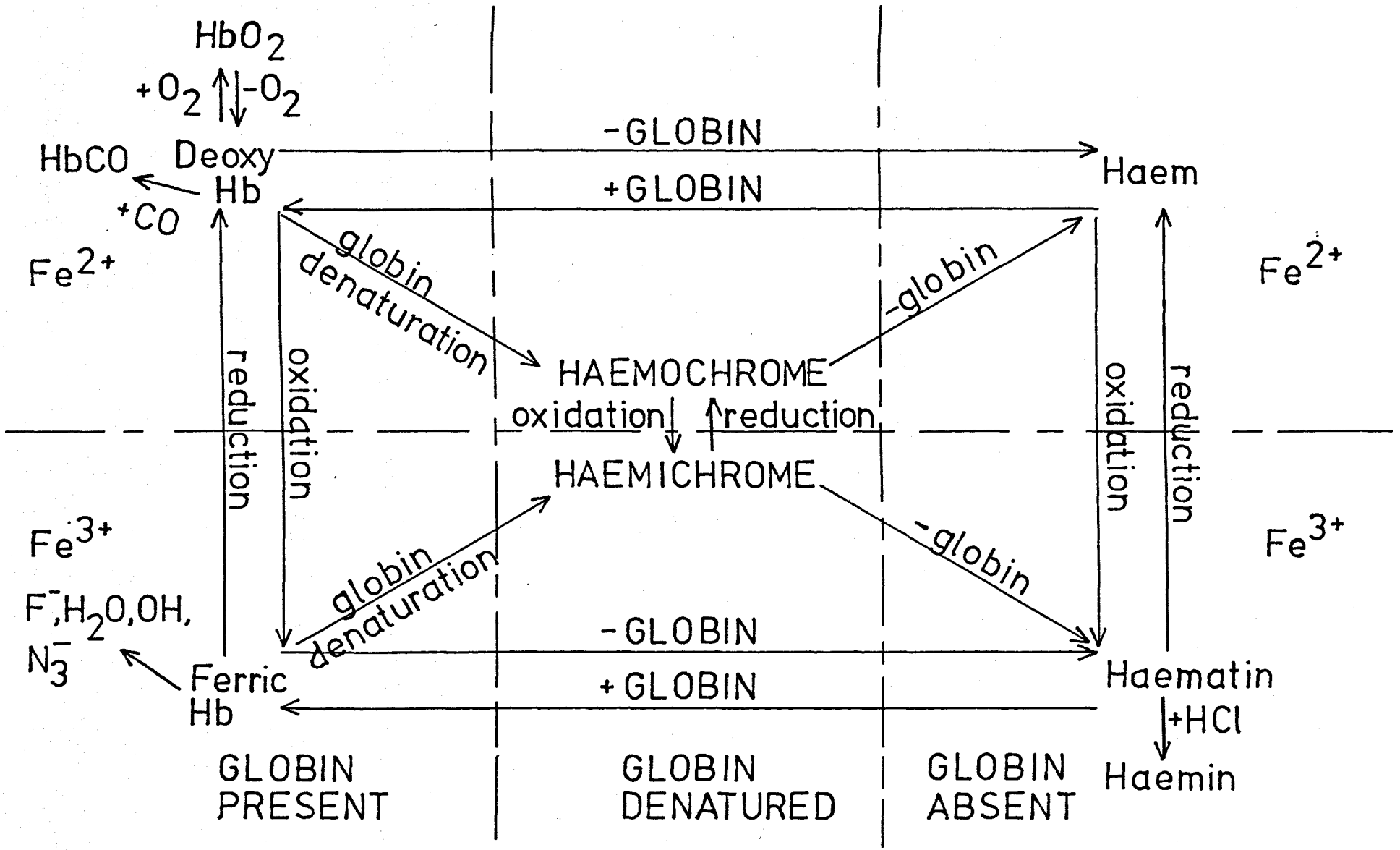
HbO2
+O2 ↑↓ -O2
HbCO
Deoxy Hb
+CO
Fe2+
-GLOBIN
+GLOBIN
Haem
Fe2+
globin denaturation
-globin
HAEMOCHROME
oxidation
reduction
HAEMICHROME
reduction
oxidation
oxidation
reduction
Fe3+
Fe3+
F-,H2O,OH,
N3-
globin denaturation
-globin
-GLOBIN
+GLOBIN
Ferric Hb
Haematin
+HCl
Haemin
GLOBIN PRESENT
GLOBIN DENATURED
GLOBIN ABSENT

Fig. 2.3

The tertiary structure appears to be stabilised by hydrogen bonds, ionic bonds and bonds between amino acid side chains. The haem is bound to the globin moiety by bonds at the periphery of the haem and on the peptide chain. Side chains of certain amino acids also form hydrogen bonds with the propionic acid groups of the porphyrin. The haem is also attached via the fifth coordination position of the ferrous ion to a histidine residue, known as the proximal histidine, via a nitrogen atom. In metmyoglobin at acid pH a water molecule occupies the sixth coordination position.

Haemoglobin is contained in the red cells of the blood of vertebrates where it comprises about 90% of the solid matter and about 97% of the protein content. The molecular weight is about 65000 (almost four times that of myoglobin); the molecule consists of four polypeptide chains, identical in pairs, and four haem prosthetic groups. The manner in which the four chains are fitted together after the tertiary folding is called the quaternary structure and the assembled molecule occupies a space of about 50 Å by 55 Å by 69 Å.

Crystal growing problems led to Perutz and his associates making a 5.5 Å resolution study of horse haemoglobin; it can be seen from this study that the haem groups are located in four pockets on the surfaces of the four peptide subunits. The arrangement of the haem groups is shown in Fig. 2.4 (Perutz, 1960, Cullis, 1961/2, Muirhead, 1963). The orientations of the haem groups were previously determined by EPR and assisted in the interpretation of the x-ray results, (Ingram, 1956).

2.2.2.4. Oxygenation.

It would seem appropriate to note the remarkable oxygenation

properties of haemoglobin and the recently proposed model which relies heavily upon the x-ray Fourier difference spectra of the deoxy and ligated forms of haemoglobin. (Perutz, 1970).

Haemoglobin is capable of reversibly binding four molecules of oxygen per protein molecule, each oxygen being attached at the metal ion of the porphyrin. It is enough to state that early researches demonstrated that the equilibrium curve between haemoglobin and oxygen was sigmoidal (Adair, 1936): this means that (in the words of Wyman, 1948) "the first oxygen enters the protein molecule with more difficulty than the second owing to the necessity of breaking up a pre-existing partnership between the haems". The energy required by each oxygen molecule to enter decreases as more oxygen molecules are bound to the protein. The sigmoidal equilibrium curve avoids the problem of low oxygen partial pressure at the tissues: if the co-operative effect were absent, then little oxygen would be surrendered at the tissues, resulting in asphyxiation. The co-operation between the haems cannot be due to a magnetic interaction because of their relatively large separations (Fig. 2.4).

This only leaves a stereochemical effect; it is suggested that the first oxygen molecule bonds and causes inter alia a change in the radius of the ferrous ion in going from the high spin to the low spin state (deoxy to oxyHb) which is transformed by the geometry of the haem group into a relatively large movement of the distal histidine. This movement is transmitted through the tertiary structure and eventually results in breakage of the salt bridges which link the chain ends of the different subunits as further oxygen molecules are attached. The affinity for oxygen is thus increased as the constraints holding the protein molecule in the deoxyHb quaternary structure have been destroyed and the

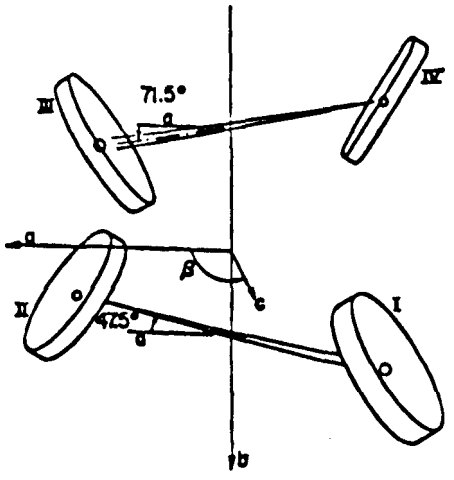

HAEM GROUPS IN HAEMOGLOBIN.

	Distance between hemes (Å)*	
	Horse Oxyhemoglobin	Human Reduced Hemoglobin
Fe_1–Fe_2	33.4	40.3
Fe_3–Fe_4	36.0	35.0
Fe_1–Fe_3	25.2	25.0
Fe_1–Fe_4	30.4	37.4

FIG. 2.4.

quaternary structure snaps over to that of oxyhaemoglobin, the remaining haems then quickly acquiring oxygen molecules. These proposals were only made possible by refining the Fourier syntheses of x-ray diffraction studies to give a resolution of 2.8 Å (Perutz, 1968).

2.2.2.5. Abnormal haemoglobins.

Examination of human haemoglobin samples from many parts of the world has led to the discovery of over one hundred mutants of the protein (Perutz, 1968); these mutations do not directly involve the haem group but are corruptions of the peptide sequence. Pathological mutation can be related to clinical symptoms such as methaemoglobinaemia. It is thought that nearly all the roughly sixty contacts between the haem and the globin are essential to the proper functioning of the protein. This expectation is supported by the sensitivity of the molecule to small stereochemical changes: in Hb Sydney the substitution of alanine for valine at E11 - 67 removes two methyl groups from contact with the haem: this results in detachment of the haem from the protein. The clinical result is called haemolytic anaemia and the protein is highly unstable at 50°C. Other mutations may lead to permanent formation of the ferric derivative which cannot reversibly bind oxygen or to low solubility leading to precipitation in the red cells ensuring their early destruction (Watson, 1961, Pauling, 1949, Perutz, 1950, 1968, V.M. Ingram, 1958).

The major justification for research into human haemoglobin must be the alleviation of these distressing symptoms, either by tampering with the DNA coding or by the use of nondegradable of replacable synthetic oxygen carriers.

2.2.2.6. Synthetic oxygen adducts.

Apart from the naturally occurring oxygen transport proteins, there exist various chelates which have the ability to take up and release molecular oxygen (Martell, 1952, Hearon, 1949, Drake, 1960). The reactions of these complexes are of interest for two prime reasons.

First, they may illuminate the necessary conditions for reversible oxygenation of the metal ion in proteins and, second, they may form the bases of physiologically useful synthetic respiratory proteins. The conditions for the formation of oxygen-chelate adducts are that the coordinating ion must be able to exist in two oxidation states at least and that the oxidation potential should have a suitable value; if it is too low there is no donation of electrons to the oxygen molecule enabling bonding to take place. If it is too high, irreversible oxidation occurs. The oxidation potential is adjusted by a suitable choice of chelating ligand; this is clearly part of the function of the globin in the protein.

Unfortunately, in the case of some synthetic oxygen carriers irreversible oxidation sets in after some hundred cycles of oxygenation and deoxygenation.

2.2.2.7. Mossbauer studies of haemproteins.

A number of ferrous and ferric complexes of ^{57}Fe-enriched rat haemoglobin and other proteins have been studied (Frauenfelder, 1962). The nucleus of the haem iron is a sensitive probe into its immediate environment in the protein molecule; this is because it is bound to the other atoms present and engages in electric and magnetic hyperfine interactions arising out of the spatial

structure. If the electronic ground state is magnetic then the considerable dilution of the metal ions (see Fig. 2.4) inhibits spin-spin interactions enabling hyperfine structure to be seen. Two parameters are useful in describing Mossbauer spectra: these are the Isomer Shift (I.S.) and the Quadrupole Splitting (Q.S.). The I.S. is the offset of the centre of gravity of the spectra from zero velocity in mm s^{-1} (Goldanskii, 1964). The Q.S. is the separation of the two lines of a Mossbauer spectrum in units of velocity relative between source and absorber, mm s^{-1}. The I.S. is due to a change in the electrostatic potential well of the nucleus when contracted in the excited state; the Q.S. is caused by the electric quadrupole moment of Fe^{57} in the 14.4 keV excited state which splits the state into two levels. The results of Mossbauer studies of haemoglobin are exhaustively listed by several authors (Lang, 1966, Gonser, 1965, König, 1961, Williams, 1966).

It has been found that in model compounds such as metal carbonyls, phthalocyanines, and cyanide derivatives there is a strong correlation between I.S. and Q.S. (Williams, 1966). On the other hand no such correlation appears to exist for all haemoglobin derivatives which probably indicates that the geometry surrounding the iron is more disturbed by the ligands. However, certain haemoglobin derivatives appear to follow a pattern, namely CN^-, OH^-, O_2 and H_2O. (see Fig. 3.19).

By analysis of the spin Hamiltonian the spin state of the metal ion has been found (although contradictions exist for certain derivatives) and the zero field splitting has been found for haemoglobin fluoride to be $2D = 14$ cm^{-1} (Lang, 1966).

2.2.2.8. Optical absorption studies of haemproteins.

Porphyrins and haemproteins are characterised by a number of optical absorption bands.

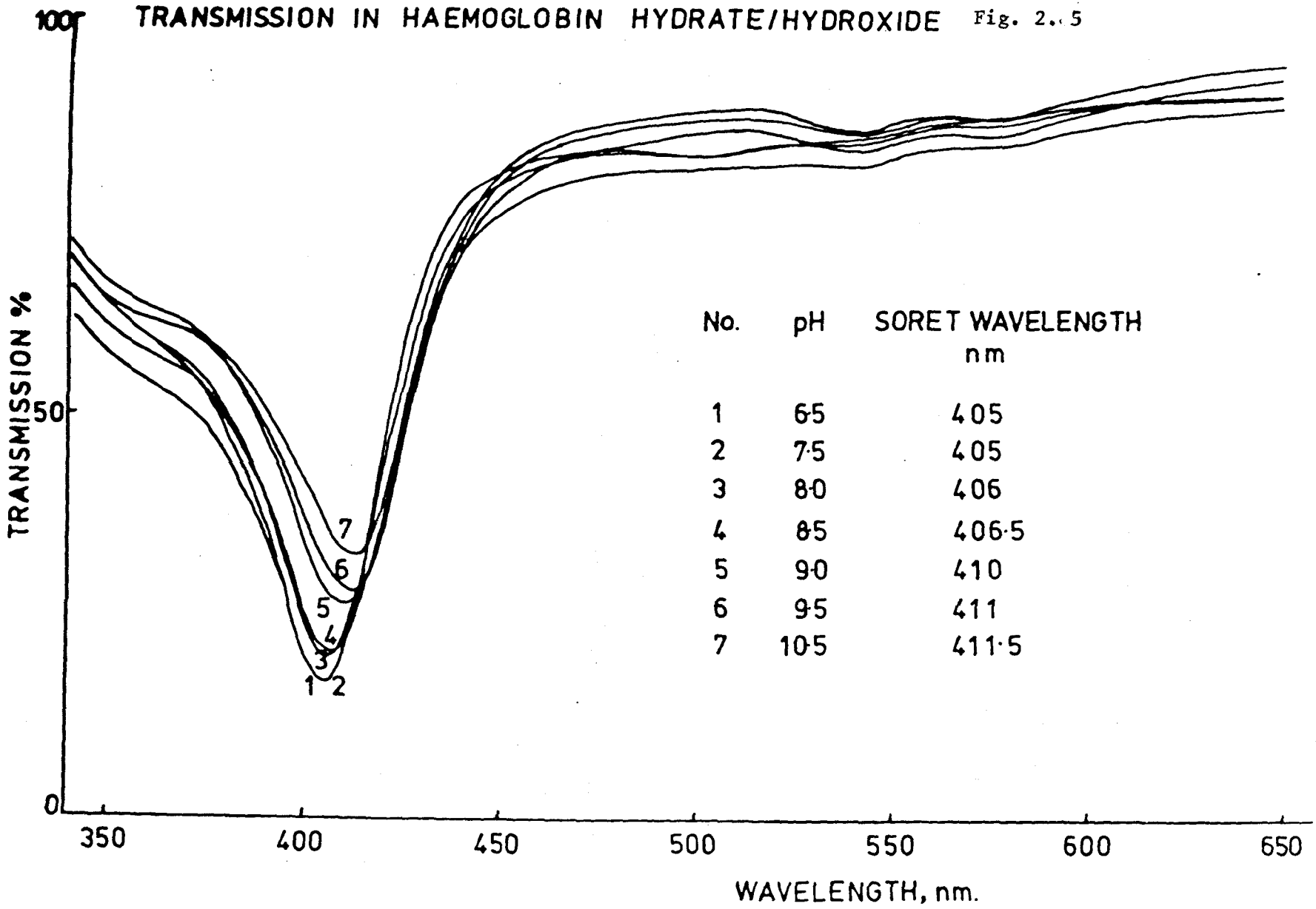
TRANSMISSION IN HAEMOGLOBIN HYDRATE/HYDROXIDE
Fig. 2.5
100
50
0
TRANSMISSION %
350
400
450
500
550
600
650
WAVELENGTH, nm.
No. pH SORET WAVELENGTH nm
1 6·5 405
2 7·5 405
3 8·0 406
4 8·5 406·5
5 9·0 410
6 9·5 411
7 10·5 411·5
1
2
3
4
5
6
7

The most intense absorption band in free porphyrins is the Soret band which occurs in the region 400 nm to 420 nm wavelength and has a molar extinction coefficient of about 130. It is thought that the Soret band arises from a transition between two molecular orbitals in a region remote from the central metal ion (Fig. 2.6).. Molecular orbital calculations for simplified porphyrins have been moderately successful in predicting the intensities and wavelengths of the Soret and other visible absorption bands (Weiss, 1965, Gouterman, 1963).

It is found experimentally that in high spin haem complexes such as myoglobin and haemoglobin fluoride the Soret band is situated at 405 nm wavelength and that in low spin complexes such as the cyanide it is shifted to 420 nm wavelength. A similar movement of the Soret band may be observed when a solution of haemoglobin hydrate is progressively changed in pH so that OH^- ions replace water molecules at the sixth coordination position of the haem; this movement may be interpreted as a change in the proportion of low spin haemoglobin present in solution: this movement is shown in the experimental curves in Fig. 2.5.

The chief characteristics of the optical absorption spectra of low spin ferric complexes of haemoglobin and myoglobin are two absorption bands, α and β , which occur at about 575 nm and 540 nm. They are certainly due to excitation from the t_{2g} orbitals of the metal ion to the ligand orbitals (Fig. 2.6).

High spin haemproteins possess absorption bands at about 630nm and 500 nm (the D and E bands) which are thought to be due to electron excitation from orbitals localized on the ligands to orbitals associated with the metal ion and vice versa. These charge transfer bands tend to disappear as the degree of covalency increases in the metal-ligand bond since the orbitals then undergo a certain degree of delocalization. The high spin complexes are

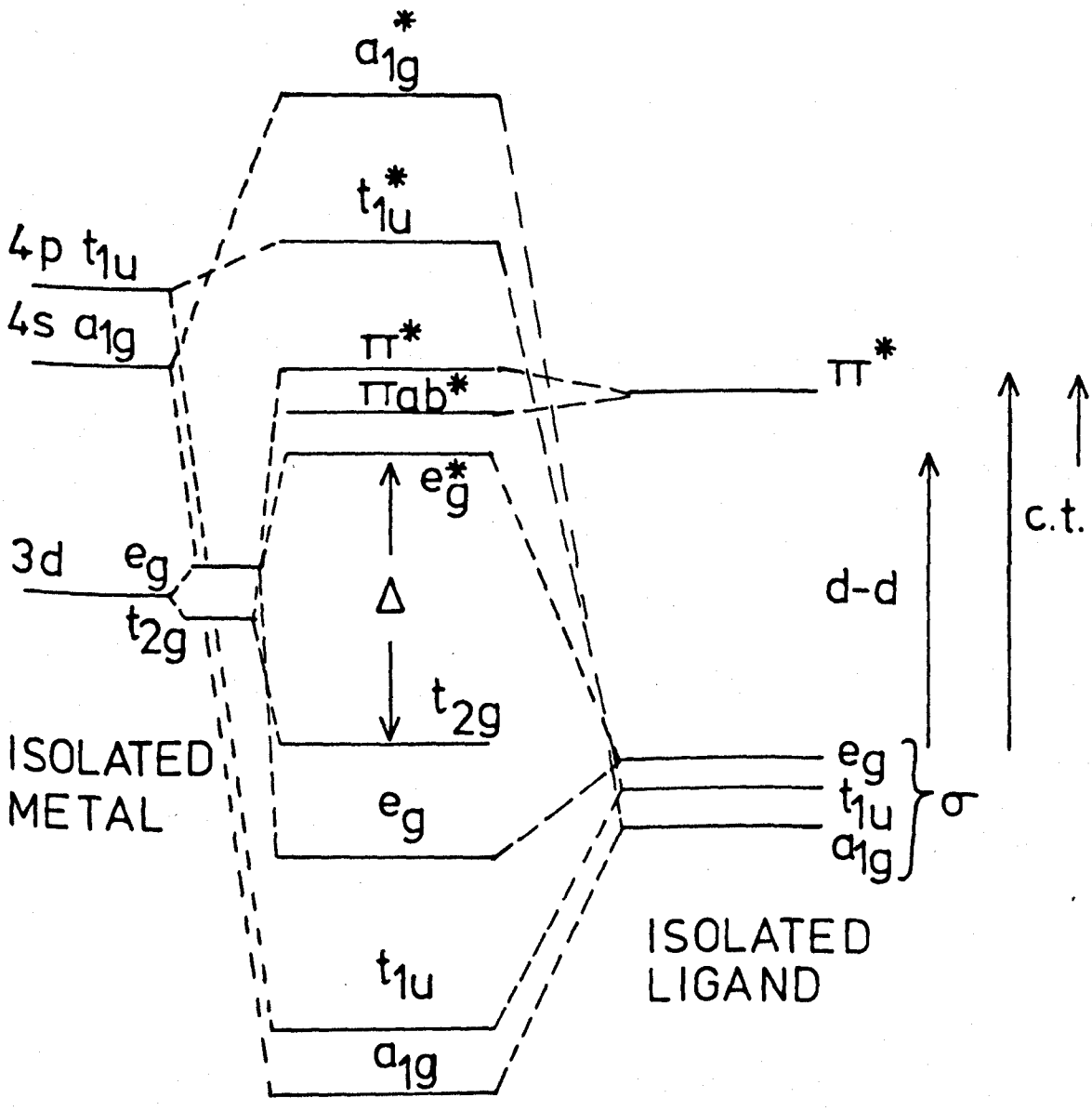

MOLECULAR ORBITAL LEVELS FOR AN OCTAHEDRAL COMPLEX.

Fig. 2.6

believed to possess minor absorption bands which are approximately coincident with the low spin alpha and beta bands; in the case of ferrous haem, these bands have been theoretically predicted (Gouterman, 1963).

The molecular orbital theory discussed in 1.6 and 1.7 gives rise to a series of energy levels resulting from the orbitals of the metal and the ligand. A knowledge of the magnetic susceptibility enables one to fill these levels with the available electrons so as to give the requisite number of unpaired spins. It is then possible to compare this energy level model with the experimental absorption spectrum of the complex. Two significant transitions are shown in Fig. 2.6; these are transitions between molecular orbitals originating in one set of d orbitals (t_{2g}) and molecular orbitals arising from the e_g orbitals, and transitions involving the transfer of an electron from an orbital associated with a ligand to an orbital associated with the metal ion or the reverse: these two types of transition are called d-d and charge transfer transitions. It is thus possible to see how the various transitions originate in haemproteins.

The d-d transitions measure the ligand field splitting and it is possible to write a series of ligands in order of increasing Δ; this is referred to as the ligand field or spectrochemical series.

I^- Br^- S^- Cl^- OH^- CO_2^- H_2O SCN^- CH_3^- CN^-

This order is approximately independent of the choice of the metal ion and it is to be noted that there is an increasing degree of covalency in the latter half of the series. It has been suggested that the ligand field splitting for any regular octahedral complex could be written as the product of two fac-

tors, the one characteristic of the metal and the other of the ligand (Jorgensen, 1962). The charge transfer absorptions are related to the degree of electron delocalization; this delocalization is thought to be due to the expansion of the charge cloud of the d electrons of the metal ion (which leads to a repulsion between the d electrons) and is believed to be caused by covalent interactions. The ligands can again be arranged in a further series, known as the nephelauxetic series:

$$F^- \quad H_2O \quad OH^- \quad CO_2^- \quad Cl^- \quad CN^- \quad Br^- \quad I^-$$

and this series is independent of the metal ion; it is observable that this series reflects the order of the ability with which ligands are able to form complexes (Orgel, 1967, Ballhausen 1962).

Experimental results for the optical absorption spectra of certain haemoglobin derivatives will be reported in Chapter 3.

2.2.2.9. Electron paramagnetic resonance studies.

The details of the occupation of the orbitals for ferric and ferrous ions indicate that certain haemoglobin derivatives will exhibit paramagnetic properties (q.v. 1.6). The extent of the paramagnetism will depend upon whether the ion concerned is in the low or high spin state.

Measurements of the magnetic susceptibility show that the ferrous derivatives oxyhaemoglobin and carbonmonoxidehaemoglobin are entirely diamagnetic (Pauling, 1936) and it is therefore not possible to observe EPR signals from these derivatives. Similarly, it is found that deoxyhaemoglobin has a spin $S = 2$ but no EPR signals have been observed from samples of this derivative. This may be because of a short relaxation time or large splittings; experiments using 50GHz microwave quanta have

been attempted without positive result (Ingram, 1963). The spin lattice relaxation time of Fe^{++} has been measured using an MgO host lattice at $1.5^{o}K$ to be 4×10^{-4} seconds, which is much shorter than that of other ions in the same host (Shiren, 1963).

The ferric haemoglobin derivatives are all paramagnetic, having $S = \frac{1}{2}$ or $S = 5/2$ states, and the temperature dependence of the optical absorption spectrum has shown that thermal equilibrium mixtures of these states may exist; this effect gives rise to intermediate values of susceptibility which were formerly ascribed to an $S = 3/2$ state (George, 1961, Griffith, 1956). EPR signals have been observed from low and high spin haemproteins at various microwave frequencies up to 35 GHz in the the case of haemoglobin (Bennett, 1957) and 70 GHz for myoglobin (Bennett, 1961, Helcke, 1968, Slade, 1972). In particular the orientations of the haem planes in a range of haemproteins from different species with respect to the crystal axes were found by examining the g value angular variation; these results were of considerable assistance in the interpretation of x-ray crystallographic data (Ingram, 1956). By making g value measurements on concentrated solutions and single crystals it is possible to calculate the zero field splitting parameter and compare with estimates obtained by other experimental techniques; using data from EPR at 35 GHz and 70 GHz, this has been accomplished for myoglobin hydrate, fluoride and formate, but there exists some lack of agreement with other results (Farrow, 1971) and it is suspected that the history of the sample may affect the g value; for example, freeze drying is thought to produce small conformational changes which may result in metal-ligand bond variations (Slade, 1968).

The angular dependence of the EPR linewidth has also been investigated at 35 GHz. in myoglobin and explained in terms of a small random misorientation of the haem groups within the crystal; for myoglobin hydrate a standard deviation of 1.6^{o} was reported (Helcke, 1968). However, at 70 GHz this theory only gives an adequate fit to the experimental results at angles removed from the haem plane; near the plane agreement was poor and it was observed that the minimum linewidth did not coincide with the maximum g value and, further, that the value of the minimum linewidth had increased in proportion to the frequency (Slade, 1968). In measurements on myoglobin pastes it was found that the EPR line could only be satisfactorily computed by using a linewidth dependent upon frequency (Farrow, 1971).

This work has therefore attempted to extend the measurements on <u>haemoglobin</u> derivatives using microwave frequencies up to 70 GHz; deoxyhaemoglobin and ferric derivatives have been examined as pastes and single crystals. It was thought important to study the angular variation of the g value at 70 GHz in single crystals and to calculate the appropriate spin Hamiltonian parameters. It was also intended to investigate the orientation dependence of the EPR linewidth at 70 GHz and compare this with the results reported for myoglobin.

2.3 References.

Ballhausen, C.J., An Intro. to Ligand Field Theory, McGraw-Hill, 1962.

Bennett, J.E., J. F. Gibson, D.J.E. Ingram, Proc. Roy. Soc.,A240,67,1957.

Bennett, J.E., J.F. Gibson, D.J.E. Ingram, Proc. Roy. Soc., A262,395,1961.

Farrow, R.H., Thesis Ph.D., University of Keele, 1971.

George, P., J.G. Beetlestone, J.S. Griffith, (in) Haematin Enzymes, (Eds.), J.E. Falk, R. Lemberg, R.K. Morton, Pergamon, 1961.

Gouterman, M., J. Mol. Spec., 11, 108, 1963.

Griffith, J.S., Proc. Roy. Soc., A235, 23, 1956.

Helcke, G.A., D.J.E. Ingram, E.F. Slade, Proc. Roy. Soc., B169, 275, 1968.

Ingram, D.J.E., J.F. Gibson, M.F. Perutz, Nat., 178, 906, 1956.

Ingram, D.J.E., (in) Para. Res., 2, 809, 1963, W. Low, (Ed.), Acad. Press.

Jorgensen, C.K., Absorption Spectra and Chemical Bonding in Complexes, Pergamon, London, 1962.

Orgel, L.G., An Intro. to Transition Metal Ion Chemistry, Methuen, 1967.

Pauling, L., C.D. Coryell, Proc. Nat. Acad. Sci. Wash., 22,210,1936.

Shiren, N,, Magnetic and Electric Resonance and Relaxation, J. Smidt, (Ed.), p. 114, North Holland, 1963.

Slade, E.F., Thesis Ph.D., University of Keele, 1968.

Slade, E.F., D.J.E. Ingram, Nat., 220, 785, 1968.

CHAPTER THREE

SPECTROSCOPIC STUDIES OF SOLUTIONS

3.1.1. Preparation of haemoglobin solutions.

Blood samples were collected from various donors by venipuncture and sodium citrate and heparin were added as anticoagulants (Quick, 1948, Surgenor, 1953). The fresh blood was centrifuged in a swing-out rotor centrifuge for twenty minutes at 6000g; the supernatent liquid was removed by suction and the remaining red cells successively mixed and washed three times with 0.9% sodium chloride solution; this treatment is designed to remove stroma and any remaining plasma. It is also effective in removing methaemalbumin; this may be shown by a photometric test (Bjerre, 1968).

The red cells were then haemolysed by the addition of an aliquot part of distilled and deionised water and left for fifteen minutes or more. Occasionally the mixture was left overnight at $4^{o}C$ without adverse effect. The haemolysis procedure causes the cells to expand and consequently their walls burst, liberating the cell contents into solution. A few drops of 35% sodium chloride solution were added to bring the chloride concentration up to 2% and the mixture was centrifuged for one hour. The clear red supernatent haemoglobin solution was pipetted off; a subsequent centrifugation sometimes yielded more haemoglobin solution.

The purpose of adding additional NaCl is to precipitate stroma; a roughly aliquot part of toluene has been recommended for this purpose (Drabkin, 1946) but this procedure was avoided for two reasons. First, it has been found that the retention of

toluene during any subsequent oxidation to ferric haemoglobin results in spectrophotometric abnormalities (Cameron, 1969) and, second, in this work it was observed that there was a tendency for the toluene to cause retention and spreading of haemoglobin solutions on molecular sieves.

The resulting protein solution contains salt and this may be removed by dialysis or with a molecular sieve. Both methods have advantages. In the latter case the solution was run through a vertical glass column containing G25 Sephadex which had been previously equilibrated with a 0.01 M solution of ammonium phosphate adjusted to pH 7.0 (Perutz, 1968). Sephadex is a dextran cross linked by epichlorhydrin which renders the dextran insoluble but enables it to retain its lyophillic qualities: the addition of water to the dry dextran causes the powder to swell into a gel which is suitable for filtration. The degree of crosslinkage determines the porosity of the gel. Molecules undergoing filtration through the gel are retained by it if sufficiently small to enter and remain in the pores whilst larger molecules pass through the gel, their size excluding them from the pores. Consequently, the haemoglobin passes through the gel far more quickly than the salt; it is advantageous to adjust the gel pH to 7.0 as an acid gel tends to exclude a proportion of small molecules from the pores (Porah, 1959).

Dialysis of haemoglobin solutions was also used to remove salt; a cellolose membrane was soaked in water, boiled to remove plasticisers and copper impurities, and filled with the protein and salt solution. The tied dialysis tubing was placed in a two litre beaker containg the dialysant (distilled and deionised water) stirred at 4°C: stirring ensures that the maximum possible concentration gradient exists across the membrane. Progress may be

monitored by measuring the water conductivity with an ohmmeter; by regularly changing the dialysant, dialysis can be halted when no further change in conductivity occurs. Dialysis of haemoglobin solutions appears to take slightly longer than that of myoglobin; this may be caused by the larger haemoglobin molecules obscuring the membrane pores. Dialysis took about one week to complete and required frequent attention; the molecular sieve method took only about two hours. Further, dialysis of ferric haemoglobin solutions has been found to perturb the optical absorption spectrum by about 1% (Cameron, 1969). The molecular sieve does not appear to affect the spectrum; dilution which occurs in the sieve method may be corrected by subsequent concentration. The actual concentration was determined by the procedures noted in 3.2.3.

For use in the EPR spectrometer it is necessary to concentrate the solutions; several methods are possible. Four methods were tried with varying degrees of success. Boiling under reduced pressure was very slow and can lead to frothing denaturation. Dry Sephadex may be used to remove water: a weighed quantity was added to the dilute protein solution, water is absorbed as the gel swells, and the remaining concentrated solution is removed by filtration under reduced pressure (Flodin, 1960). However, the recovery of haemoglobin was only 80% and the method would be better employed for large quantities of dilute solution (Deutsch, 1963).

The concentration method used most often was the removal of water by tablets of a commercial polyacrylamide hydrogel, Lyphogel. Each tablet absorbs a fixed weight of water but does not take up large molecules. The loss of protein is consequently small and the degree of concentration can be readily estimated from the weight of Lyphogel added; the tablets can be removed with

the aid of forceps after about four hours at 4°C, when the concentration process is complete.

A further method which was tried at a late stage in the work and found very adequate involved the use of an ultrafiltrator (manufactured by the Amicon Corporation, Inc.); in this device pressures up to 40 p.s.i. were applieed to the solution which dialyses through a specially strengthened and supported membrane. The rate of dialysis is considerably enhanced by the pressure. As in the case of normal dialysis, the protein molecules are too large to pass through the membrane pores and are retained the gradually concentrating solution on the input side of the membrane.

3.1.2. Ligation of haemoglobin in solution.

The haemoglobin obtained in solution is mostly oxyhaemoglobin and remains so provided that oxidising agents are absent from buffer solutions and the water used in the preparation. This is never quite the case and there is thus a slow oxidation to ferric haemoglobin (sometimes referred to as methaemoglobin).

3.1.2.1. Deoxyhaemoglobin.

Deoxyhaemoglobin solution was prepared by the chemical reduction of oxyhaemoglobin. Freshly prepared ferrous citrate has been commonly used (Perutz, 1955) but this is unsuitable for EPR work as the iron oxidises to the ferric form and is readily seen as an impurity signal. The use of sodium dithionite, described in 3.2.3., does not give rise to this problem. The resulting purple deoxyhaemoglobin solution is stored in a sterile specimen tube in a sealed Kilner jar, both containg nitrogen gas, at 4°C.

3.1.2.2. Haemoglobin hydrate (methaemoglobin).

Haemoglobin hydrate may be prepared by oxidizing oxyhaemoglobin. It is important to add no more than a thrice molar excess of oxidising agent since excess over this level has been found to perturb the optical spectrum (Cameron, 1969) by about 7%. The use of potassium ferricyanide is to be avoided because of the presence of iron. Sodium nitrite A.R. was used as an oxidizing agent and the solution dialysed at once against 0.1 M phosphate buffer to remove excess nitrite; if this is not done a Hb-$NaNO_2$ complex may form (Lemberg, 1949).

3.1.2.3. Ferric haemoglobin derivatives.

The fluoride was prepared by the addition of potassium fluoride until the final molar concentration was 400 times that of the haem (Li, 1969). Methaemoglobin azide was prepared by the dialysis of a 5% haemoglobin solution against 0.15 M sodium azide solution. The preparation of the organic monobasic acid derivatives is described in 3.3.1.

3.2. Spectrophotometric studies of haemoglobin derivatives.

3.2.1. Introductory note.

The chief features of the optical absorption spectrum of haemoglobin have been described in 2.2.2.8. In this work experimental spectra have been obtained for derivatives not previously studied and an attempt is made to interpret these results.

3.2.2. Quantitative measurement of absorption.

The measurement of absorption is based on two fundamental laws relating the incident and transmitted radiation intensities.

Lambert's law states that for monochromatic light, each successive unit thickness of the absorbing medium absorbs an equal fraction of the light transmitted through it. This may be expressed as

$$I = I_o \cdot 10^{-kt}$$

where $1/k$ is the path length reducing the incident intensity I_o to $I_o/10$ and k is the extinction coefficient.

Beer's law states that, if the solvent absorption is compensated for, then the extinction coefficient is directly proportional to the concentration of the solution, thus

$$I = I_o.10^{-Ect}$$

where $E = k/c$ is the extinction coefficient for unit concentration.

In cases where the molecular weight is not precisely known it is usual to write the unit of concentration as a superscript in per cent, and the unit of optical path length or the wavelength of measurement as the subscript, i.e.

$$E^{1\%}_{540\ nm} = \log_{10} (I_o/I)\ cm^{-1}$$

where the value of the right hand side is the extinction

coefficient for unit per cent concentration and one centimetre optical path length at the cited wavelength.

Beer's law as stated above is obeyed by haemproteins in solution (Day, 1967).

3.2.3. Determination of solution concentrations.

The concentrations of the prepared haemoglobin solutions were determined optically by two methods.

A known quantity of the haemoglobin solution (the stock solution) was diluted to 1:100 with distilled water. One ml of this solution was added to 9 ml water buffered to pH 5.8 with a mixture of ammonium hydrogen phosphate and diammonium phosphate solutions. Using the value of $E^{1\%}_{540nm} = 5.97\ cm^{-1}$ for haemoglobin hydrate (Li, 1969), the concentration was obtained from the absorption at 540 nm.

One half ml of the stock solution was diluted with about 20 ml distilled water and made up to exactly 100 ml with 0.07 M potassium hydrogen phosphate solution; about 0.2 gm of sodium dithionite was added to reduce the haemoglobin and the solution was saturated with carbon monoxide from a bench cylinder. The optical absorption spectrum was determined at once and the concentration calculated by dividing the optical density at 540nm wavelength by 8.03 (Perutz, 1968).

Both of these determinations gave the concentration of the stock solution as 6.06%; assuming a molecular weight of 65000 this is about 1 mM.

In general, various haemoglobin complexes were examined as follows. For transmission measurements, the stock solution was diluted 1:100 and 5 ml added to 5 ml of molar solutions of the desired ligand buffered with concentrated phosphate solutions

to the required value of pH. Absorption measurements were made on the stock solution directly diluted with molar solutions of ligands. All absorption spectra were obtained using a Perkin-Elmer-Hitachi EPR3 spectrophotometer with appropriately buffered ligand solutions as reference samples.

3.3.1. Monobasic acid derivatives of haemoglobin.

Molar solutions of sodium formate, sodium acetate, sodium propionate, and sodium n-butyrate were prepared from the BDH Analar range; An approximately 0·1 M solution of potassium iso-butyrate was prepared by titrating iso-butyric acid with potassium hydroxide.

Transmission and absorption spectra were obtained for all these derivatives; all the spectra exhibited the conventional shift of the Soret band with pH and both the charge transfer D and E bands and the alpha and beta bands were present. The extinction coefficients of these derivatives are given in Table 3.1 for a pH value 8.0; the absorption spectra are shown in Fig. 3.0 at the same pH.

Examination of the variation in transmission with pH reveals the following points:

(a) there is a Soret band movement to longer wavelengths with increasing pH; this indicates an increase in the proportion of the low spin component present. A significant contribution may be due to successful OH^- competition with the desired ligand at large pH values.

(b) the absorption in the D charge transfer band at 635 nm shows a gradual decrease with rising pH except for the n-butyrate which shows an unusual minimum at pH 9.5: a gradual decrease of absorption in this band indicates an increasing

Table 3.0.

Extinction coefficients, $E^{1\%}_{1\ cm}$

Derivative / Band	Formate	Acetate	Propionate	iso-butyrate	n-butyrate
D	4.2	3.1	3.7	4.1	4.4
alpha	6.0	5.7	6.6	6.2	7.5
beta	6.8	7.0	8.0	8.3	9.1
E	7.0	7.5	8.2	8.8	9.4

proportion of low spin state population (Fig. 3.1).

(c) changes in transmission in the alpha and beta bands were smaller than in the D and E bands and the data is not so reliable but the n-butyrate clearly displays different behaviour from the other haemoglobin derivatives, that is, a decrease in transmission with increasing pH indicating the formation of a low spin state or its increasing preponderance. Between pH 7.5 and pH 9.5, the other derivatives show a decrease in transmission which takes an upward turn beyond pH 9.5; these trends are exhibited in both the alpha and beta bands. In the case of the acetate, propionate and iso-butyrate, they may suggest the presence of more low spin. The formate does not display this behaviour to the same extent and this may indicate that it has a greater propensity to remain in the high spin state (Fig.3.2).

(d) a graph of the difference between transmissions in the D and alpha bands is shown in Fig. 3.3; the interpretation of such difference spectra requires care since band movements may blur the graph. All error bars were doubled for this graph. What is to be seen is a quite definite increase in differential transmission of D over alpha with rising pH. The increase in differential transmission with pH starts between pH 7.5 and 8.5 except for the n-butyrate when it starts at pH 9.5. The graph suggests an overall rise in low spin component for all derivatives.

(e) the intensity of the E band at about 480 nm is thought to depend on the Soret band intensity (about 410 nm) since mixing may occur; a plot of the Soret band wavelength with transmission in the E band shows that E transmission increases as the Soret band moves to longer wavelengths (with rising pH) although this trend is strangely reversed for the n-butyrate.

TRANSMISSION IN THE D BAND WITH pH. Fig. 3.1

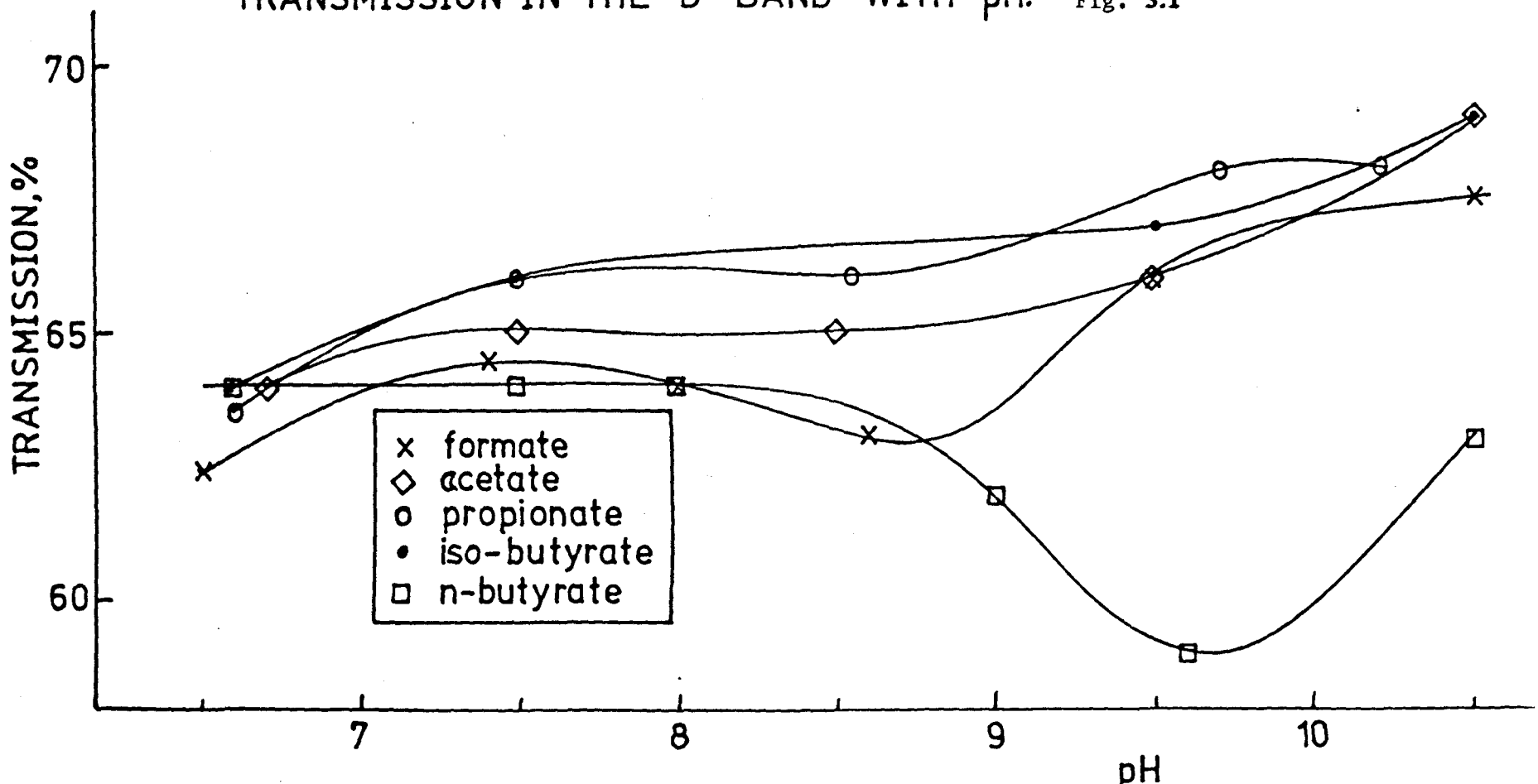

In considering what conclusions may be drawn from these results one should bear in mind that the alpha and beta bands may coincide with minor high spin bands as noted in 3.5.3.1. The movement of the Soret band and the decrease in absorption in the D band with rising pH indicate an increasing preponderance of low spin state component. In support of this, one notes that the differential transmission in the D and alpha bands increases with pH and that, omitting interpretation of the middle pH range, the alpha and beta bands show a decrease in transmission at large pH.

These remarks may be complicated by the following factors:

(a) competition between the desired ligand and OH^- ions may occur at large pH.

(b) the upswing in transmission in the alpha and beta bands at pH values greater than 9.5 for the acetate, propionate, and isobutyrate may suggest the formation of high spin haem complexes dissociated from the globin.

(c) it has been assumed that all bands occur at the same respective wavelengths in all derivatives; this is not strictly the case and a full lineshape analysis would be necessary for a complete appreciation.

(d) most important of all, the general move to low spin is not shared by the n-butyrate; in the beta and alpha bands, the n-butyrate shows a pronounced move to low spin with increasing pH but at pH 9.6 there is a repeatable peak in the transmission; this is matched by a fall in transmission in the D band at pH 9.6. The E band may indicate a similar effect but this could be a Soret band effect. The conclusion to be drawn is that as the pH increases, a high spin n-butyrate complex is formed. This is not at all similar to the other derivatives and is made more unusual by the succeeding move to low spin. This may be

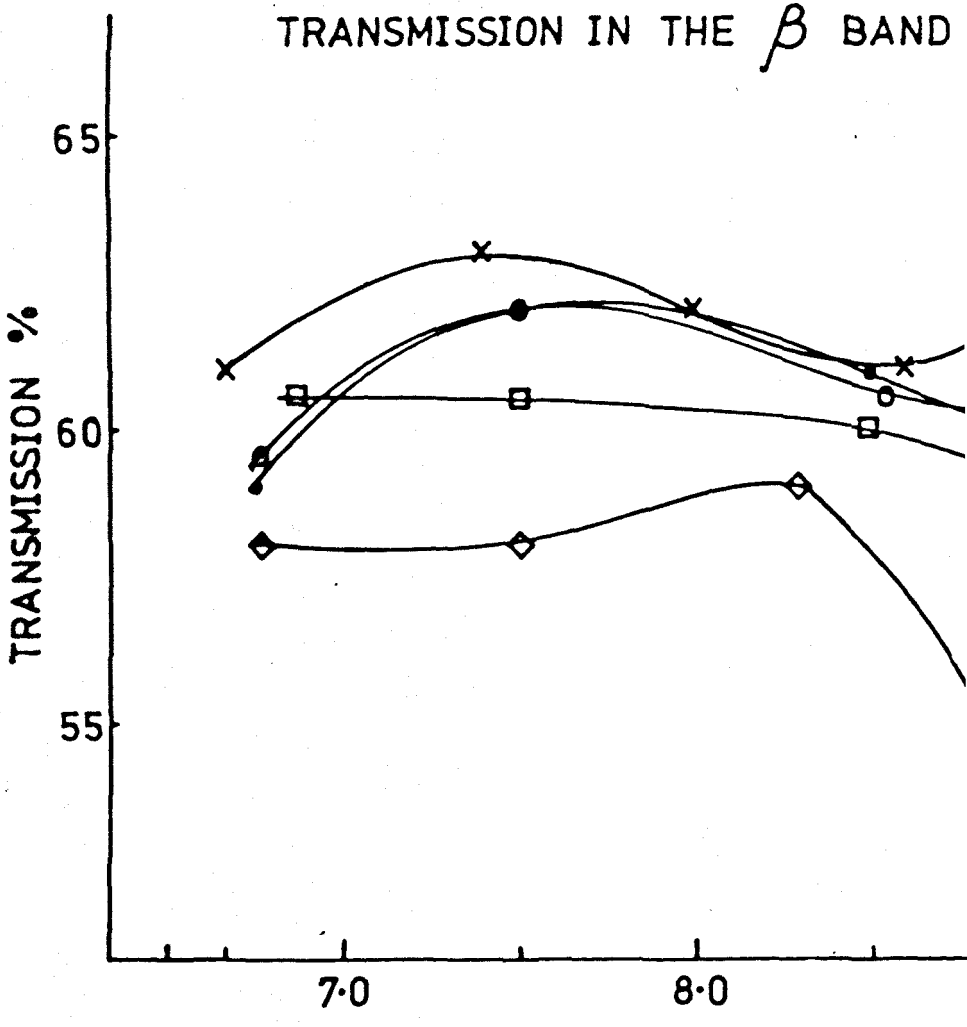
TRANSMISSION IN THE β BAND
TRANSMISSION %
65
60
55
7·0
8·0

AGAINST pH. Fig.3.2

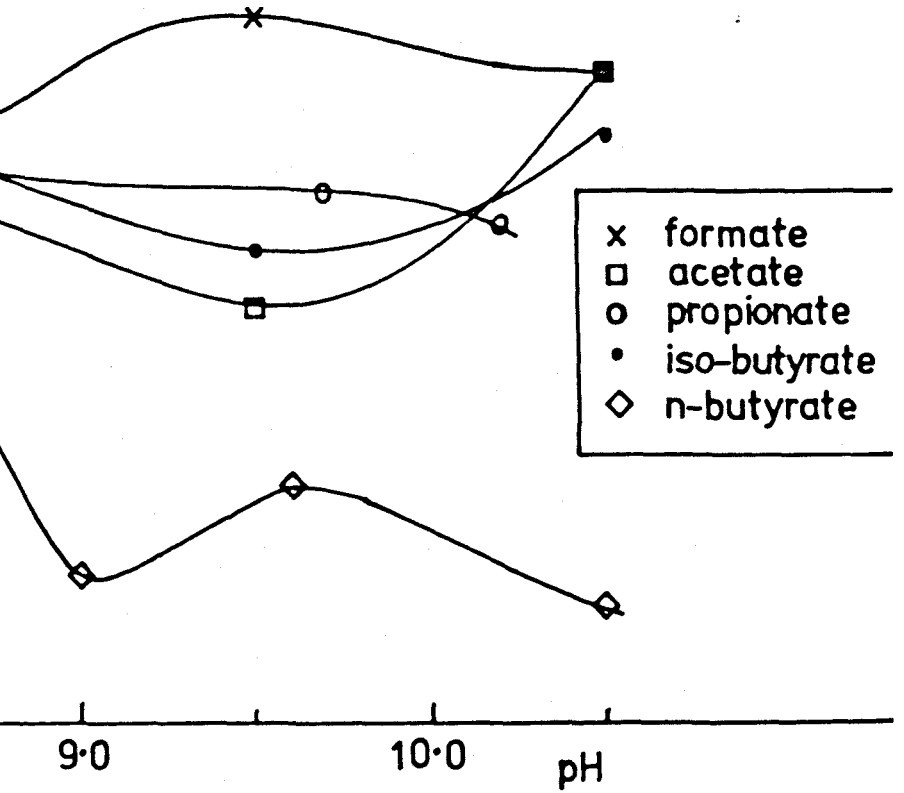

caused by the formation of a denatured haemoglobin derivative ligated with n-butyrate which then rapidly changes to the low spin hydroxide as the pH is further increased.

It is tentatively suggested that the reason for the different behaviour of the n-butyrate is due to steric hindrance; the sizes of the monobasic acid ligands are shown below, together with the sizes of ethyl iso-cyanide and tert-butyl-isocyanide. The sizes were determined by measurements on a space filling model to $\pm 0{\cdot}1$ Å. (The size is defined as the distance from the oxygen ion of the carboxyl group to the furthest atom of the ligand.)

Formate	$H - COO^-$	2.4 Å
Acetate	$CH_3 - COO^-$	2.7 Å
Propionate	$CH_3 - CH_2 - COO^-$	3.3 Å
n-Butyrate	$CH_3 - CH_2 - CH_2 - COO^-$	3.9 Å
iso-Butyrate	$CH_3 - CH(CH_3) - COO^-$	3.3 Å
ethyl iso-cyanide	$CH_3 - CH_2 - CH_2 - COO^-$	3.7 Å
tert-butyl isocyanide	$CH_3 - CH_2 - NC$	5.2 Å

From the electron density maps of haemoglobin (Perutz, 1968) it appears that the maximum linear molecule which can gain admission to the haem pocket is about 4 Å long. The difference in the structural formulae of the two butyrate isomers would mean that the n-butyrate - the longer ligand - would have greater difficulty entering the pocket to bind to the iron than the smaller iso-butyrate. It is apparent from this that an attempt to ligate the anions of the next largest monobasic acid, valeric acid, would fail despite the existence of four

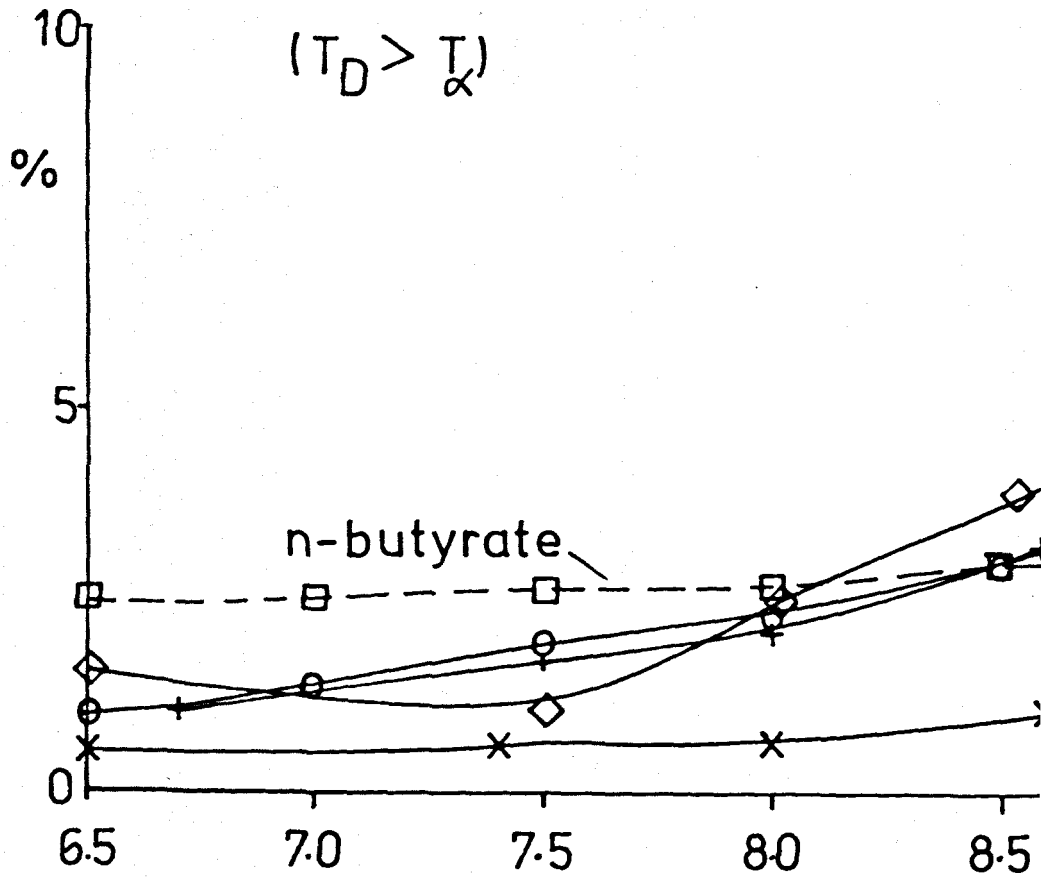
DIFFERENTIAL TRANSMISSION IN D
(T_D > T_α)
10
%
5
0
n-butyrate
6.5
7.0
7.5
8.0
8.5

AND ALPHA BANDS Fig. 3.3.

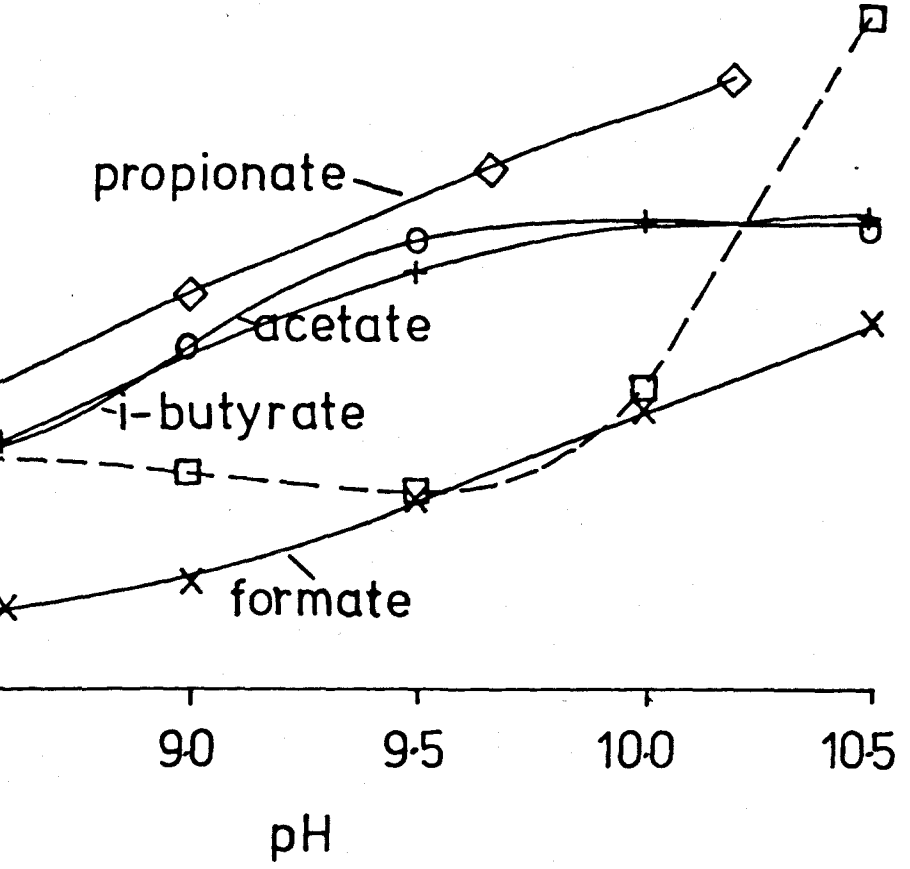

isomers.

The unusual behaviour of the n-butyrate when compared with the other radicals in this series in its optical absorption spectra suggests that it is not bound in the usual manner.

A similar effect has been observed in the case of ethyl iso-cyanide and tert-butyl-iso-cyanide (Nobbs, 1966). It was found that ethyl isocyanide binds to the iron of the haem but that tert-butyl-iso-cyanide does not (Nobbs, 1966b). That groups as large as ethyl-isocyanide and the iso-butyrate may be diffused into the protein molecule and occupy the sixth ligand site at the haem is initially suprising but it is likely to be due to the ability of the distal histidine residue to rotate, this being permitted by the relatively large distances involved in its van der Waals bonding to other residues (4.9, 6.2 Å). A similar rotation of the distal histidine to permit binding of the azide radical has been deduced to occur from the EPR spectrum (Helcke, 1968).

It is therefore suggested that the iso-butyrate radical is similar to the ethyl isocyanide molecule in that it is sufficiently compact to enter the haem pocket and bind but that the n-butyrate and tert-butyl-isocyanide are too large to do this.

It has been suggested that the wavelength separation of the alpha and beta bands is dependent upon the actual ligand in the sixth coordination position at the haem (Braterman, 1964). One may compute the following wavelength differences for the monobasic acid derivatives at pH 8.5

Formate	40 nm
Acetate	35 nm
Propionate	40 nm
iso-Butyrate	30 nm
n-Butyrate	33 nm

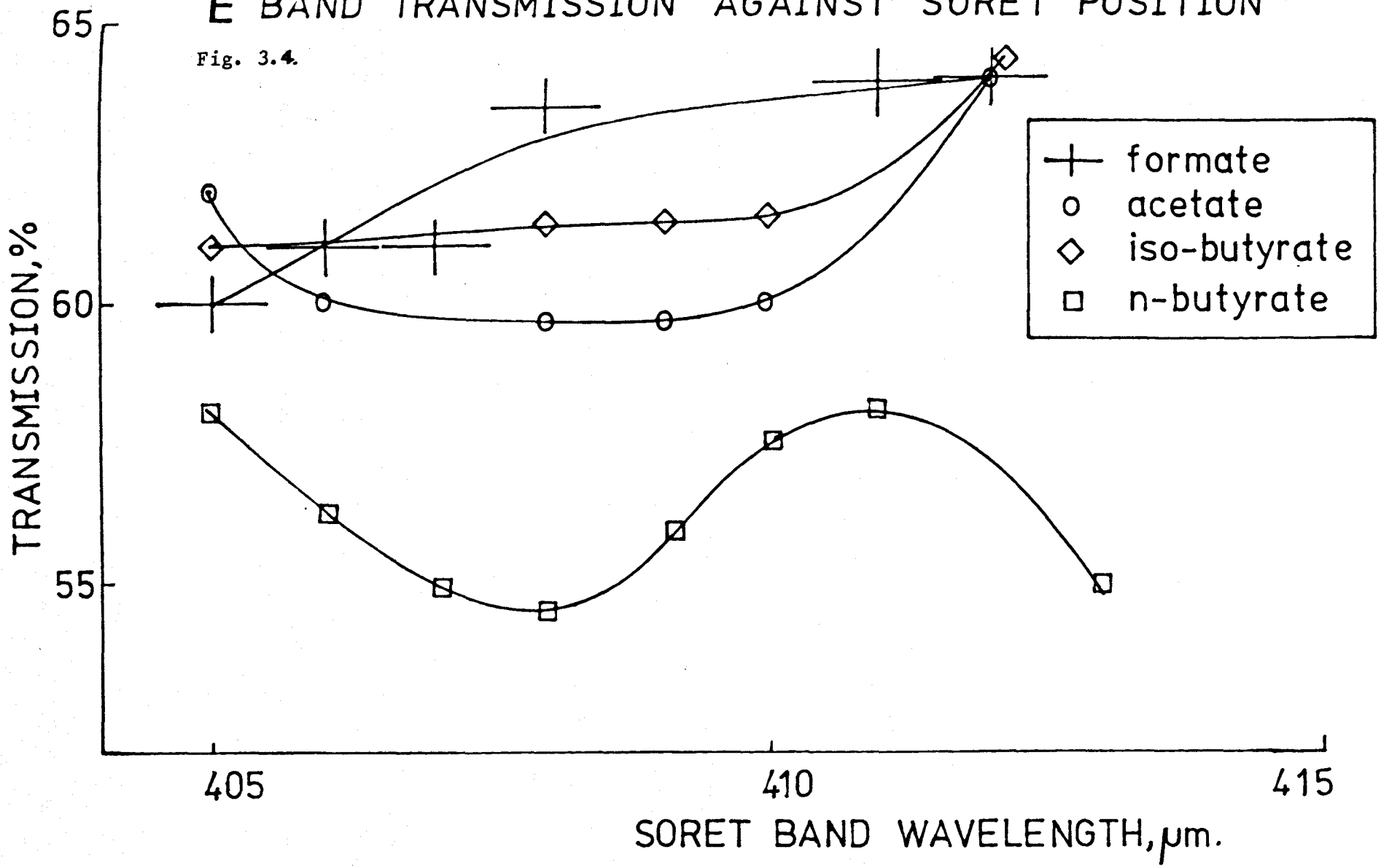
E BAND TRANSMISSION AGAINST SORET POSITION
Fig. 3.4.
65
60
55
TRANSMISSION,%
formate
acetate
iso-butyrate
n-butyrate
405
410
415
SORET BAND WAVELENGTH, μm.

ABSORPTION IN THE MONOBASIC ACID DERIVATIVES. Fig. 3.4a.

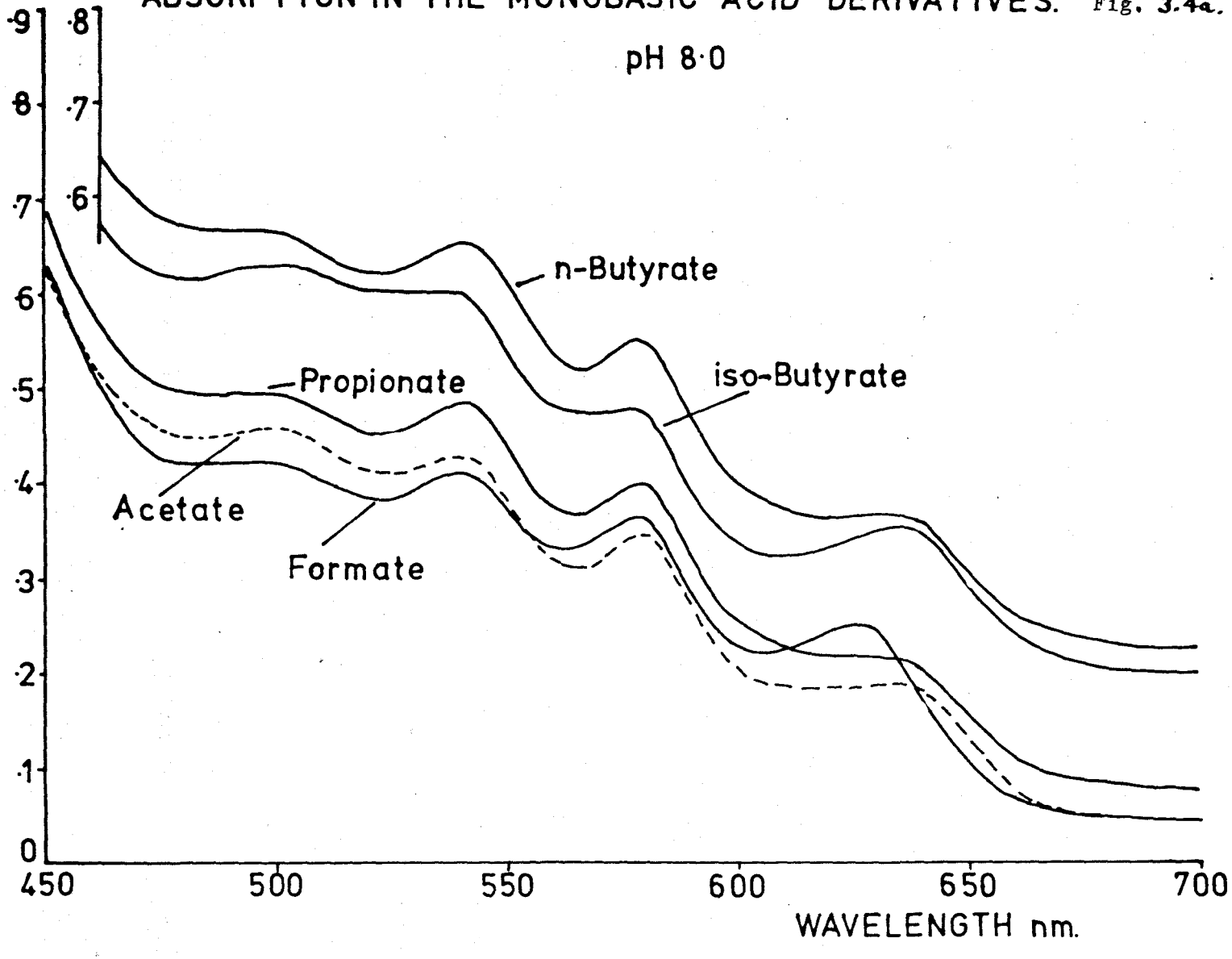

It has been suggested that, for ferrous haem complexes, the wavelength separation is greater for high spin than low spin complexes. Supposing that this were the case for ferric complexes, one might tentatively bracket the formate and propionate as predominantly high spin and the iso-butyrate as low spin at room temperature. It has been reported that myoglobin formate comprises two high spin forms (Farrow, 1971). Magnetic susceptibility results indicate that the formate and the acetate are essentially high spin at room temperature (Schoffa, 1964). This means that the acetate is slightly anomalous since the wavelength separation of the alpha and beta bands is not so great as for the formate. It might be possible that OH^- competition occurs more readily in the presence of the acetate ligand - this would lead to a smaller wavelength difference but would not contradict the magnetic susceptibility result obtained at pH 6.84.

3.3.2. Halide derivatives, F^-, Br^-, Cl^-.

Solutions of sodium fluoride and chloride and potassium bromide were made up in molar concentrations and buffered to desired pH values using phosphate buffer. They were added to the haemoglobin solution as described in 3.2.3. and permitted to incubate at room temperature for about thirty minutes, after which the transmission and absorption spectra were measured.

3.3.2.1. Fluoride.

The transmission spectrum of haemoglobin fluoride is reproduced in Fig. 3.5 over the pH range 5.8 to 10.5 where it may be noted that the Soret band occurs at 402 nm and 412 nm at the extremes of pH.

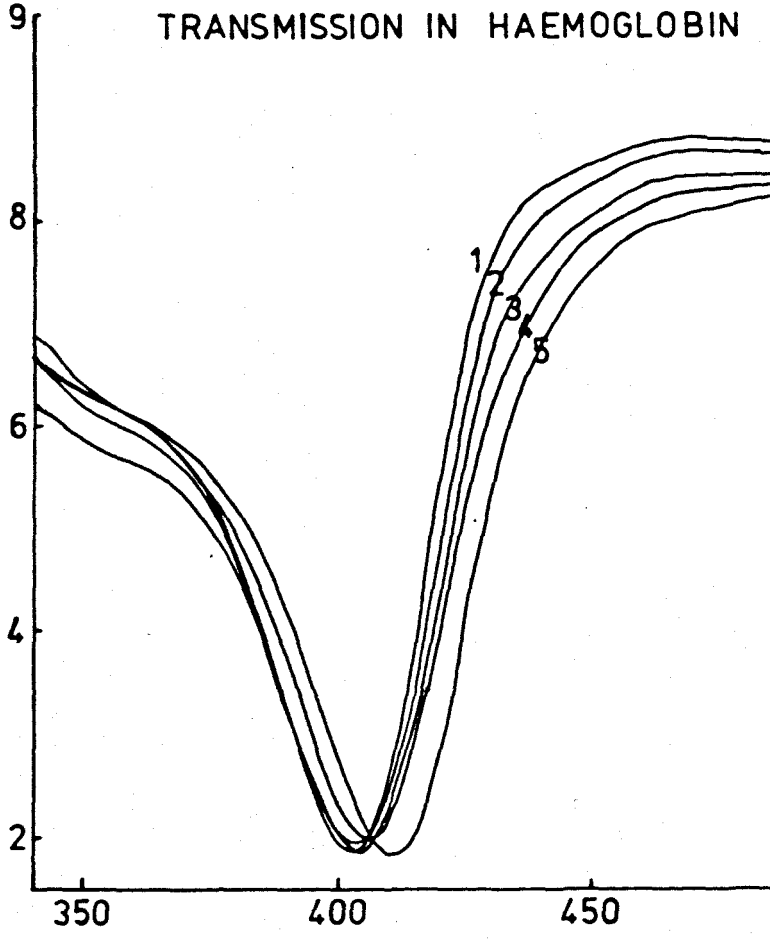
TRANSMISSION IN HAEMOGLOBIN
9
8
6
4
2
1
2
3
5
350
400
450

FLUORIDE. Fig. 3.5

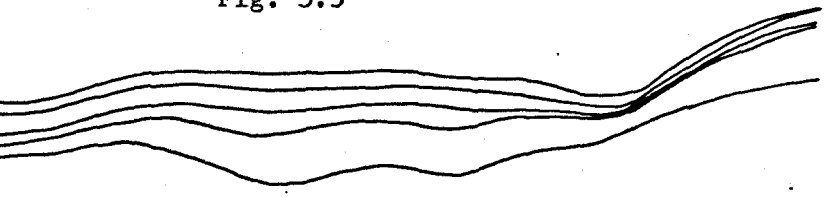

	pH
1	5·8
2	6·5
3	7·5
4	8·5
5	9·5

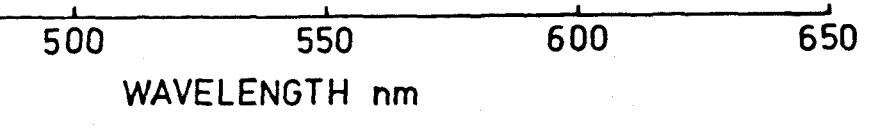

It is well known that the fluoride is an almost solely high spin state derivative so that changes in the optical spectrum with pH must be presumed due to successful OH^- competition with the F^- in the bonding process. This is, in part, substantiated by the movement of the Soret band to 412 nm at pH 10.5 which coincides with the wavelength obtained for the hydroxide at the same pH.

3.3.2.2. Bromide and Chloride.

The optical spectra of mixtures of haemoglobin and sodium chloride or potassium bromide solutions displayed the same properties as those of the haemoglobin alone as the pH was varied and it is thus deduced that neither of these anions binds at the haem. Construction of a simple space filling model of the haem plane indicated that the fluoride ion would sit quite neatly into the sixth coordination position but that the larger halide ions would be compelled to take up positions at greater distances from the iron ion.

3.4.1.1. Cyanate and thiocyanate.

Myoglobin cyanate has been prepared and the temperature dependence of magnetic susceptibility determined down to $77^{\circ}K$ (Iizuka, 1969); it was found that this derivative was comprised of two components I and II. It was suggested that II is probably denatured and entirely in the low spin state and that MbOCN(I) is a thermal equilibrium mixture of spin states with a high spin ground state. Myoglobin thiocyanate was found to be almost completely insoluble. The magnetic susceptibilities of myoglobin and haemoglobin (horse) cyanates and thiocyanates have been determined (Schoffa, 1964).

Human haemoglobin cyanate and thiocyanate were prepared by incubating haemoglobin solution with solutions of sodium cyanate and thiocyanate, buffered to desired pH values. In each case the ligand was present in at least eight times molar excess. There was no evidence of precipitation in either case; both mixtures were centrifuged and no residue was seen. In the case of the thiocyanate it was noted that the brown colour of the haemoglobin became a wine red during the preparation.

The binding of the cyanate to haemoglobin is rather more complicated than to myoglobin. Haemoglobin, as noted in chapter two, contains terminal amino groups and sulphydryl groups. It has been demonstrated that cyanate binds to both these groups according to the equation (Stark, 1963, 1965, Smith, 1967)

$$R - NH_2 \quad + \quad HCNO \quad = \quad R - NH.CONH_2$$

It is not clear whether the thiocyanate binds in a similar fashion; clearly, the cyanate will attache itself to the peptide chain at several places and also probably at the haem.

3.4.1.2. Cyanate.

The optical absorption spectrum of haemoglobin cyanate for a range of pH between 5.8 and 10.5 is depicted in Fig. 3.6. It will be observed that the Soret band moves only 1 nm in wavelength over the entire pH range whereas in haemoglobin hydrate the Soret shift is 8 nm between pH 6.5 and 10.5. The extinction coefficients at pH 7.8 are:

632 nm	(D)	$E^{1\%}_{1\ cm}$ 2.3
576 nm	(alpha)	$E^{1\%}_{1\ cm}$ 8.5
542 nm	(beta)	$E^{1\%}_{1\ cm}$ 11.4

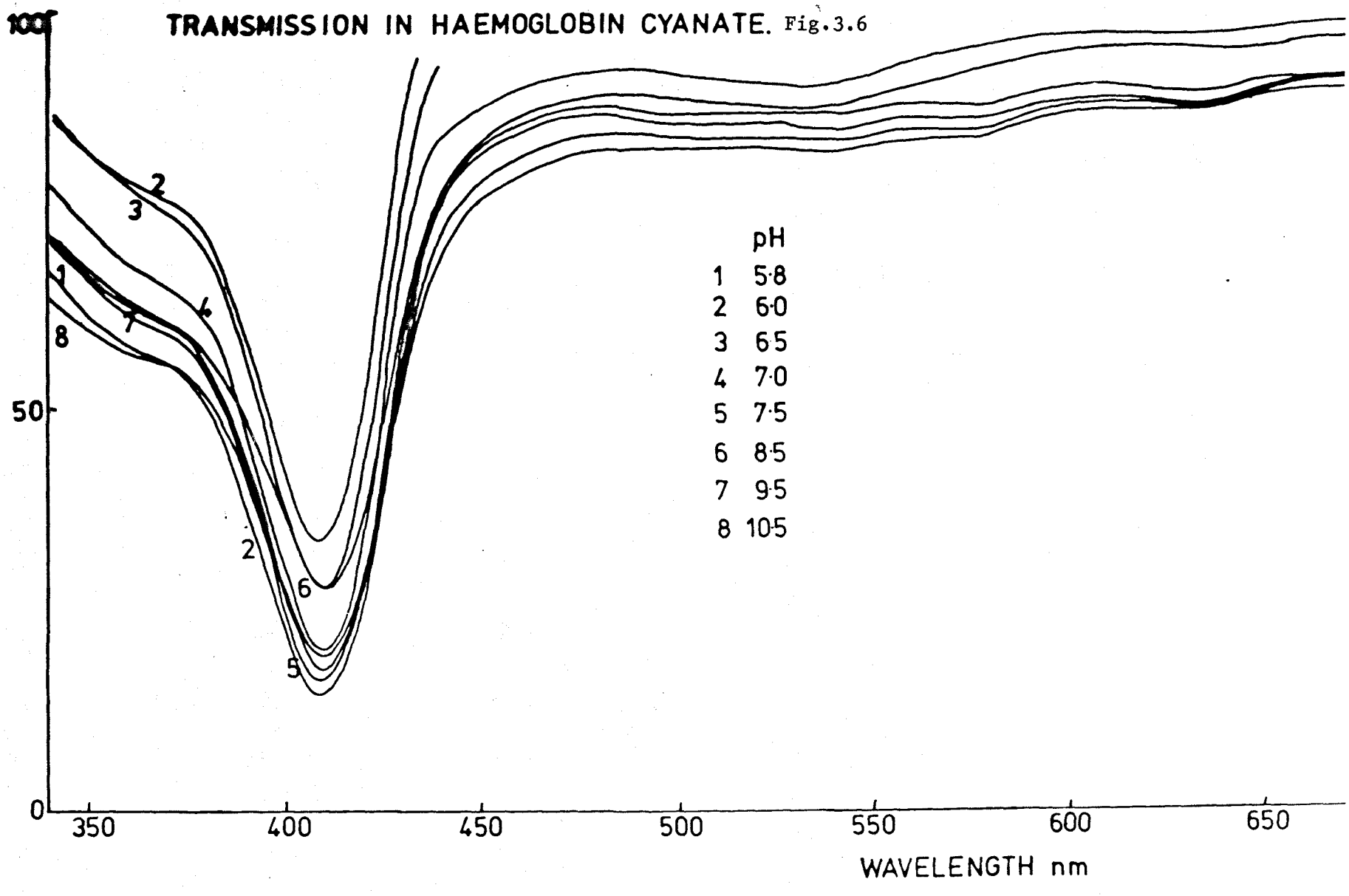
TRANSMISSION IN HAEMOGLOBIN CYANATE. Fig.3.6
100
50
0
350
400
450
500
550
600
650
WAVELENGTH nm
pH
1 5·8
2 6·0
3 6·5
4 7·0
5 7·5
6 8·5
7 9·5
8 10·5

No value is given for the E band because it was not readily discernible. It seems very likely that the binding of the OCN^- ion changes the conformation of the entire molecule such that the binding of OH^- ions at large pH is not possible; further comment on this point is made in the following section.

3.4.1.3. Thiocyanate.

The thiocyanate ion (SCN^-), like cyanide (CN^-) and carbon monoxide (CO) is an ambidentate ligand (Alben, 1968). This means that it contains more than one potential sigma donor site, only one of which is involved in coordination at a given time. The thiocyanate of haemoglobin, of which there has been little study apart from the unpromising result that myoglobin thiocyanate is insoluble (Iizuka, 1969), may bind at either the sulphur or nitrogen terminals; this has been the subject of much study in tetrahedrally and octahedrally coordinated iron complexes (Forster, 1965) and in other transition metal ion complexes (Norbury, 1970).

The mode of coordination may often be discovered for a particular complex by using infrared spectroscopy, in particular, by examining the shifts of the CN and CS stretching frequencies and the NCS flexing frequency from their values for the free ion (Larsson, 1969). The actual mode of bonding of the thiocyanate ion from metal to metal depends upon its rather equitable electronic charge distribution (Ahrland, 1958) but the preferred mode in a given case will be determined by the nature of the acceptor site. The bonding mode may be correlated with the presence of a properly orientated pair of electrons on the acceptor atom. The equity between the N and S terminals means that bonding is very susceptible to small changes in the acceptor; in this context, the thiocyanate ligand could be used as a sensitive probe

into the electronic properties of the haem iron in the protein environment.

The infrared transmission properties of haemproteins and similar compounds have been previously investigated with a view to obtaining information about the binding of small ligands (McCoy, 1969). Because aqueous solutions are very strongly absorptive in the infrared, it was initially necessary to use haemoglobin thiocyanate in suspension in Nujol (liquid paraffin) between discs of sodium chloride and also pressed into discs of potassium bromide, using a hydraulic press at a pressure of about 30,000 p.s.i.

To enable measurements to be made of an aqueous solution, a cell of calcium fluoride was constructed. Discs of CaF_2 were sawn off a one inch diameter rod of the material and ground to a thickness of 1 mm. The discs were separated by an aluminium shimstock spacer of 0.025 mm thickness containing a one centimetre diameter hole into which the sample protein solution could be introduced; the discs and spacer were clipped together to form the absorption cell. Calcium fluoride is possessed of good transmissive properties between 4000 cm^{-1} and 880 cm^{-1} and it was thus possible to examine the CN frequency. A more suitable cell could be constructed from silver bromide which has a cut-off at 400 cm^{-1} and is also insoluble in water. This would enable measurements to be made on the NCS and CS frequencies although the water absorption bands may cause difficulty at the NCS band.

The band positions obtained from these measurements are tabulated in Table 3.2., together with the characteristics of the Perkin-Elmer 337 spectrophotometer used. The transmission of the thiocyanate in KBr is shown in Fig. 3.7.

It will be seen from the table that the frequencies of the CN, CS, and NCS stretching and flexing oscillations are the same

Table 3.1.

Infrared absorption bands in haemoglobin thiocyanate.

	Wavenumber, cm^{-1}		
	CN	CS	NCS
Dispersed in KBr discs			
$Hb(SCN^-)$	2065	740	465
NaSCN	2070	742	465
HbH_2O	2055	-	-
Suspended in Nujol between NaCl discs*			
$Hb(SCN^-)$	2065	720	-
NaSCN	2060	720	-
HbH_2O	2060	720	-
In aqueous solution between CaF_2 discs**			
$Hb(SCN^-)$	2065	-	-
NaSCN	2068	-	-

Notes.

* The absorption of NaCl is considerable beyond 500 cm^{-1}

** The absorption of CaF_2 increases sharply at about 1300 cm^{-1}

Perkin-Elmer 337: Accuracy $\pm$ 1.9 cm^{-1}

Reproducibility $\pm$ 1.3 cm^{-1}

Resolution $\pm$ 5 cm^{-1}

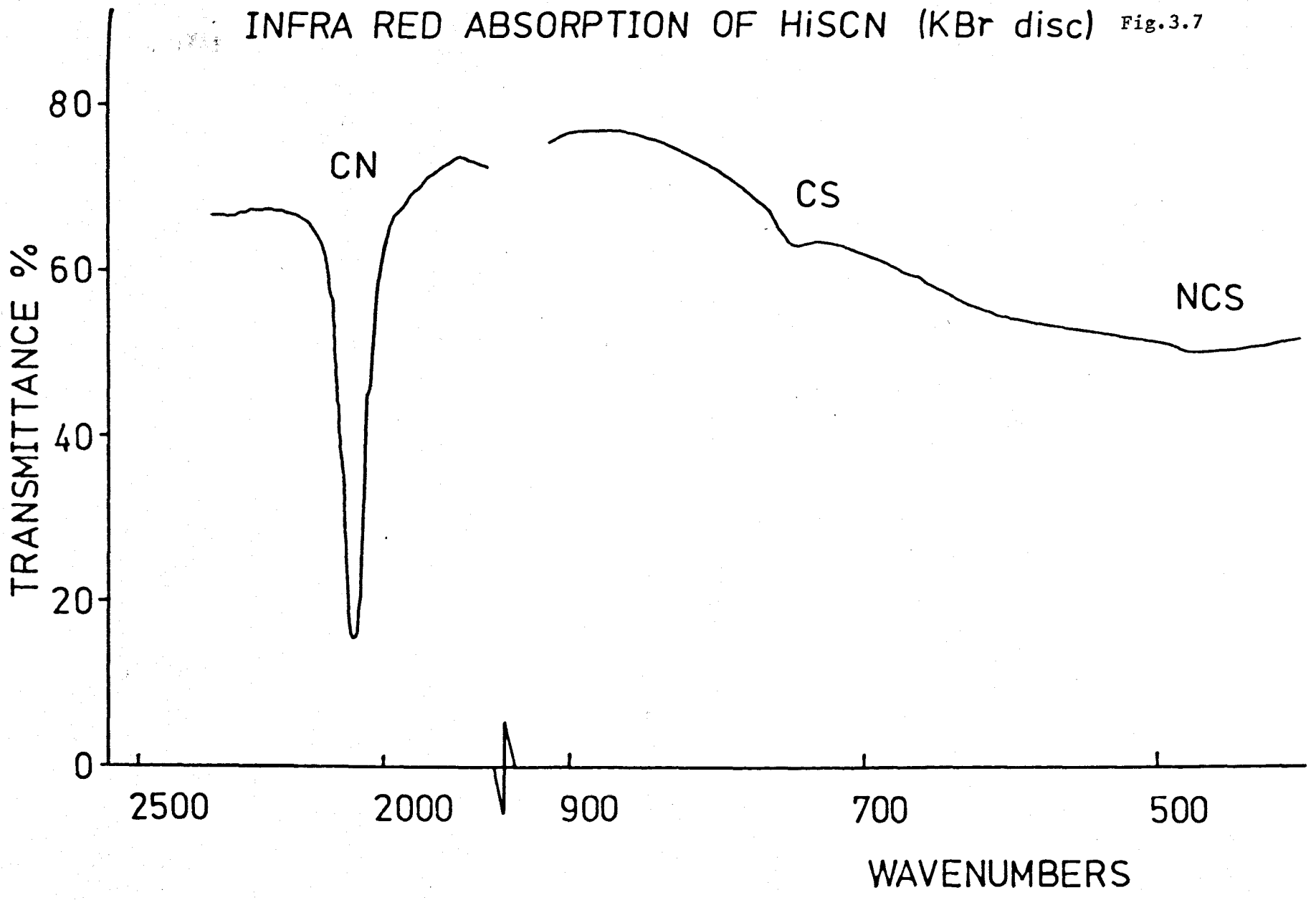
INFRA RED ABSORPTION OF HiSCN (KBr disc) Fig.3.7
80
60
40
20
0
TRANSMITTANCE %
CN
CS
NCS
2500
2000
900
700
500
WAVENUMBERS

in the NaSCN sample used and in the HbSCN. The spectral lines of the haemoglobin hydrate sample are also tabulated and it is seen that there are lines at the CN and CS frequencies; this is to be expected since the haem plane contains CN bound to the iron and CS is present in the amino acid residues cysteine and methionine.

Within the limitations of the infrared spectrophotometer it may be deduced that the SCN^- bound to haemoglobin is predominantly bound in the same mode as in NaSCN, that is, via the sulphur terminal.

Upon adding sodium thiocyanate solution to haemoglobin at pH 6.0, the colour changed from brown to a distinct red. This latter colour could be either due to the presence of oxyhaemoglobin after reduction of the ferric ions to ferrous or to the characteristic colour of ferric ions in combination with SCN^-; the distinctive red colour of $Fe^{3+}(SCN^-)_2$ is often used as a sensitive test for SCN^-. The former possibility is unlikely since thiocyanates are not reducing agents; however, it may be possible for the binding of the SCN^- ion to the peptide chain NH_2 termini to result in a conformational change resulting in a change of spin state of the iron.

Examination of the thiocyanate at 9 GHz and 35 GHz using EPR spectroscopy revealed no $g = 6$ signal (nor any other signal) although a $g = 6$ signal was clearly observed for an acid met haemoglobin solution of the same concentration. It could be argued that this means that the iron was in the ferrous low spin state ($S = 0$) as HbO_2 or that the hypothetical attachment of SCN^- at the peptide chain brings about conformational changes resulting in a change in the spin lattice relaxation time.

Comparison of the optical absorption spectra for the OCN^-

and SCN^- derivatives of haemoglobin shows that considerable similarity exists (Fig. 3.8). It is interesting to note that the ratios of absorptions in the beta and D bands for these derivatives at pH 7.8 are

$HbOCN^-$	5.1
$HbSCN^-$	2.5

suggesting that at room temperature the ratio of high spin to low spin states in the cyanate is less than in the thiocyanate. The Soret band positions at pH 7.5 are

$HbOCN^-$	409.5 nm
$HbSCN^-$	410.5 nm
HbH_2O	405.0 nm

indicating a substantial proportion of low spin population at room temperature.

The room temperature magnetic susceptibility of $HbSCN^-$ has been measured as $\mu_{eff} = 5.06$ at pH 6.6 (compared with 4.66 for $HbOH^-$ at pH 9.7 and 5.40 for HbOCN at pH 7.6). No measurements appear to have been made for human HbSCN: the above values refer to horse haemoglobin. (Schoffa, 1964). The value for HbSCN is intermediate and suggests that HbSCN (like HbOCN and HbOH) may be a thermal mixture of spin states with a substantial low spin component at room temperature. However, as has been stated, no EPR signals were observed from HbSCN at 77°K; at the present time this may be ascribed to a short spin lattice relaxation time brought about by conformational changes initiated by binding of SCN^- ions to the peptide chains.

It is suggested that investigation might be made of the SCN^- ligand using neutron diffraction; various cyanides have been investigated using this approach (Curry, 1968, Fenn, 1970). There

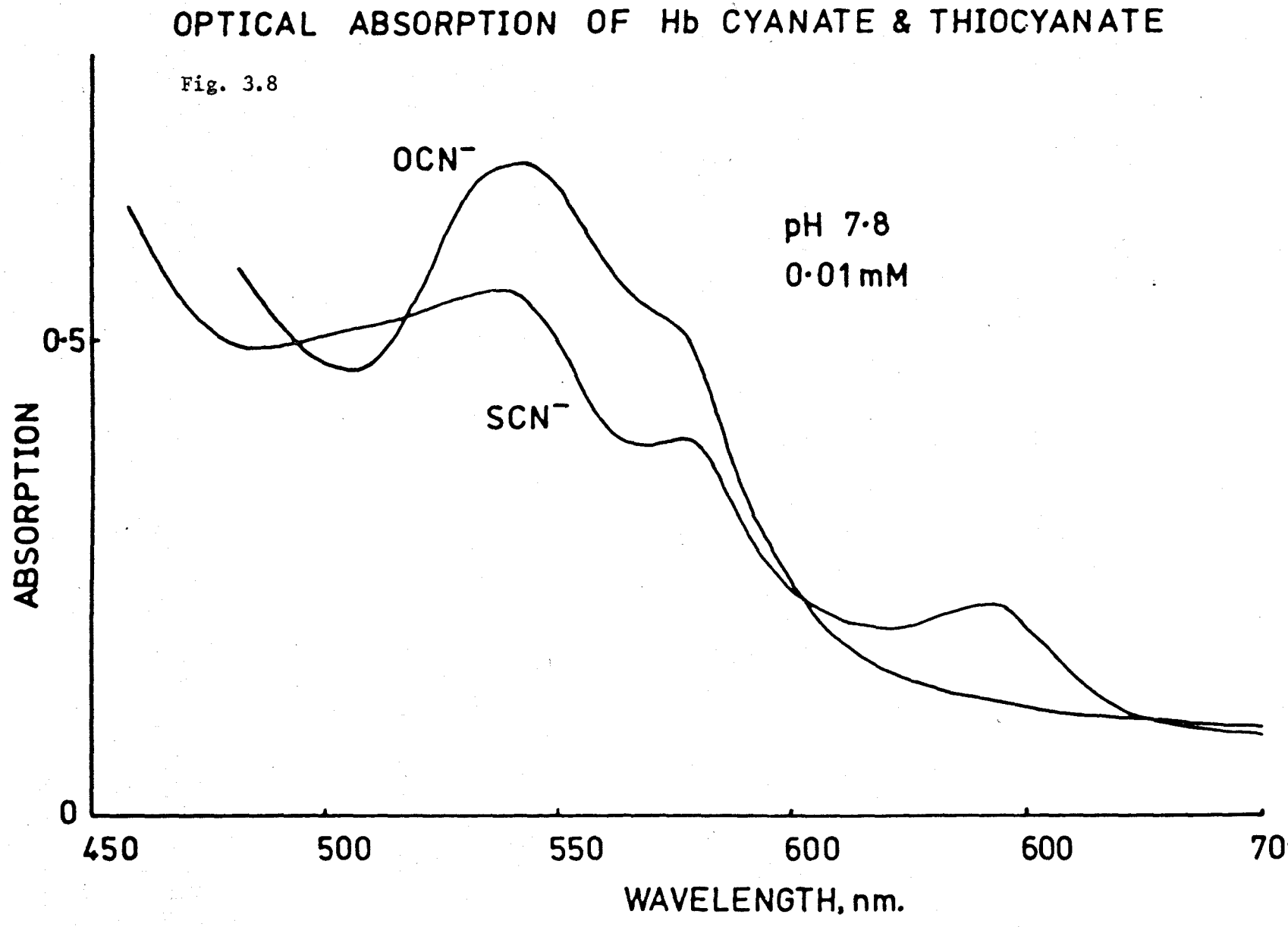
OPTICAL ABSORPTION OF Hb CYANATE & THIOCYANATE
Fig. 3.8
OCN⁻
SCN⁻
pH 7·8
0·01mM
ABSORPTION
0·5
0
450
500
550
600
600
70
WAVELENGTH, nm.

are significant differences in the neutron scattering for nitrogen, carbon and sulphur atoms. A reduction in the incoherent scattering background radiation in the haemoglobin could be perhaps achieved using deuterium substitution (Hodgkin, 1970).

3.4.2. Summary.

Solutions of various haemoglobin derivatives have been prepared from fresh human red cells. The quantity of haemoglobin in the samples was determined spectrophotometrically.

Investigation of the monobasic organic acid derivatives of haemoglobin revealed that the n-butyrate possessed rather different optical absorption properties from its isomer, iso-butyrate, and from the smaller preceding acid radicals in the series: formate, acetate, propionate. It is suggested that the linear dimension of the n-butyrate radical is too large for it to fit into the haem pocket. This may be analogous to the inability of tert-butyl-isocyanide to bind at the haem.

The absorption spectra of the fluoride has been obtained over a range of pH. It is thought that neither Cl^- nor Br^- bind at the haem plane.

The cyanate and thiocyanate derivatives have been compared. The optical absorption spectra are rather different. By the use of infrared spectrophotometry the mode of attachment of the SCN^- ion has been investigated; it is believed that this ion is bound via the sulphur atom. There exists also the possibility that the SCN^- ion may be bound to the peptide chains; it is suggested that there has been a change in the spin lattice relaxation time brought about by a conformational change.

3.5. Temperature dependence studies of optical absorption spectra.

3.5.1. Introduction.

As has been previously indicated, the ferric ion situated in a ligand field has either S = 5/2 or S = ½ ground spin states. This is, in its turn, determined by the actual ligand co-ordinated in the sixth co-ordination position. Measurements of the magnetic susceptibility of haemproteins at room temperature (Schoffa, 1964, Scheler, 1956a,b) show that, while there are derivatives which correspond to predominantly high and low spin states, there are also complexes which possess intermediate values of magnetic moment; this led to an initial belief that there might exist protein complexes with intermediate spin state, S = 3/2. This idea has been substantially discounted by Griffith who showed that in axially distorted octahedral symmetry the $^4T_1$ state (S = 3/2) can never be the ground state (Griffith, 1964). It has also been suggested that derivatives with intermediate values of magnetic susceptibility are either chemical mixtures or thermal equilibrium mixtures of high and low spin complexes (Theorell, 1951, Taube, 1952). Clearly, if the energy difference between the ground state and the first excited state is comparable with kT at room temperature then the two spin states will coexist in thermal equilibrium (Iizuka, 1969).

As will be appreciated from section 3.2. the magnitude of the absorption in the α and β bands and the D and E bands is related to the spin state of the haemprotein. This is made very clear by the relationship known to exist for the intensity of absorption in the β band and the magnetic susceptibility of a derivative, and the wavelength of the Soret band (Smith, 1968, Scheler, 1956b). Remarkably little work has been done on this aspect of the optical absorption spectra of the haemproteins (Conant, 1930).

It has been reported that the absorption spectrum of alkaline ferrihaemoglobin changed to the same form as the acid met haemoglobin hydrate upon cooling to ''liquid air temperatures'', a result obtained under dynamical temperature conditions (Keilin, 1949). Cytochrome-c has been investigated under quasistatic temperature conditions (Yonetani, 1966) and three haemprotein derivatives have been studied optically down to 77°K (Iizuka, 1969a).

Difference spectra between optical absorption in haemoglobin hydroxide samples at 5°C and 35°C demonstrated the presence of a spin state thermal mixture with a low spin ground state (George, 1961). Spectral variations with temperature should correlate with measurements of the magnetic susceptibility at the same temperatures; magnetic susceptibility measurements at low temperatures have been used to typify spin states in various myoglobin derivatives (Iizuka, 1969b).

3.5.2. Experimental details.

The measurements of optical absorption were made in the EPR3 spectrophotometer previously used; cylindrical glass cuvettes were supported in a 3" glass Dewar vessel which was closed with a gastight rubber seal. Nitrogen gas was blown through the Dewar after being cooled in a copper heat exchanger immersed in liquid nitrogen. Cold helium gas was blown through the system by siphoning liquid helium from a storage vessel. The sample compartment of the spectrophotometer was continuously flushed with gas to avoid condensation on the Dewar seal and on the optical windows of the sample chamber. The temperature of the sample was measured using a copper-constantin thermocouple and a Hewlett-Packard digital voltmeter; the reference junction of the thermocouple was situated in melting ice and the device was previously calibrated in freezing

mixtures and liquid nitrogen and liquid helium. In a subsidiary experiment it was found that the temperature difference between the sample and reference cuvettes did not exceed 2°K under static conditions of temperature.

It was previously observed that freezing produced a considerable increase in absorption: this was thought due to optical path increases brought about by multiple internal reflections (Keilin, 1950). In these experiments it was necessary to increase the photomultiplier voltages to provide additional detection sensitivity, resulting in a slightly noisier spectrum but with the desired features quite distinct. The sensitivity was in fact increased by a factor of about ten times.

The measurement of optical absorption at low temperatures is attended by some degree of difficulty owing to problems peculiar to frozen samples. Upon freezing a protein solution to very low temperatures (77°K or below), the water freezes to ice I_h which is the normal hexagonal structured form of ice, and the phase diagram of ice-water shows that only ice I_h is present below 2 kBar pressure between 153°K and 273°K (Zeemansky, 1957). A metastable cubic ice I_c may form when water vapour is deposited onto a surface below about 170°K in temperature and there is a slow transition to ice I_h upon warming above this temperature (Dowell, 1960). If there is any region where ice I_c is the stable polymorph it must be well below 170°K and the transformation from ice I_h to ice I_c would then be effectively prevented by the slow rate of the molecular processes involved at these low temperatures. Accordingly, phase transitions are not expected to obtrude upon the measurements. However, the stresses imposed in the freezing processes cause comminution of the ice crystallites. Several cycles of temperature variation will probably result in a distribution of crystal sizes.

It is also possible that small air bubbles will be trapped in the frozen liquid. Both of these will act as scattering centres. Rayleigh scattering intensity is proportional to the incident intensity, the square of the scattering centre volume, and to the inverse fourth power of the wavelength (Jenkins, 1957). This kind of scattering may be considered as due to the re-radiation of light energy by an electric dipole induced by the oscillating electric field of the incident electromagnetic radiation. If the size of the scattering centre is comparable with the wavelength, the re-radiation field is no longer similar to that due to a simple dipole because, as the size of the scattering centre increases, interference effects occur. This form of scattering is called Mie scattering (Mie, 1908) and the overall result is to increase the path length traversed by some relatively large factor related to the density of scattering centres; this lead to a substantial reduction in transmitted intensity. The total light intensity scattered per unit cross sectional area per second is given by

$$I = \frac{\lambda^2}{2\pi} \sum_{n=1}^{\infty} (2n + 1)(|a_n|^2 + |p_n|^2)$$

for a transparent scattering site, where the functions a_n and p_n are complex functions of r/λ, where r is the radius of the scattering site, and of the refractive index. The above sum has been tabulated by many authors (Johnson, 1947).

The intensity of the scattered light at some angle to the direction of incidence is given by

$$I = \lambda^2 (i_1 + i_2)/8\pi^2 R^2$$

where the angular distribution functions i_1 and i_2 are functions of r/λ, refractive index, and orientation; R is the distance to the scattering site.

Clearly, the efficiency of the scattering is wavelength dependent and the transmitted intensities at longer wavelengths will

differ markedly from those at shorter wavelengths. In Fig. 3.9 is shown the ratio of scattering at wavelengths of 630 nm and 524 nm as a function of the radius of the scattering site (Sratton, 1949); it is clear that a distribution of scattering site radii (in this case, a distribution of ice crystallite sizes) would yield a mean value of this ratio. Lack of data on the intensity distribution around frozen ice samples at various temperatures prevents one from investigating the form of this distribution. It may however be argued that in difference spectrophotometry the scattering effect will be of only minor consequence since it should occur to an equal extent in both the sample and reference cuvettes. Although this may be broadly correct it must be admitted that the presence of the protein solute in the sample cuvette may influence the distribution of the ice crystallite size achieved by temperature cycling; this difference might result in a shift in the peak of the distribution function and also a change in its width, both effects having an effect on the scattering ratio of Fig. 3.9. The contribution of Rayleigh scattering from protein molecules is negligible.

A further problem arises from the deliberate choice of cylindrical cuvettes; because of the high risk of fracture of ordinary rectangular cuvettes on cooling to very low temperatures owing to the stresses imposed by the freezing samples these latter cuvettes were not used. Instead cylindrical glass specimen tubes were matched by trial and error using the spectrophotometer and pairs of tubes selected with transmissions differing by $\pm 2\%$ or less. However, the shape of the tubes means that there is a lens action; path lengths followed by light rays in different parts of the incident beam cross-section are not equal because the light is refracted in the liquid or solid contents. If it is assumed that refraction in the

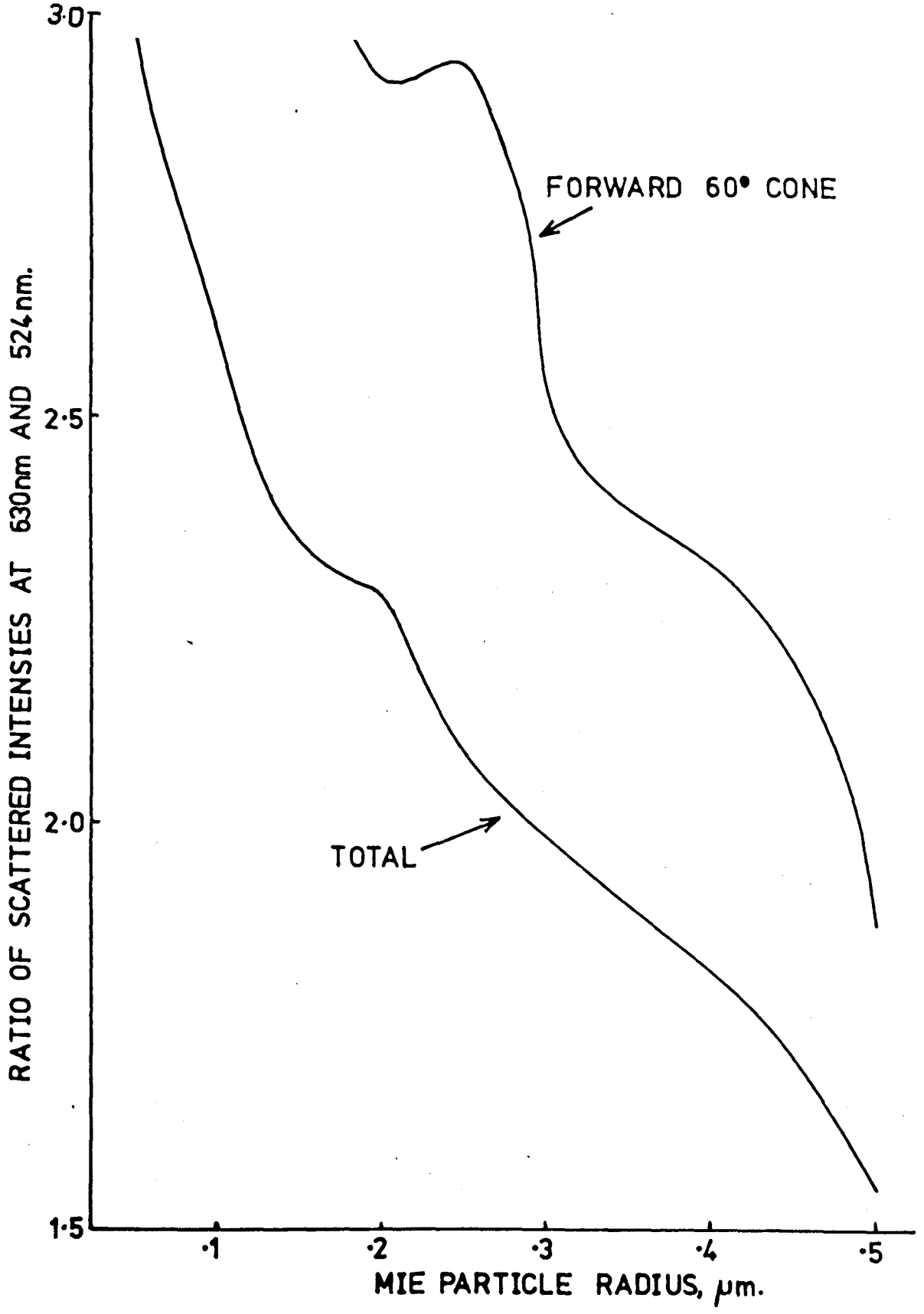
3·0
2·5
2·0
1·5
RATIO OF SCATTERED INTENSIES AT 630nm AND 524nm.
FORWARD 60° CONE
TOTAL
·1
·2
·3
·4
·5
MIE PARTICLE RADIUS, μm.

Fig. 3.9

walls of the tubes is negligible and that the incident beam is restricted in aperture then numerical integration leads to the following tabulation of the apparent absorption coefficient:

A_{actual}	0·1	1·0	2·0
$A_{apparent}$	0·0976	0.975	1.950

for a refractive index of 1·33. This shows that the value of the absorptivity is somewhat reduced and that the error is almost independent of sample concentration (Meehan, 1964). Small differences in refractive index between the contents of sample and reference cuvette will cause small absorption differences.

The cylindrical shape of the cuvettes and the solid nature of the samples may also produce photometric errors. The lens action leads to a spread of light across the window of the detecting photomultiplier tube. Further, unless the opposing faces of the frozen sample are symmetrical and free from strains, the light beam will deviate on passing through the sample and its position on the detecting surface of the photocathode will shift. These effects will vary somewhat from sample to sample but will largely depend for their effect upon the manner in which the photomultiplier responds to off-axis illumination.

3.5.3. Results of low temperature studies.

Using the experimental technique detailed in the previous section, the optical absorption spectra of various derivatives of haemoglobin were obtained over a range of temperature below 273°K; the samples were cycled between room temperatures and low temperatures by controlling the flow of cold gas and various sets of measurements were made as the sample warmed. Generally, it took about ten minutes to cool the sample and about two hours to make measurements on warming.

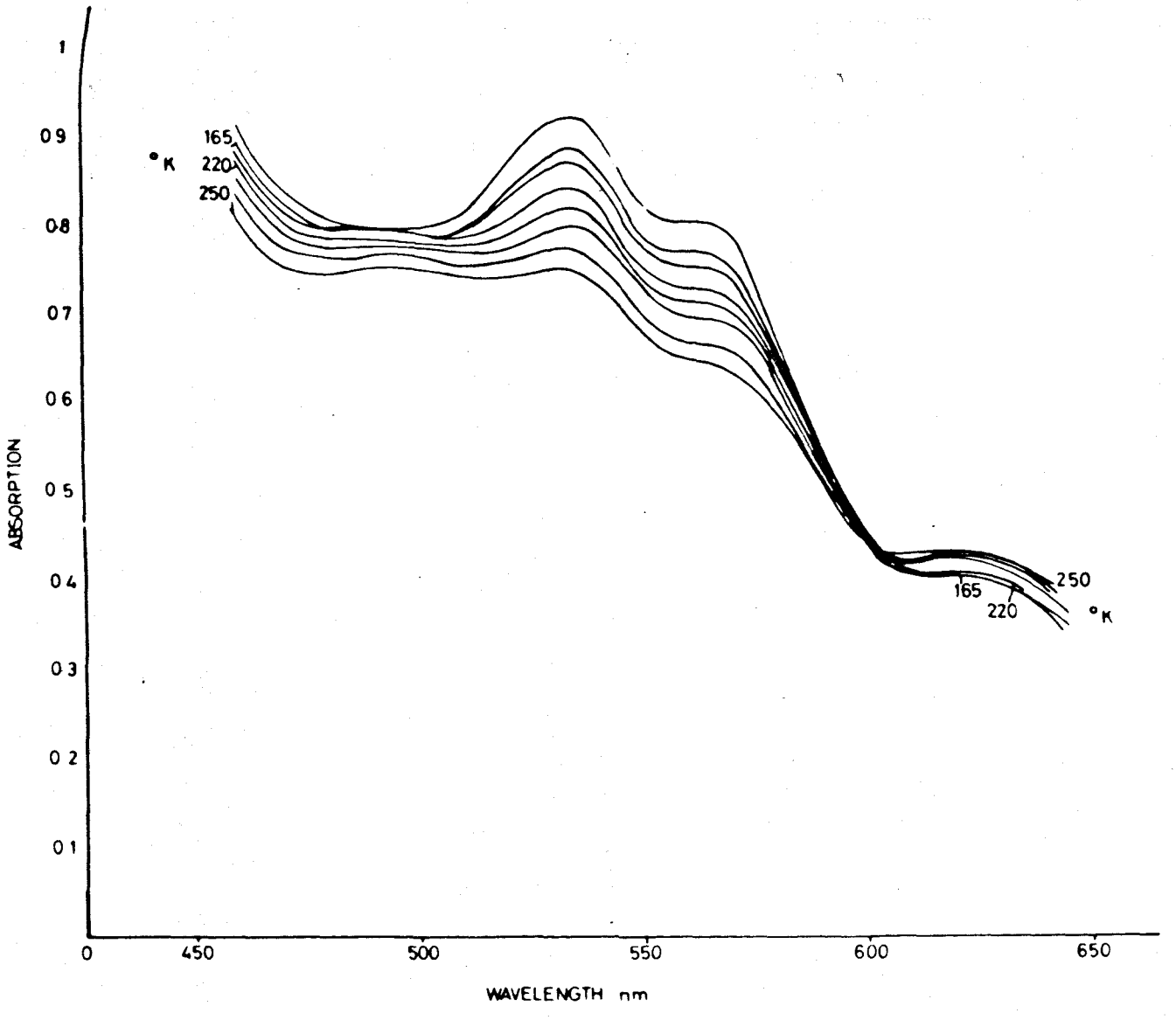

THE OPTICAL ABSORPTION SPECTRUM OF met Hb(H_2O), pH 6.5, WITH TEMPERATURE

Fig. 3.10

3.5.3.1. Haemoglobin hydrate.

The results for this derivative are reproduced in Fig. 3.10 as a series of absorption spectra at various temperatures in the range 131°K to 261°K.

It is at once observable that the absorption increases in the beta band as the temperature falls. There appears to be an isobestic point at 595 nm wavelength and the absorption in the D charge transfer band is increased at higher temperatures. The ratio of absorptions in the beta and D bands is plotted in Fig. 3.11 where it may be seen that this ratio falls with increasing temperature. Measurements with the spectrophotometer in the transmission mode (i.e., without the use of the electrical analogue circuits required to obtain absorption scales) showed that the ratio of transmissions in the beta and D bands increased in a regular manner as the temperature increased over the range 88°K to 240°K; since absorption and transmission are defined to be in an inverse logarithmic relationship, this demonstrates that the absorption ratio between the beta and D bands decreases with rising temperature.

Previous measurements of magnetic susceptibility have indicated that haemoglobin hydrate is a thermal mixture of two spin states with a high spin ground state (Iizuka, 1969b); subsequent optical studies at low temperatures seemed to contradict this conclusion and support the hypothesis that the hydrate is a mixture of two chemical components, I being in the high spin state over the entire temperature range studied and the other, II, being a thermal equilibrium mixture with a low spin ground state. Thus the high spin EPR signal of haemoglobin hydrate would be attributable to component I. Furthermore, a reassessment of the Mossbauer spectra (Lang, 1966) might lead to a reinterpretation in terms of a two component model; previous attempts to reconcile the fluoride and

hydrate Mossbauer spectra have depended upon the assumption that there exists considerable covalency which would distort the spatial distribution of the five d electrons, giving rise to the large observed quadrupole splitting.

This is an important problem since it casts a serious doubt on the ability of magnetic susceptibility measurements at low temperatures to determine spin states correctly, or suggests that the usefulness of cryogenic optical absorption studies is destroyed by some unknown mechanism. For this reason particularly it was felt that it was important to repeat the hydrate measurements and extend them to other derivatives.

The experimental results indicate that absorption in the beta band at 540 nm wavelength increases with falling temperature and that the converse is true for the D charge transfer band. These movements imply that there is more low spin and less high spin population at lower temperatures; this is in conflict with the published description based on magnetic susceptibility measurements and supports the optical results of Iizuka (1969a). This trend from low spin to high spin as the temperature is increased is shown more clearly in the graph of the absorption ratio in Fig. 3.11, where it is seen that the ratio falls with rising temperature. This trend is confirmed by a graph of the transmission ratio for the beta and D bands which rises with rising temperature.

Unfortunately, it is not possible to use the absorption ratio as an index to the low spin/high spin population ratio. This arises because of several factors: the presence of minor high spin bands at about the same wavelength as the beta band prevents the use of the absorption ratio in this manner (Brill, 1961). As a hypothesis it is worth remarking that the behaviour of the beta band alone could be brought about by increasing intensity in these

RATIO OF ABSORPTIONS AT BETA AND D BANDS IN Hb HYDRATE (pH 6·5).

Fig. 3.11

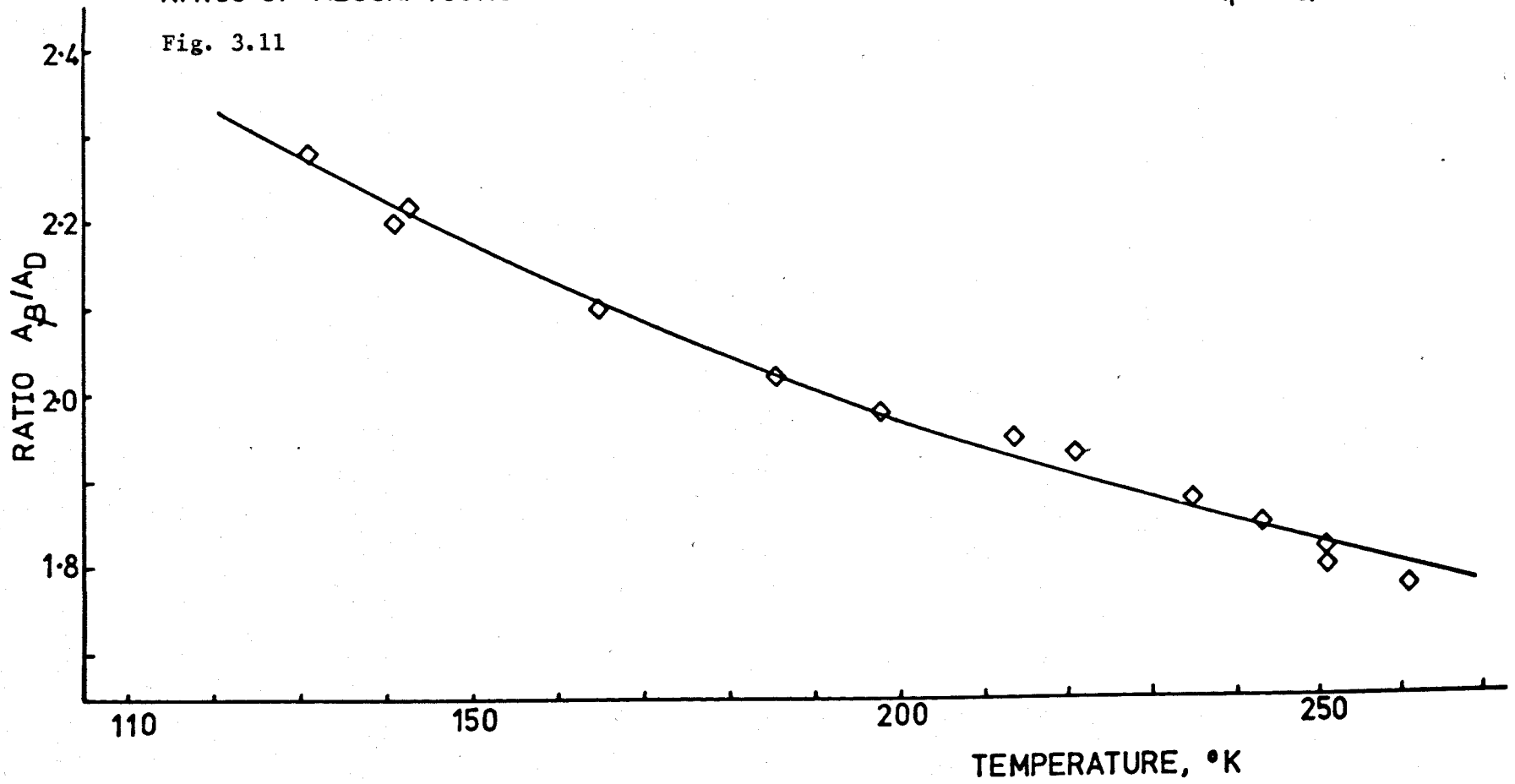

minor bands as the temperature falls but this cannot be a large effect since it is not noticeable in other high spin derivatives and also the behaviour of the D band leads to the same general conclusions as the behaviour of the beta band. It should also be born in mind that the ratio of absorptions is dependant upon line widths and the wavelengths of the bands; somewhat different line shapes may be observed for the same bands in different derivatives at room temperature and the wavelength of occurrence is not fixed. It is therefore possible that the hypothetical componenents I and II may possess such spectral differences and that such effects might obscure any trend in the absorption spectra due to temperature changes.

In an attempt to relate the optical and magnetic behaviour at low temperatures, the absorption ratio is plotted against the thermal equilibrium constant K over a range of temperature; K is the ratio of low spin to high spin populations obtained from the magnetic susceptibility measurements and in the same Fig. 3.12 is graphed the molar susceptibility against absorption in the beta band over a range of temperature. (It should be noted that these curves are not functions and therefore end at the initial and final points plotted).

Consideration of these curves shows that as the temperature falls, the molar susceptibility rises sharply to its maximum value at the curve end indicating a high spin ground state; however, the absorption in the beta band is increasing, suggesting a low spin ground state. It is most unlikely that this result could be brought about by chemical action; the detachment of a water molecule and the attachment of a hydroxyl ion would indeed bring about a low spin ground state but would also reverse the trend of the magnetic susceptibility with temperature and we must also query

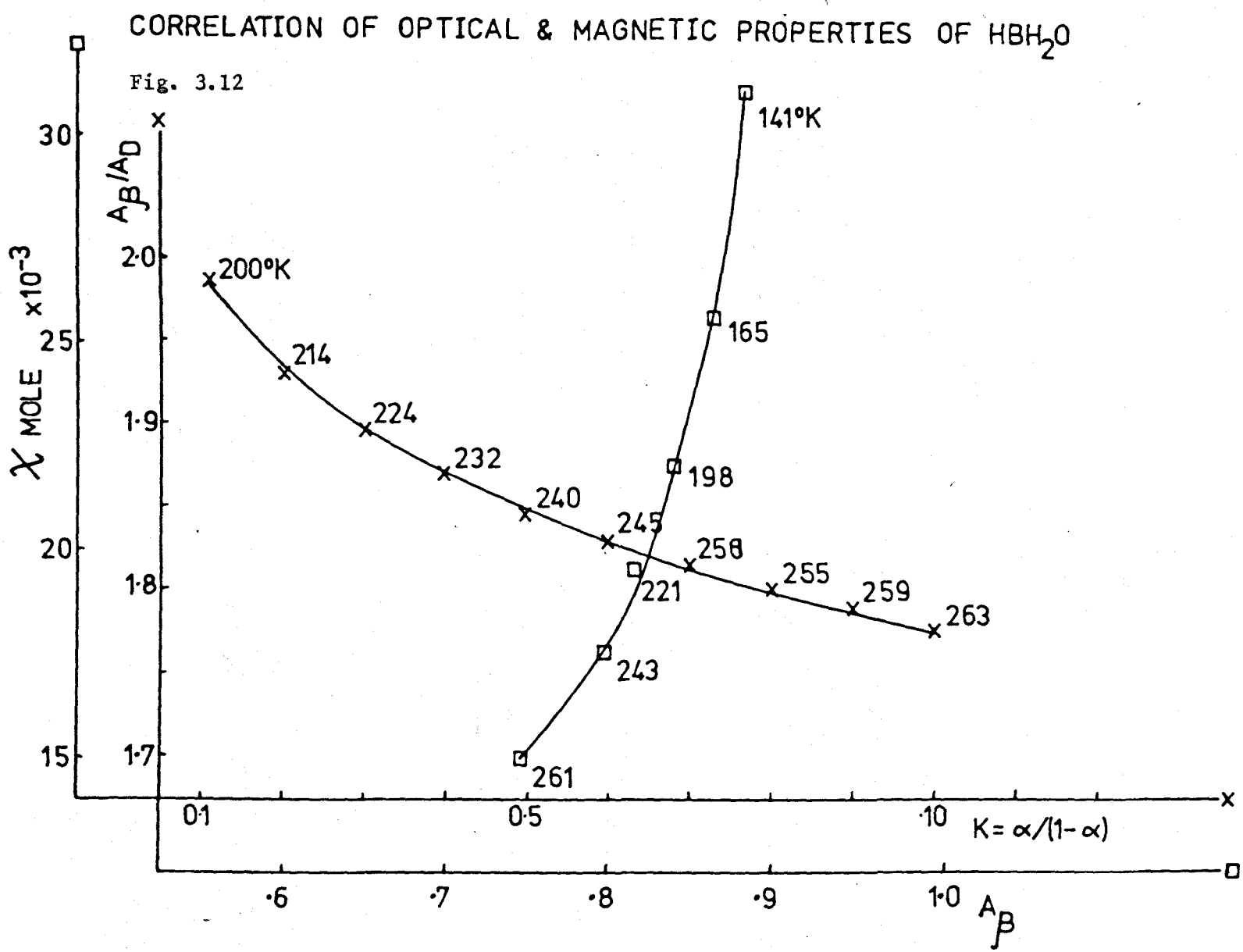
CORRELATION OF OPTICAL & MAGNETIC PROPERTIES OF HBH_2O
Fig. 3.12
χ MOLE $\times 10^{-3}$
A_B/A_D
30
25
20
15
2·0
1·9
1·8
1·7
200°K
214
224
232
240
245
258
255
259
263
141°K
165
198
221
243
261
0·1
0·5
·10
K = $\alpha/(1-\alpha)$
·6
·7
·8
·9
1·0
A_B

the possibility on three other grounds. First, the general shapes of absorption bands in haemoglobin hydrate are different from those in the hydroxide (q.v.); second, the pH is too low for such an event to occur in solution at room temperature; third, ionic mobilities become smaller at reduced temperatures: no data appears to be available for ionic mobilities in haemoglobin solutions but in ionic crystals mobility is facilitated by an increase in available thermal energy (Etzel, 1950).

The curve correlating the absorption ratio of the beta and D bands with the equilibrium constant K cannot be readily extended below 200°K on a linear scale because K becomes rather small and errors increase.

Overall, we observe that the optical and magnetic results do not support each other and some feasible explanation must be found. It is tentatively suggested that the explanation might lie in one of the following: the freezing process, the minor high spin bands, or inadequacy of the two spin state model.

Problems arising from the freezing process have been discussed in the previous section; these were related to possible phase changes in the ice and to the size and size distribution of the ice crystals. However, it is not impossible that the stresses imposed in freezing might be communicated to the protein molecule and give rise to small conformational changes. These conformational changes could reflect back as electronic changes at the haem ion; there is no evidence for this effect and it is suggested that microphotometric studies should be made of single crystals of haemoglobin hydrate at low temperatures. The results could be compared with EPR measurements and room temperature optical absorption results for single crystals (Day, 1967). Furthermore, careful examination should be made of Mie scattering from ice at 540 nm and 630 nm over several cycles of temperature between 77°K and 273°K and the effect of

different buffers and other solutes determined.

That the presence of minor high spin absorption bands might greatly influence the results is possible but if a minor high spin band located under the beta band at 540 nm wavelength were growing as the beta band was declining in absorption, then one would expect to observe a crossover where the total absorption of the two bands would reach a turning point. It is strong evidence against this hypothesis that no such minimum has been observed over the range of temperature employed.

It has been suggested that the hypothesis that the hydrate is comprised of a thermal equilibrium mixture of spin 5/2 and spin $\frac{1}{2}$ state populations is too simple to adequately explain the results and a "two component" chemical hypothesis has been proposed. The results reported here are in general support of this hypothesis (Gray, 1972). It is, however, curious that the ratio of statistical weights of the high and low spin states - which is a function of the degeneracy of the two spin states involved and of contributions from other degrees of freedom within the molecule - varies considerably from one derivative to another; these ratios have been obtained from magnetic susceptibility studies and tabulated (Iizuka, 1969a,b). They vary between 4.12×10^{-6} for myoglobin imidazole to 2.58×10^{4} for cytochrome-c hydroxide; this rather large variation is important since it may relate to changes in the conformation of the protein molecule.

3.5.3.2. Haemoglobin hydrate with Inositolhexaphosphate.

Various organic phosphates including 2,3-diphospho-D-glyceric acid (DPG) and Inositolhexaphosphate (IHP) complex with haemoglobin and shift the oxygen dissociation curve (Benesch, 1967, Chanutin, 1967); it is believed that IHP causes ferric haemoglobin to assume a

completely high spin form at room temperature (Perutz, 1972).

Spectrophotometric measurements were made between 91°K and 246°K on a sample of haemoglobin (ferric) hydrate to which had been attached IHP. (This sample was kindly supplied by Dr. M.F. Perutz.) It was found that the ratio of the absorptions in the bands at 540 nm and 630 nm remained constant within the experimental error between the temperatures quoted. This ratio is shown as a function of temperature in Fig. 3.13.

It is considered that the invariance of this ratio implies that the haemoglobin hydrate + IHP complex is entirely in one spin state at room temperature since reducing the temperature does not change the optical spectrum; if there were a mixture of spin states then one would expect that lowering the temperature would cause the ground spin state to predominate in the population. It remains possible that the high spin state observed is the ground state in a thermal mixture and that if one were to raise the temperature well above room temperatures an increase in low spin content might be observed: however, such a process would be of limited value since a substantial rise in temperature would denature the protein.

3.5.3.3. Haemoglobin Fluoride.

Examination of the optical absorption spectrum of the fluoride in Fig. 3.13 shows that there is little variation between 100°K and 205°K and that the ratio of absorptions in the beta and D bands is flat as a function of temperature within the experimental error. Some possible fine structure was observed in the beta band but this may have been an instrumental artifact, possibly noise or pen response effects; further measurements to determine this point could be made using greater wavelength resolution and lower noise

ABSORPTION RATIO A_β/A_D : HbH_2O+IHP, HbF^-, HbN_3^-.

Fig. 3.13

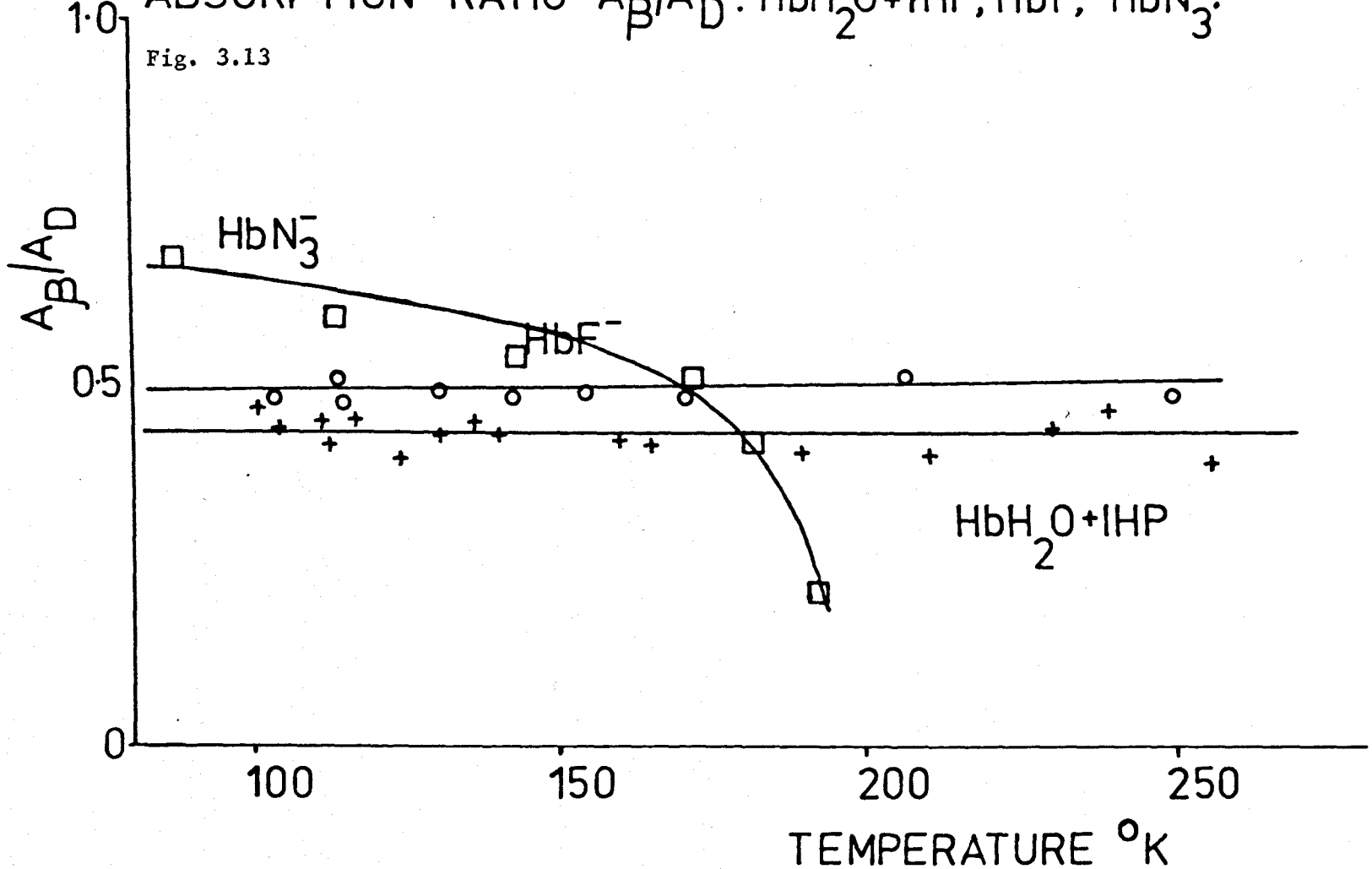

detection.

The results indicate a very similar case to that of haemoglobin hydrate with IHP attached. It has long been considered that haemoglobin fluoride is almost entirely in the high spin state (Beetlestone, 1961); there is alleged to be about 3% of the low spin state present at room temperature.

Because of the well known nature of the fluoride, it is gratifying to observe that the results reinforce the belief that the absorption ratio A_{540nm}/A_{630nm} is a useful indication of spin state changes.

3.5.3.4. Haemoglobin hydroxide.

The optical absorption spectrum of the hydroxide is shown in Fig. 3.14 where it may be seen that absorption at 540 nm wavelength decreases as the temperature increases; a graph of transmission in the same band as a function of temperature shows an increase with temperature. It is thereby deduced that there is an increasing proportion of high spin state at higher temperatures.

At large values of pH the OH^- radical attaches to the haemoglobin in place of the water molecule (see Fig. 2.5). Various workers have estimated the proportion of low spin component present at room temperature to lie between 31% and 36% on the basis of magnetic susceptibility and optical absorption measurements (Smith, 1968 Beetlestone, 1964, Farrow, 1971). The results reported here indicate that $HbOH^-$ is a derivative with a low spin ground state and this result is in agreement with measurements of the magnetic susceptibility. It is not possible in this case to calculate the absorption ratio owing to the small value of A_{630nm}. If the value of A_{540nm} is plotted as a function of temperature, a small change in slope of the curve occurs at about 175°K; this is matched by a similar

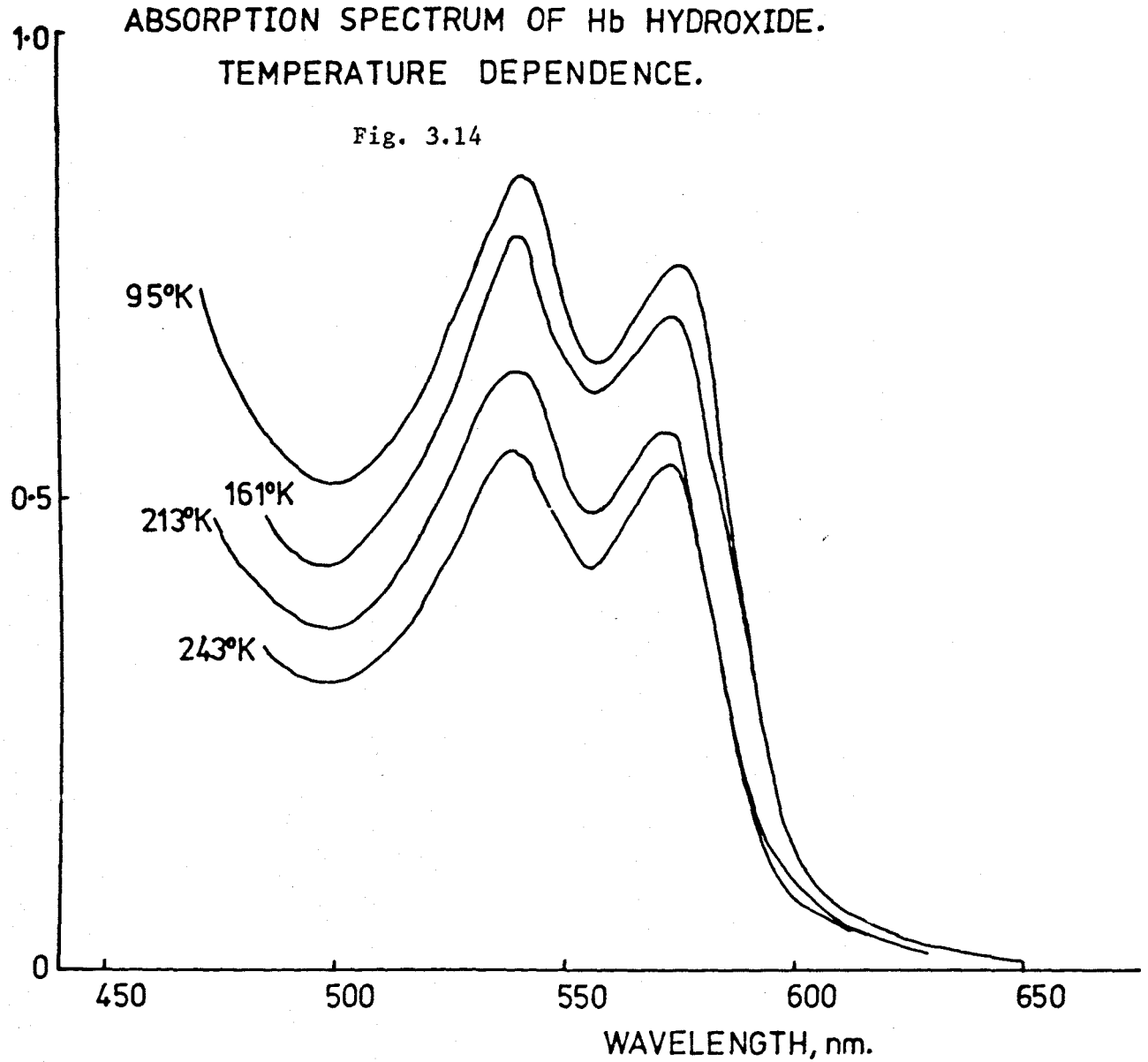
ABSORPTION SPECTRUM OF Hb HYDROXIDE.
TEMPERATURE DEPENDENCE.
1·0
0·5
0
95°K
161°K
213°K
243°K
450
500
550
600
650
WAVELENGTH, nm.

Fig. 3.14

effect on the graph of n^2_{eff} against temperature (Iizuka, 1969a). These optical results are in accord with those previously reported but variations at 602 nm and 636 nm were not observed, possibly because of lack of sensitivity.

3.5.3.5. Haemoglobin Azide.

The general trend exhibited by the absorption spectrum of the azide derivative, HbN_3^-, is a reduction in absorption as the temperature rises and a small gradual increase in A_{630nm}: this can be seen in Fig. 3.13. The behaviour of the absorption bands becomes somewhat unusual above 195°K but the absorption ratio A_{540nm}/A_{630nm} undergoes a gradual decrease with increasing temperature.

It is thought that the peculiar behaviour at 195°K and above is caused by small macroscopic sample movements which would have the effects discussed in 3.5.2. The consistent progress of the absorption ratio, however, indicates that there is an increasing proportion of high spin state population with rising temperature. This supports the hypothesis that haemoglobin azide possesses a low spin ground state.

3.5.3.6. Haemoglobin Formate.

The variation of the optical absorption spectrum shown in Fig. 3.15 is that of haemoglobin formate ($HbH.COO^-$) as a function of temperature. It was found that this spectrum fluctuated very little between 90°K and 185°K and hence only the 90° curve has been reproduced; above about 190°K the spectrum began to change substantially and measurements were made up to a temperature of 244°K and are given in Fig. 3.15. The absorption at 540 nm is plotted as a function of temperature in Fig. 3.16 and may be seen to be almost invariant below about 200°K. The ratio

A_{540nm}/A_{630nm} is plotted as a function of temperature up to $200^{o}K$ and is seen to be a gradually falling function of temperature. Note that the error bars change gradually in size because of the gradually decreasing magnitude of the denominator A_{630nm}.

The reduction in the absorption ratio as the temperature rises suggests that the high spin component is increasing in magnitude. This is not in agreement with the high spin EPR signal obtained from myoglobin formate (Farrow, 1971) but is in accord with the high spin value of magnetic susceptibility obtained at room temperature (Schoffa, 1964). Variation of the magnetic susceptibility with temperature has apparently not been published.

The high spin EPR signal obtained from $Mb.COO^{-}$ strongly suggests the presence of two kinds of formate; a rotation of the principal axes of two g tensors has been found and this may indicate that the ligand is bound in two different orientations at the haem plane. This is markedly similar to the hypothesis that the ligands may be bound in two different fashions in myoglobin and haemoglobin azide (McCoy, 1970); it was suggested in this latter study that there were two kinds of azide (possibly low and high spin forms) but x-ray diffraction measurements do not confirm this (Stryer, 1964).

It may be the case that haemoglobin formate contains two equilibrium systems; first, two different modes of binding at the haem with different spin states; second, that one binding mode would be a thermal equilibrium mixture with a low spin ground state. It is possible that the local steric arrangements near the haem plane favour two orientations of the same radical; this would probably be determined largely by the proximal histidine residue.

ABSORPTION SPECTRUM OF HB FORMATE
AS A FUNCTION OF TEMPERATURE.

Fig. 3.15

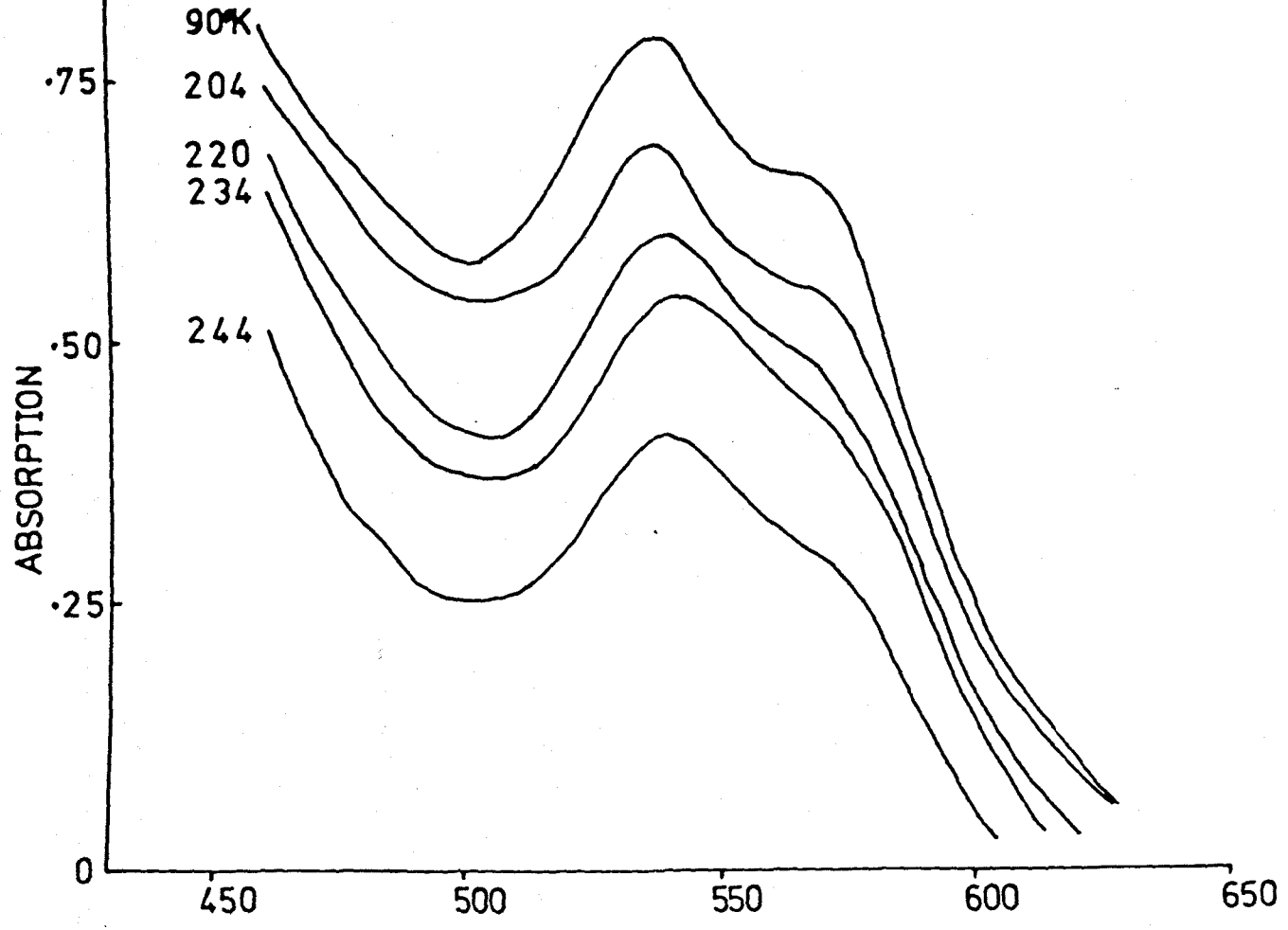

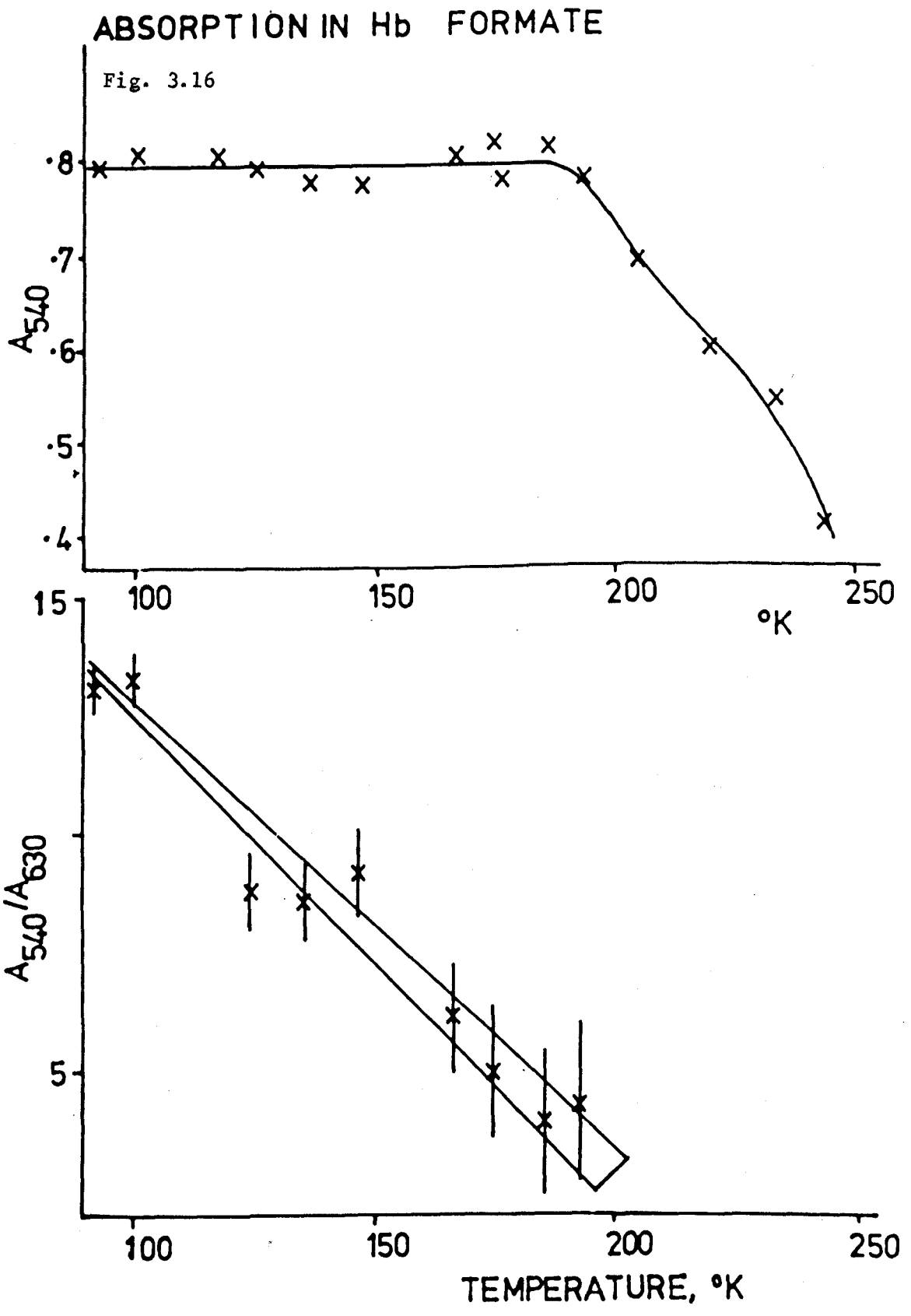
ABSORPTION IN Hb FORMATE
Fig. 3.16
·8
·7
·6
·5
·4
A540
100
150
200
250
°K
15
5
A540/A630
100
150
200
250
TEMPERATURE, °K

3.5.3.7. Haemoglobin cyanate.

Only fragmentary results were obtained for the cyanate and a full spectrum was not examined. The magnitude of the absorption at 540 nm wavelength was found generally to decrease with rising temperature between 100°K and 215°K but with an anomalous region between 80°K and 100°K where absorption increased with rising temperature; this curious result was repeated several times. One obvious explanation is that some local liquifaction of the cold nitrogen gas may have occurred in the reference beam of the spectrophotometer and have obscured the beam.

3.5.3.8. Oxyhaemoglobin.

The optical absorption spectrum of oxyhaemoglobin was found to behave in the manner shown in Fig. 3.17 where it may be seen that the absorption bands at 540 nm and 575 nm increase in magnitude as the temperature rises. The dependence of absorption in the beta band at 540 nm is shown in Fig. 3.18 as a function of temperature. HbO_2 does not possess any charge transfer bands at 630 nm or 480 nm (Li, 1969).

Little related information is available on the magnetic properties of this derivative except for the room temperature magnetic susceptibility; the room temperature optical absorption spectrum has been obtained and the Mossbauer spectrum of the haem iron has been obtained over a range of temperature.

The room temperature magnetic susceptibility indicates that oxyhaemoglobin is diamagnetic at room temperature (S = 0). The results of Mossbauer spectroscopy are curious. It will be noted from Fig. 3.19 that oxyhaemoglobin lies in the group of haem complexes with small I.S. and large Q.S. (q.v. 2.2.2.7.) and this has led spectroscopists to suggest that the ground state

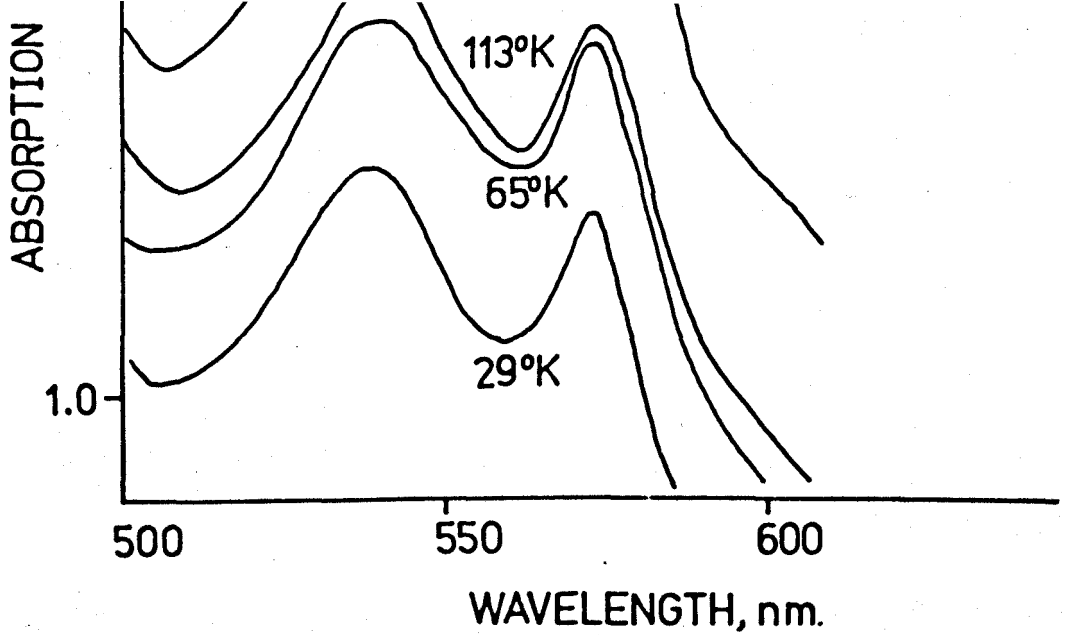
ABSORPTION
1.0
113°K
65°K
29°K
500
550
600
WAVELENGTH, nm.

Fig 3.17

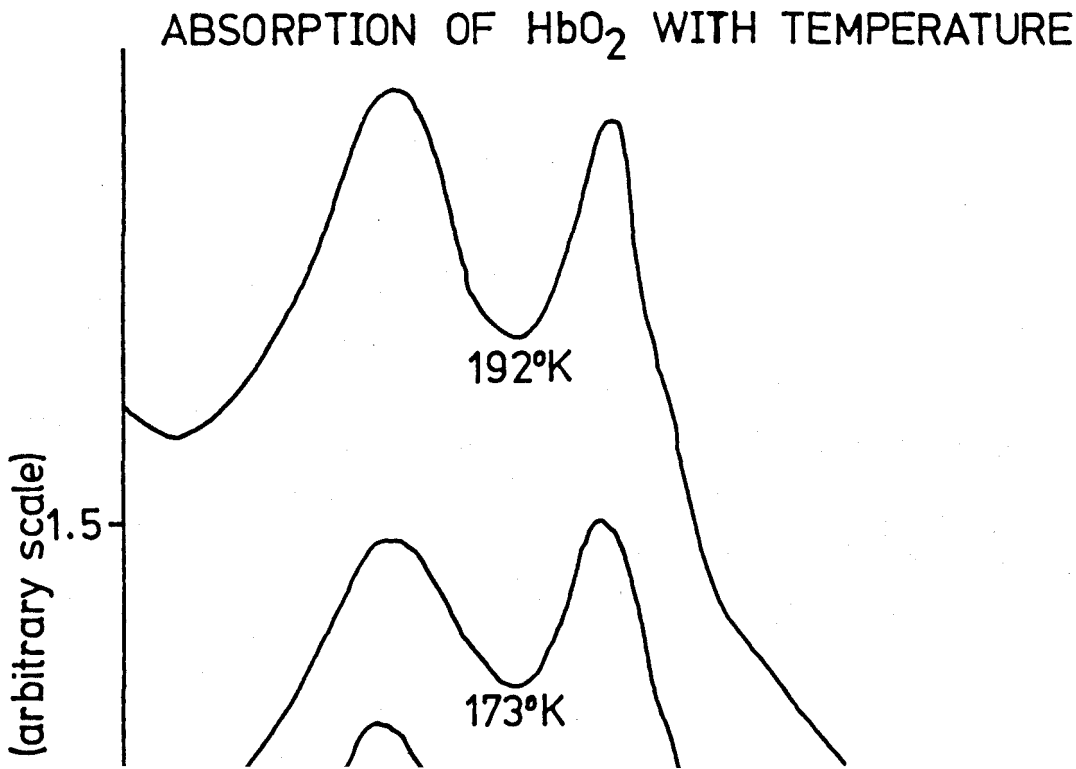
ABSORPTION OF HbO_2 WITH TEMPERATURE
192°K
173°K
(arbitrary scale)
1.5

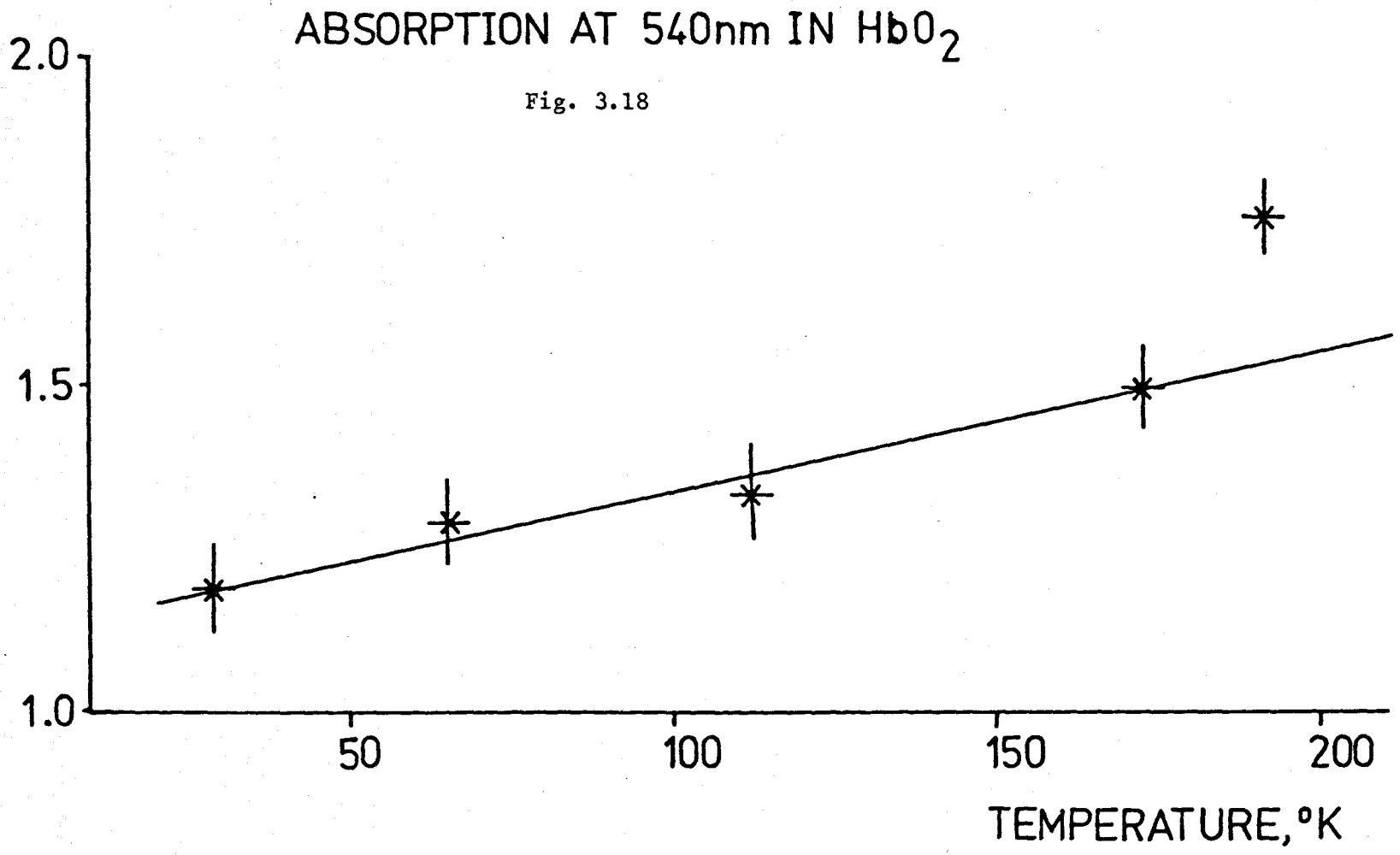
ABSORPTION AT 540nm IN HbO_2
2.0
1.5
1.0
50
100
150
200
TEMPERATURE, °K

Fig. 3.18

is $S = \frac{1}{2}$ (Maling, 1969); this apparent contradiction may be partially resolved if electron transfer is assumed to take place between the iron and the oxygen molecule. This effect would not be discerned by the magnetic susceptibility measurements since the magnetic moment of the molecule as a whole is determined. Further, it is well known that the ground state of the oxygen molecule is $S = 1$; if the oxygen molecule is assumed to lie parallel to the haem plane, the consequent reduction in symmetry about the oxygen-oxygen axis may lead to $S = 1$ not being the state with lowest energy and thus tentatively explains why oxyhaemoglobin has no paramagnetic properties (Griffith, 1956).

Also, temperature dependence of the Q.S. has been observed (Lang, 1966); it has been proposed that this is due to the presence of low lying excited states having appreciable occupation at 195°K (Lang, 1962). This suggestion is unlikely to be the case since these states would give rise to paramagnetism observable at room temperature; it may be that the reduction in the Q.S. is due to improved rotation of the oxygen molecule as the temperature rises.

No EPR signals have been observed from oxyhaemoglobin samples at low temperatures up to microwave frequencies of 70 GHz.

Assuming that no spin mixing occurs (Harris, 1968) three possibilities present themselves:

(a) that HbO_2 has an $S = \frac{1}{2}$ ground state. This would be supported by the Mossbauer data but refuted by measurements of the magnetic susceptibility and lack of EPR signals (Maling, 1969).

(b) that the spin state is always $S = 0$ irrespective of the temperature; this is in accord with the diamagnetic properties at room temperature and the lack of EPR signals but in this case one would not expect to observe any changes in the optical absorption spectrum as the temperature varies.

Fig. 3.19

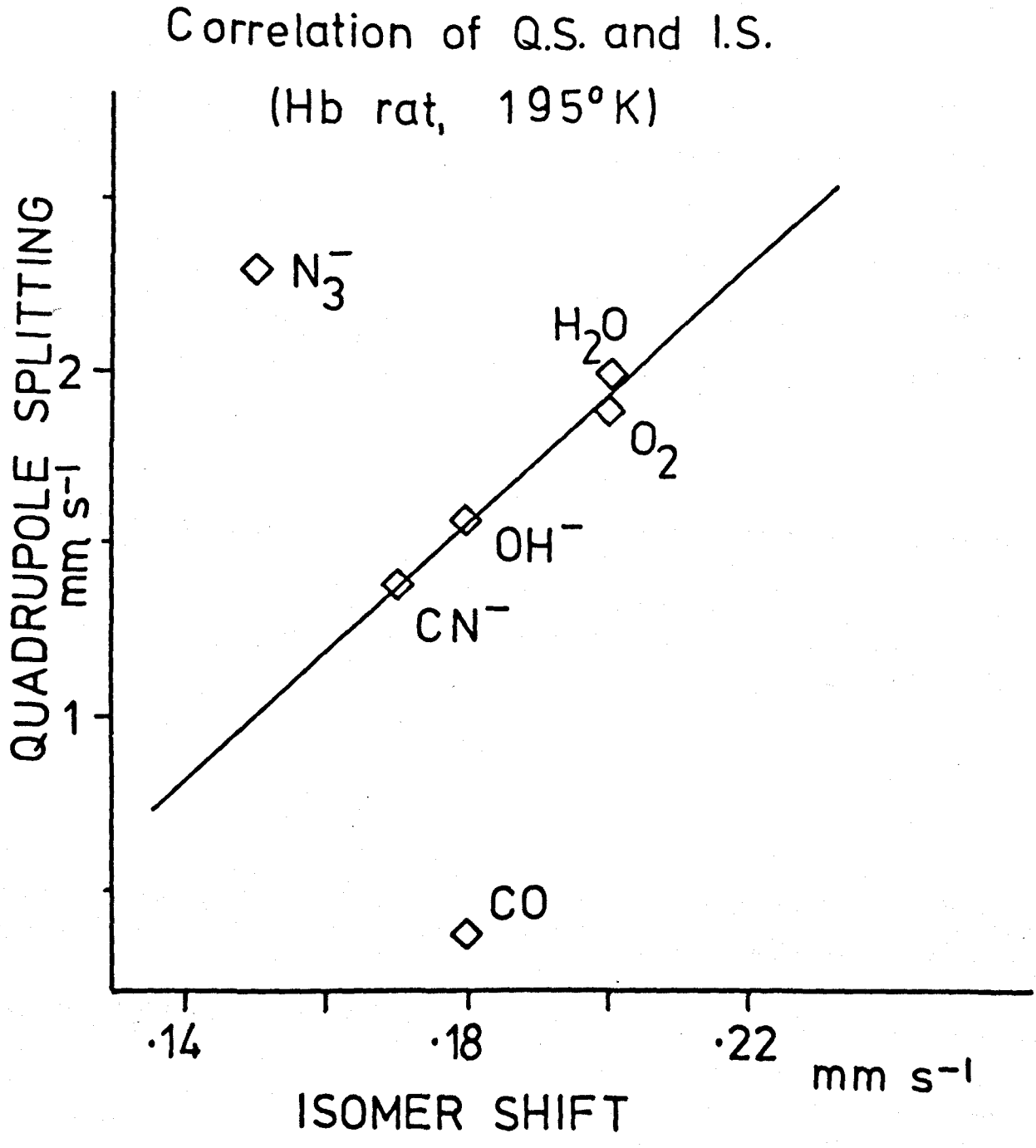
Correlation of Q.S. and I.S.
(Hb rat, 195°K)
QUADRUPOLE SPLITTING
mm s⁻¹
2
1
N_3^-
H_2O
O_2
OH^-
CN^-
CO
·14
·18
·22
mm s⁻¹
ISOMER SHIFT

(c) that the ground state is S = 2 and that thermal equilibrium of spin states exists to yield an S = 0 population growing with temperature. It is thought that the ground state cannot be S = 1 if S = 0 and S = 2 occur (Griffith, 1956, 1964). This hypothesis would be in agreement with the change in optical absorption with temperature. However, it would also imply a detectable magnetic moment at room temperature unless the statistical weight of the S = 2 state were particularly low. (Iizuka, 1969). Some support for this hypothesis is lent by the Mossbauer results; the temperature dependence of the Q.S. suggests a paramagnetic species. The unlikely suggestion of low-lying excited states could be replaced by the existence of an S = 2 ground state. An S = 2 ground state would not necessarily conflict with the lack of EPR signal since no signals have been observed from samples of deoxyhaemoglobin which has an S = 2 spin state (at 50 GHz microwave frequency by Ingram, 1963, or in this work at 70 GHz); this lack of signal could be due to an inadequate size of microwave quantum or a rapid spin lattice relaxation effect.

An S = 2 ion in a low symmetry crystalline electric field has the degeneracy of the five m_s spin states completely removed. Since there is no Kramers' degeneracy for an S = 2 ion, EPR signals may be absent if the microwave quanta are smaller than the zero field splitting. We must however take care in extrapolating from deoxyhaemoglobin to HbO_2 since the crystal field symmetry in deoxyhaemoglobin is lower since the iron is only pentacoordinated.

There is the further possibility that in oxyhaemoglobin S is no longer a good quantum number and that spin mixing occurs (Harris, 1968) as it may for certain porphyrin complexes but no calculations appear to have been attempted for ferrous porphyrin complexes investigating possible spin mixing.

3.5.4. Further remarks and suggestions.

The measurement of optical absorption at cryogenic temperatures appears to be in need of some development. A comprehensive study of light scattering from water frozen to low temperatures would enable conclusions to be drawn about the effects of possible transitions between different polymorphs of ice. Furthermore, by examining the light scattered azimuthally around the sample, the distribution of sizes of ice crystals could be obtained; the effects of cycling the temperature of the sample and the rate of temperature change upon the distribution could be studied. This knowledge about the distribution is important because the ratio of light scattered in the forward direction at two different wavelengths is dependent upon the ice crystal sizes; in double beam spectrophotometry this effect is probably far less important than when using a single beam, but it should be confirmed that both sample and reference cuvettes contain the same ice crystal distribution if they have undergone the same temperature cycles.

It would also be advantageous to modify the low temperature sample holder so that the cold gases were not in contact with the sample, probably by the use of a copper post between sample and liquid gas. This would obviate the possibility that locally liquified gas could obscure a light beam.

It has been shown that the magnetic susceptibility of a haem protein derivative is related to the optical absorption in the 540 nm band (Smith, 1968). It is not possible to demonstrate this relationship for haemoglobin hydrate because of the anomalous behaviour of this derivative; however, in the case of the hydroxide this relationship can be demonstrated. In Fig.3.20 is graphed n_{eff}^2 against absorption in the 540 nm band over the temperature range

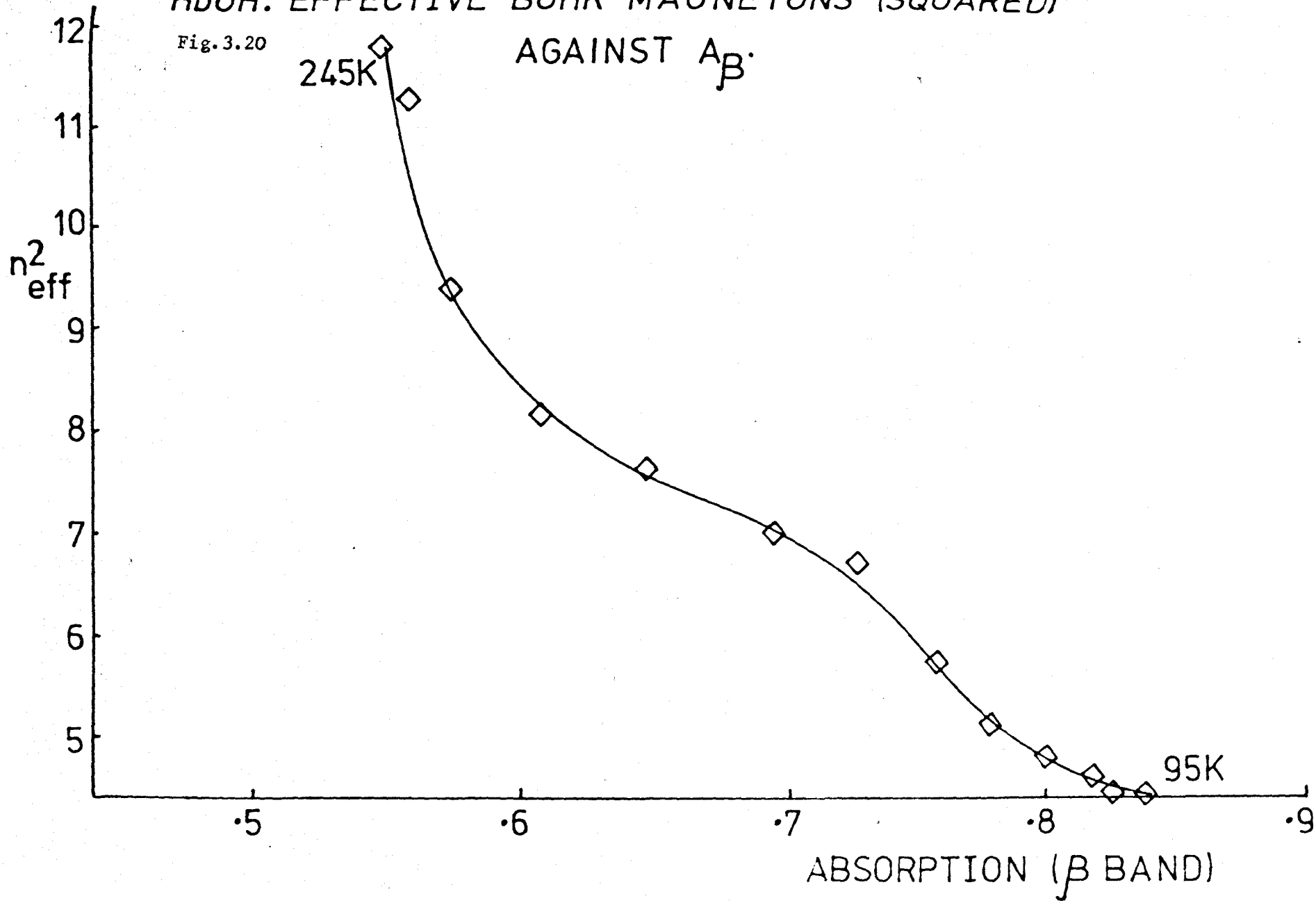
HbOH: EFFECTIVE BOHR MAGNETONS (SQUARED)
AGAINST A_β.
Fig. 3.20
245K
95K
n^2_{eff}
12
11
10
9
8
7
6
5
·5
·6
·7
·8
·9
ABSORPTION (β BAND)

95°K to 245°K. It may be observed that a smooth curve may be drawn through the points and that, as the paramagnetism of the hydroxide diminishes the absorption in the 540 nm band increases; the azide which also has a low spin ground state, shows indications of following the same pattern but most of the change in susceptibility is between 220°K and room temperature, in which range macroscopic sample movements obscured the optical measurements. It is not possible to draw a similar graph for the formate because no low temperature magnetic susceptibility data was available.

The optical absorption studies of haemproteins and their investigation by electron spin resonance serve to complement each other; generally, EPR has been used at low temperatures with frozen samples whereas optical absorption has commonly been used at room temperature. In this way a great deal of useful data has been obtained. However, by using optical techniques at low temperatures, the two techniques may support each other.

3.6 References.

Adair, G.S., M.E. Adair, Proc. Roy. Soc., B120, 422, 1936.

Anfinsen, C.B., Proc. Nat. Acad. Sci. Wash., 47, 1309, 1961.

Benesch, R., R.E. Benesch, Biochem. Biophys. Res. Comms.,26, 162, 1967.

Berg, P., Ann. Revs. Biochem., 30, 293, 1961.

Braterman, P.S., R.C. Davies, R.J.P. Williams, Adv.Chem.Phys.,7,359,1964.

Brill,

Burton, J.D., Nat., 212, 976, 1966.

Chanutin, A., R.R. Curnish, Arch. Biochim. Biophys., 121, 96, 1967.

Conant, J.B., F.A. Crawford, Proc.Nat.Acad.Sci.USA, 16, 552, 1930.

Corey, R.B.,L.Pauling, Rc. Inst. lomb. Sci. Lett., 89, 10, 1955.

Cullis, A.F., Proc. Roy. Soc., A256, 15 and 161, 1961/2.

Dalton, J., C.A. McAnliffe, D.H. Slater, Nat., 235, 388, 1972.

Day, P., D.W. Smith, R.J.P. Williams, Biochem., 6, 3747 and 1563, 1967.

Dowell, L.G., A.P. Rinfret, Nat., 188, 1144, 1960.

Drake, J.F., R.J.P. Williams, Nat., 182, 1084, 1960.

Etzel, H., R.J. Maurer, J. Chem. Phys., 18, 1003, 1950.

Frauenfelder, H., The Mossbauer Effect, Benjamin, N.Y., 1962.

Ghirreti, F., (in) Oxygenases, C. Hayaishi, (Ed.), Acad. Press, N.Y., 1962.

Gibson, Q.H., E. Antonini, J. Biol. Chem., 238, 1384, 1963.

Gol'danskii, V.I., The Mossbauer Effect, Consultants Bureau, N.Y.,1964.

Gonser, U., R.W. Grant, Biophys. J., 5, 768, 1965.

Gray, K., E.F. Slade, Biophys. Biochem. Res. Comms., 48, 1019, 1972.

Green, D.W., V.M. Ingram, M.F. Perutz, Proc. Phys. Soc., A225, 287, 1954.

Griffith, J.S., The Theory of Transition Metal Ions, C.U.P., 1964.

Harris, G.M., Theoret. Chim. Acta, 10, 119, 1968.

Hearon, J.Z., D. Burk, J. Nat. Cancer. Inst., 9, 337, 1949.

Iizuka, T., M. Kotani, Biochim. Biophys. Acta, 194, 351, 1969a.

Iizuka, T., M. Kotani, Biochim. Biophys. Acta, 181, 275, 1969b.

Ingram, D.J.E., J.F. Gibson, M.F. Perutz, (in) Paramagnetic Resonance, (Ed.) W. Low, 2, 809, 1963, Acad. Press, N.Y.

Ingram, V.M., Biochim. Biophys. Acta, 28, 539, 1958.

Jenkins, F.A., H.E. White, Fundamentals of Optics, 1957, p.457.

Johnson, I., J. Amer. Chem. Soc., 69, 1184, 1947.

Jorgensen, C.K., (in) The Biochemistry of Copper, (Ed.), J. Peisach, Acad. Press, N.Y., 1966.

Keilin, D., E.F. Hartree, Nat., 164, 254, 1949.

Keilin, D., E.F. Hartree, Nat., 165, 504, 1950.

Keilin, J., Biochem. J., 45, 440, 1949.

Kendrew, J.C., Science, 139, 1259, 1963.

Kendrew, J.C., Nat., 181, 662, 1958.

Kendrew, J.C., Nat., 185, 422, 1960.

Klotz, I.M., S. Keresztes-Nagy, Biochem., 2, 445, 1963.

Konig, E., K. Madeja, Chem. Comm. (London), 1961, 61, 1961.

Kovalskii, V.V., L.T. Rezaeva, Zh. Obsch. Biol., 25, 339, 1964.

Lang, G., S. DeBennedetti, R.I. Ingalls, J.Phys.Soc.Japan, Supp.B1,17,131,1962

Lang, G., W. Marshall, Proc. Phys. Soc., 87, 3, 1966.

Li, T-K., B.P. Johnson, Biochem., 8, 3638, 1969.

Maling, J.E., M. Weissbluth, (in) Solid State Biophysics, (Ed.), S.J. Wyard, McGraw-Hill, N.Y., 1969, p. 329.

Martell, A.E., M. Calvin, Chemistry of the Metal Chelate Compounds, Prentice-Hall, N.J., 1962, p. 336.

McCoy, S., W.S. Caughey, Proc. 54th Nat. Meeting Amer. Chem. Soc., Chicago, Ill., 1957.

McCoy, S., W.S. Caughey, Biochem., 9, 2387, 1970.

McCoy, S., W.S. Caughey, (in) Structural Probes for the Function of Proteins and Membranes, (Eds.), B. Chance, T. Yonetani, in the press, 1972.

Meehan, E.J., (in) Koltoff-Elving's Treatise on Analytical Chem., 5(1), 2773, 1964, Wiley.

Mie,, G., Ann. Physik, 25, 377, 1908.

Muirhead, H., M.F. Perutz, Nat., 199, 633, 1963.

Nobbs, C.L., J.C. Kendrew, H.C. Watson, Nat., 209, 339, 1966.

Nobbs, C.L., (in) Hemes and Hemeproteins, (Eds.), B. Chance, R.W.Estabrook, T. Yonetani, Acad. Press, N.Y., 1966, p. 143.

Pauling, L., Science, 120, 543, 1949.

Pauling, L., R.B. Corey, H.R. Bronson, Proc.Nat.Acad.Sci.USA.,37,205,1951.

Perutz, M.F., J.M. Mitchison, Nat., 166, 677, 1950.

Perutz, M.F., Nat., 185, 416, 1960.

Perutz, M.F., J. Cryst. Growth, 2, 54, 1968.

Perutz, M.F., Nat., 219, 139, 1968.

Perutz, M.F., Nat., 242, 89, 1968.

Perutz, M.F., H. Lehmann, Nat., 219, 902, 1968.

Perutz, M.F., H. Muirhead, J.M.Cox,,L.C.G. Goaman, Nat., 219, 131, 1968.

Perutz, M.F., Nat., 178, 906, 1970.

Perutz, M.F., A.R. Ferscht, S.R. Simon, J.G. Beetlestone, E.F. Slade, to be published, 1972.

Redfield, A.C., Biol. Rev. Cantab. Phil. Soc., 9, 175, 1934.

Robertson, J.M., J. Chem. Soc., 225, 1195, 1936.

Roche, A., J. Roche, Bull. soc. chim. biol., 17, 1494, 1935.

Scheler, W., G. Schoffa, F. Jung., Biochem. Z., 329, 232, 1956b.

Scheler, W., G. Schoffa, F.,Jung, Naturwiss., 43, 1959, 1956a.

Schoffa, G., Adv. Chem. Phys., 7, 182, 1964.

Simpson, W.T., J. Chem. Phys., 17, 1218, 1949.

Slade, E.F., R.H. Farrow, Biochim. Biophys. Acta, 278, 450, 1972.

Smith, D.W,, R.J.P. Williams, Biochem. J., 110, 297, 1968.

Sratton, J.A., N.B.S. Applied Math. Series 4, Tables of Scattering Functions for Spherical Particles, 1949.

Stryer, L., J.C. Kendrew, H.C. Watson, J. Mol. Biol., 8, 96, 1964.

Walter, R.I., J. Biol. Chem., 196, 151, 1952.

Watson, A.C., J.C. Kendrew, Nat., 190, 663, 1961.

Watson, J.D., F.H.C. Crick, Nat., 171, 737, 1953.

Weiss, C.H., H. Kobayaishi, M. Gouterman, J. Mol. Spec., 16, 4125, 1965.

Weissbluth, M., Struc. Bond., 2, 1, 1967.

Williams, R.J.P., (in) Hemes and Hemeproteins, (Eds.), B.Chance, R.W. Estabrook, T. Yonetani, Acad. Press, N.Y., 1966.

Wilkins, M.F.H., Nat., 171, 738, 1953.

Wyman, J., Adv. Protein Chem., 4, 407, 1948.

Yonetani, T., D.F. Wilson, B. Seamonds, J. Biol. Chem., 241, 5347, 1966.

Zeemansky, M.W., Heat and Thermodynamics, McGraw-Hill, 1957.

CHAPTER FOUR

EPR STUDIES OF HAEMOGLOBIN SOLUTIONS.

4.1. Experimental procedure.

Concentrated solutions and pastes of haemoglobin hydrate, fluoride, formate and cyanate were studied by EPR at 35 GHz and 70 GHz. At Q band the sample was placed in a P.T.F.E. tubular sample holder situated axially in the microwave cavity; low loss ceramic sample containers machined from Stykast Lo-K were also used. At 70 GHz it is not possible to introduce a relatively bulky sample holder into the microwave cavity and consequently the paste sample was placed carefully on the cavity endplate.

Much of the techniques of EPR spectroscopy at 70 GHz are modified or improved methods used at lower frequencies. In particular, microwave components are correspondingly smaller and an improved surface finish is required on the internal surfaces of tapers and microwave cavities.

At 70 GHz (4 mm) the millimetre waves were generated by a reflex klystron YK1010 giving an output of 100 mW; after passing through an isolator and a 10 dB coupler, the waves arrived at a magic tee. A wavemeter was provided after the coupler for approximate wavelength measurements. Between the magic tee and the microwave cavity the waveguide is oversized from 4 mm standard guide to 35 GHz waveguide in order to reduce attenuation; tapers are used to achieve this which are long in comparison with the wavelength. The microwave cavity operates in the TE_{012} mode and is turned out of nonmagnetic brass, bored and reamed to the correct dimensions. The cylindrical bore and

cavity endplates are diamond polished to give the cavity a high Q factor; the cavity was thoroughly washed with water and acetone and diamond polished after use to preserve the Q factor. The signal is detected by a Philips crystal detector which may be optimised using a shorting plunger. The details of this spectrometer have been described elsewhere (Slade, 1968/9).

In the course of this work it was necessary to incorporate a superconducting magnet into the spectrometer; a split coil magnet was supplied by the Oxford Instrument Co. Ltd. The magnet was mounted on a three inch diameter stainless steel tube at the bottom of an eight inch diameter helium cryostat. It was possible to rotate the magnet by means of a worm and wheel through a gas tight seal thereby permitting angular orientation studies to be made. The mounting of the magnet was so contructed that the magnet could be mounted also with the two inch bore vertical. This admitted a demountable three piece re-entrant cryostat tail not supplied by the manufacturers which was used in calibrating the magnet. In normal use with this re-entrant tail fitted to the cryostat the loss of liquid helium was about 500 ml per hour; without the tail the boiling off of helium was reduced to some 300 ml per hour.

Owing to difficulties experienced by the manufacturers, the two coils of the magnet did not possess equal numbers of turns on their respective windings; a centre tap was therefore provided through which a small balancing current could be passed to one coil. The calibration data reported was 0.16548 Tesla ampere^{-1}.

Upon installation in the laboratory the magnet was again calibrated using an NMR probe with both proton and deuterium samples and also at one value of the magnetic field using 35 GHz microwave radiation; the latter frequency was determined

Fig. 4.1

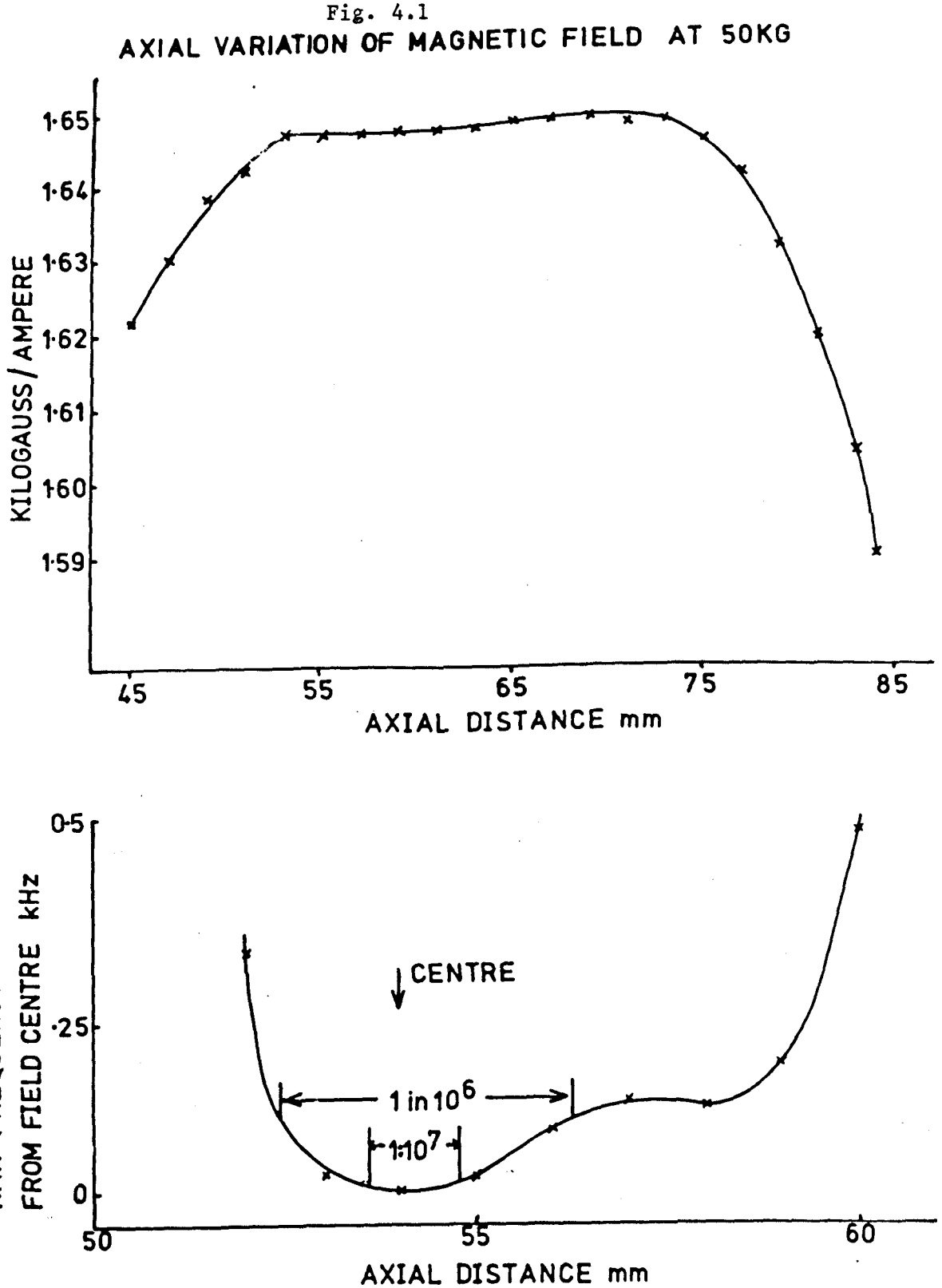
AXIAL VARIATION OF MAGNETIC FIELD AT 50KG
KILOGAUSS/AMPERE
1·65
1·64
1·63
1·62
1·61
1·60
1·59
45
55
65
75
85
AXIAL DISTANCE mm
NMR FREQUENCY DIFFERENCE FROM FIELD CENTRE kHz
0·5
·25
0
CENTRE
1 in 10^6
1:10^7
50
55
60
AXIAL DISTANCE mm

from the EPR signal of a small sample of d.p.p.h. in the field of a previously calibrated electromagnet. In the NMR calibrations a solid state marginal oscillator using the high input impedance of an FET across the r.f. resonant circuit was used; noise proportional to 1/f is also reduced by this technique (Idoine, 1971). The data obtained were as follows:

NMR (^1H and ^2H)	0.1648(6) $\pm$ 0.0007 T Amp^{-1}
EPR (d.p.p.h.)	0.1648(8) $\pm$ 0.0001 T Amp^{-1}

This result agrees with that of the manufacturer within the experimental error of 0.0007 T Amp^{-1}. The axial variation of the magnetic field was measured at 1 T and 5 T; the result for 5 T is shown in Fig. 4.1 in terms of T Amp^{-1} against axial dimension. At 5 T the optimum centre tap current was 280 $\pm$ 20 mA and the axial homogeneity of the field was 1.4 parts in 10^7 over the NMR sample size. The limits of homogeneity are indicated in Fig. 4.1.

At 35 GHz the magnetic field was provided by a Newport Instruments Ltd. electromagnet. Measurements of the magnetic field were made using an NMR marginal oscillator. When a liquid helium cryostat was inserted between the pole pieces of the magnet there was insufficient space available to insert the NMR probe. Accordingly a flat Hall probe was cemented to the centre of a pole piece and the Hall voltage measured with a Pye potentiometer when a constant current was passed through the Hall plate. The magnetic field strength at the centre of the magnetic field was related to the Hall voltage using the NMR probe in the absence of the cryostat.

4.2. Experimental results at 35 GHz and 70 GHz.

The samples of haemoglobin hydrate, fluoride, formate and cyanate were prepared as described from fresh human red cells (q.v. 3.1).

EPR signals were observed from samples of the hydrate, fluoride and formate but not from the cyanate. It was found that it was essential to make use of distilled and deionised water and several times recrystallized ammonium sulphate in the preparation of samples for use in the 70 GHz spectrometer otherwise impurity signals were present. Measurements at 35 GHz were made at 77°K; in the 70 GHz spectrometer the sample was contained in the microwave cavity immersed in liquid helium at 4.2°K. No signal was observed from haemoglobin cyanate at 35 GHz at a temperature of 4.2°K; nor was any signal seen from a cyanate sample at 77°K in a 9 GHz spectrometer. It is interesting to note that no signals have been observed in this case; there may be some similarity to myoglobin cyanide (Farrow, 1971) for which difficulties have been encountered by many workers in trying to measure the g values. In the case of $HbOCN^-$ all that may be said is that substantial distortion may be present at the haem plane, reinforced by bonding of the OCN^- to the peptide chain ends, and this may have led to an unsuitable spin-lattice relaxation time.

The signals observed from the hydrate, fluoride and formate are reproduced in Figs. 4.2,3,4. The signals seen at 35 GHz and 70 GHz are shown side by side for comparison purposes; although the experimentally observed peak to peak linewidths and the g values of the peaks of the first derivative absorption lines are useful in describing the experimental spectrum, it is far more valuable to determine g_x, g_y, g_z, and the paramagnetic linewidth ΔB. The

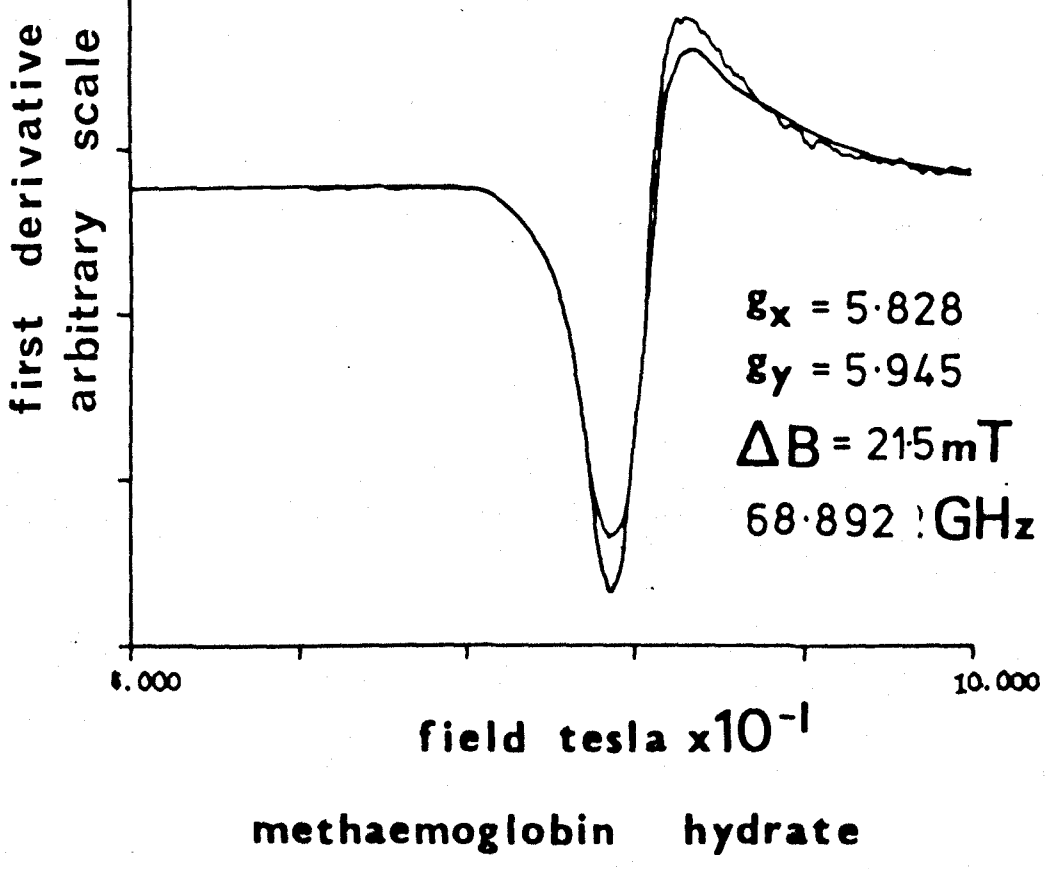
first derivative
arbitrary scale
$g_x = 5{\cdot}828$
$g_y = 5{\cdot}945$
$\Delta B = 2{\cdot}15\,mT$
68·892 GHz
8.000
10.000
field tesla $\times 10^{-1}$
methaemoglobin hydrate

Fig. 4.2

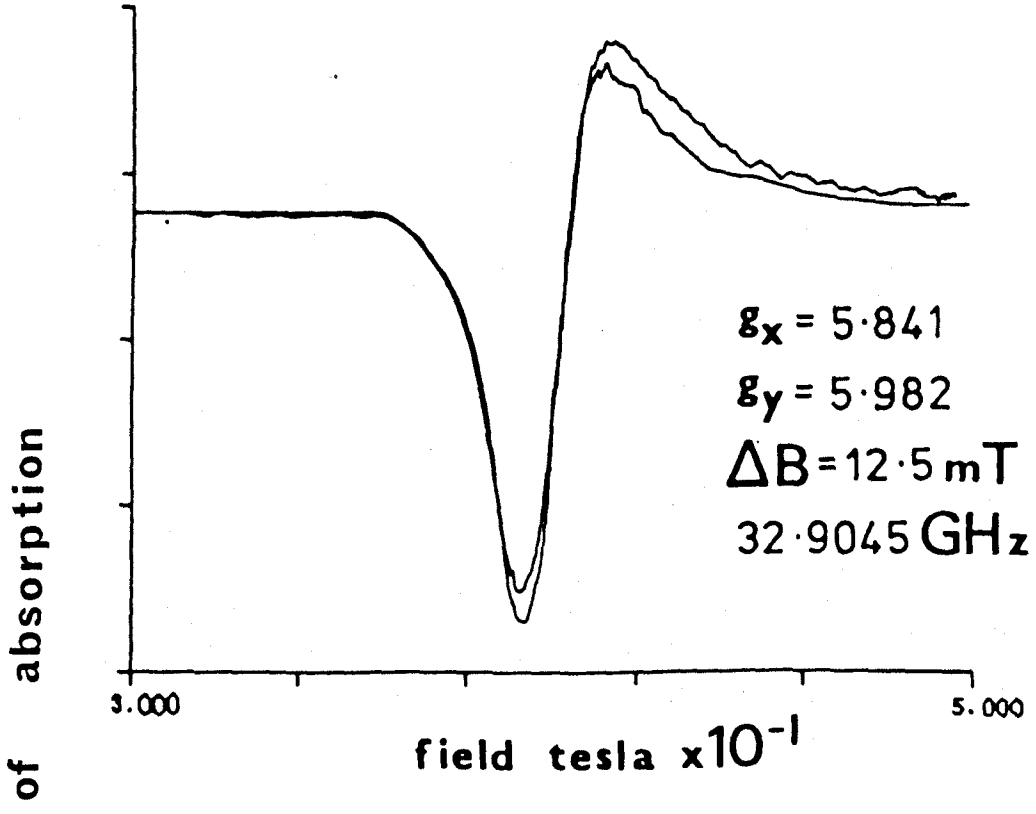
$g_x = 5{\cdot}841$
$g_y = 5{\cdot}982$
$\Delta B = 12{\cdot}5\,mT$
$32{\cdot}9045\,GHz$
3.000
5.000
field tesla $\times 10^{-1}$
of absorption

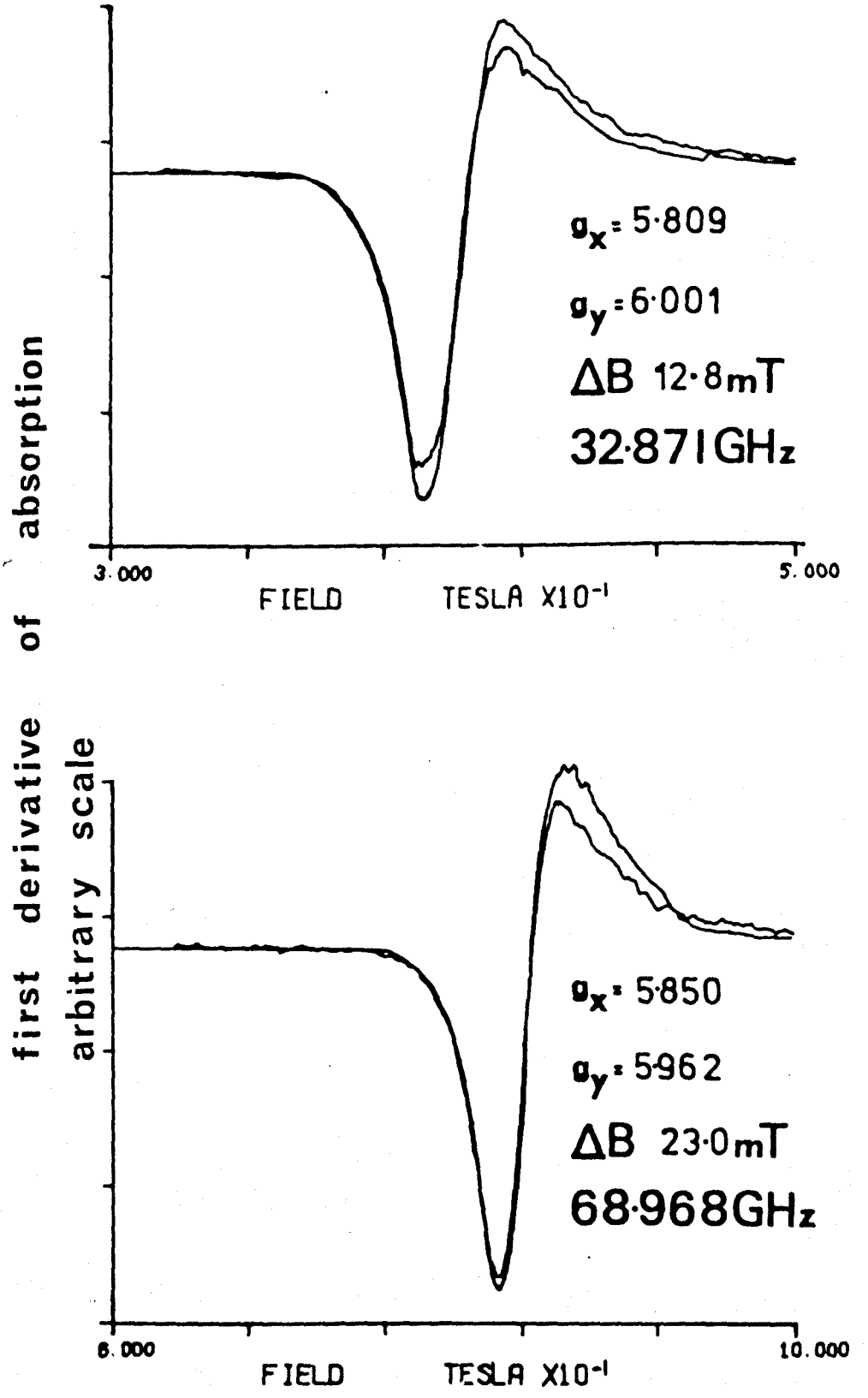

methaemoglobin fluoride

Fig. 4.3

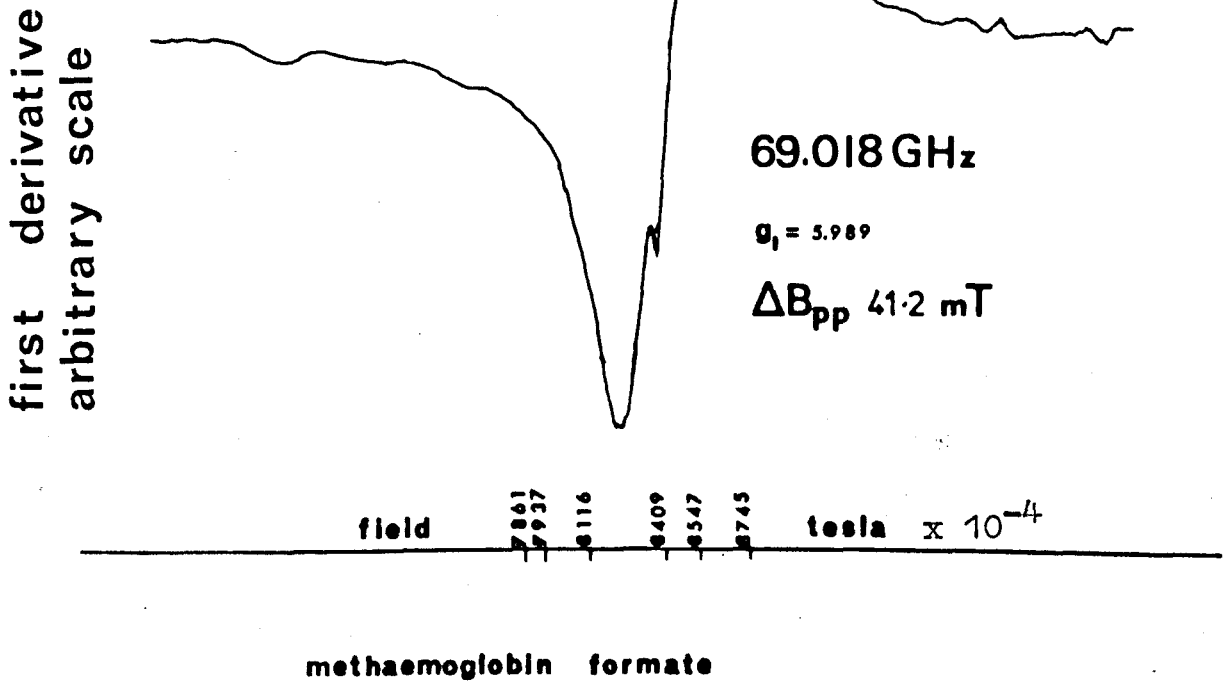
first derivative
arbitrary scale
69.018 GHz
g_1 = 5.989
ΔB_{pp} 41·2 mT
field
7861
7937
8116
8409
8547
8745
tesla x 10^{-4}
methaemoglobin formate

Fig. 4.4

of absorption

manner in which this is done is described in the next section.

It is of interest to note from the experimental spectra that all show an anisotropic lineshape with larger linewidths at the higher frequency. Also a small inflexion is to be seen on the formate spectrum at 70 GHz which may reflect large g value anisotropy not present in the other two derivatives.

4.3. Computation of g_x, g_y, and g_z.

The simulation of polycrystalline or paste spectra requires a spatial averaging process since the absorption lineshape is a function of the orientations of the crystalline electric field symmetry axes of individual paramagnetic molecules in the static magnetic field. It is necessary to incorporate the variation of the transition probability with the relative orientation of the static and microwave magnetic fields and to make use of two premises:

(a) that the distribution of molecular orientations is random. In haemoglobin, where there are four paramagnetic centres in one molecule, it is assumed that one centre in each molecule is randomly orientated. To a high degree of approximation, the other three paramagnetic centres will then also be randomly orientated since they are rigidly orientated with respect to the first; in fact this is not strictly true because small thermal movements of parts of the molecule are reported (Watson, 1968).

(b) that there is a lineshape which may be assumed; a Lorentzian lineshape function has been used throughout.

The simplest treatment is that of axial anisotropy in $\bar{g}$ without fine or hyperfine interaction terms so that the system may be defined by the Hamiltonian

$$H = \beta \cdot \bar{B} \cdot \bar{g} \cdot \bar{S}$$

Assuming a delta lineshape function, the spectrum may be integrated in terms of B_{11} , B_L as a function of magnetic field (Eleaney, 1950, Sands, 1955) and a lineshape function may also be incorporated (Ibers, 1962, Slade, 1968). In the case of lower symmetry when $g_x \neq g_y \neq g_z$ then no closed form expression is available but such spectra may be computed numerically (Swalen, 1964, Kneubuehl, 1960, Burns, 1961).

In spherical polar coordinates the Hamiltonian becomes

$$H = g(\theta,\phi)\,\beta\, BS_x$$

where

$$g(\theta,\phi) = (g_z^2\cos^2\theta + g_x^2\sin^2\theta\cos^2\phi + g_y^2\sin^2\theta\sin^2\phi)^{\frac{1}{2}}$$

and since only the Zeeman term is present

$$h\upsilon = g(\theta,\phi)\,\beta\, B$$

a line shape function may be inserted in terms of

$$\upsilon(B,\theta,\phi,) = B - h\upsilon/\beta\, g(\theta,\phi)$$

Assuming random orientation in the paste, the fraction of paramagnetic centres with magnetic axes in the angular increment

$$\phi \longrightarrow \phi + \Delta\phi$$
$$\theta \longrightarrow \theta + \Delta\theta$$

is directly proportional to $\Delta\phi\sin\theta\Delta\phi$ which becomes $d\phi\sin\theta d\theta$ as $d\theta$, $d\phi$ tend to zero.

Averaging the line shape function L over all possible orientations gives

$$I(B) = \int_{\phi=0}^{\pi/2}\int_{\theta=0}^{\pi/2} L(\theta,\phi)\sin\theta\, d\theta\, d\phi$$

for the intensity which may be transformed by a choice of parametric variable $x = \cos\theta$ to

$$I(B) = \int_{\phi=0}^{\pi/2} \int_{x=0}^{1} L(\theta,\phi)\, dx\, d\phi$$

It has been suggested that the dependence of transition probability upon relative orientation of static and dynamic magnetic fields should be incorporated (Bleaney, 1960, Kneubuehl, 1961) and a suitable function has been derived as (Pilbrow, 1969)

$$P(\theta,\phi) = g_x^2 g_y^2 \sin^2\theta + g_y^2 g_z^2 (\sin^2\phi + \cos^2\theta\cos^2\phi) + g_z^2 g_x^2 (\cos^2\phi + \cos^2\theta\sin^2\phi)$$

The lineshape function is thus

$$L_{Lorentzian} = P(\theta,\phi) / (\upsilon^2 + \tfrac{3}{4} W^2)$$

where W is the line width at maximum slope; introducing the line shape function into the integral gives

$$I(B) = \int_{\phi=0}^{\pi/2} \int_{x=0}^{1} \frac{P(\theta,\phi)}{(\upsilon^2 + \frac{3}{4}W^2)}\, dx\, d\phi$$

Similar integrals have been transformed into functions of elliptic integrals in closed form (Bloembergen, 1953, Kohin, 1958, Poole, 1967) but taking account of $P(\theta,\phi)$ prevents this and numerical integration is necessary. A computer program in Fortran IV was written for an I.C.L. 4130 for this purpose; the parameters required are g_x, g_y, g_z, microwave frequency and paramagnetic linewidth.

Attempts have been made to determine anisotropic g tensors using automatic fitting subroutines (Johnson, 1965, Dowsing, 1969) based upon least squares estimations (Marquardt, 1963) but they

suffer from the heavy disadvantage that the form of the actual function to be minimised is often such that at points near the desired minimum the steepest descent is not directed to that minimum and so convergence may not occur (Dowsing, 1970). The use of a grid search technique might overcome this problem.

Because of these difficulties a visual comparison method was adopted. Experimental spectra were transformed into pairs of coordinates using a D-Mac digitising table which corresponded to the intensity of the first derivative EPR spectrum at a given value of magnetic field.

The simulated and experimental first derivative EPR spectra were plotted by the computer to the same scale on the same axes and the input parameters varied until the best approach to coincidence was obtained. The effect of doing this may be seen in Fig. 4.2,3,4.

The values of the g tensor and the paramagnetic linewidth obtained are given with the appropriate spectrum.

4.3. Simulation of anisotropic linewidths.

It has been assumed that the linewidth of a paramagnetic centre is isotropic; this may not necessarily be the case and the transition probability may be modified to take account of linewidth anisotropy. It is initially assumed that the coordinate transformation diagonalising the $\bar{g}$ tensor also diagonalises a width tensor. This technique has been applied but the transition probability used was later found to be in error (Johnson, 1965, Pilbrow, 1969). Following the same method but incorporating the correct expression for transition probability, we define the principal values of the linewidth tensor in relation to the corresponding linewidth at maximum slope as

$$w_x = \tfrac{3}{4} W_x^2$$

$$w_y = \tfrac{3}{4} W_y^2$$

$$w_z = \tfrac{3}{4} W_z^2$$

and the appropriate linewidth function is

$$R(x,\phi) = w_z^2 + (w_y^2 - w_z^2)(1 - x^2) + (w_x^2 - w_y^2)(1 - x^2)\cos^2\phi$$

which reduces to

$$R(x,\phi) = \tfrac{3}{4} W_i^2$$

when $W_i = W_x = W_y = W_z$ in the isotropic case.

To simplify the choice of initial linewidth parameters, syntheses were first performed with isotropic linewidths and then developed with anisotropic values. In this case the expression for the intensity becomes

$$I(B) = \int_{\phi=0}^{\pi/2} \int_{x=0}^{1} \frac{P(x,\phi)\, dx\, d\phi}{\nu^2 + R(x,\phi)}$$

It was found that many iterative adjustments were necessary to obtain a good fit to the experimental curves; this resulted in a substantial increase in computing time and, for this reason, the procedure has only been followed through for the hydrate at 70 GHz.

It was found that the parameters giving the best fit were $W_x = 12.0$ mT : $W_y = 11.6$ mT : $W_z = 13.2$ mT. However, these values are within the experimental error in measuring the linewidth; a more accurate linewidth determination to ± 0.1 mT is essential for such an anisotropy analysis. (Helcke, 1968).

4.4 Hamiltonian parameters for haemoglobin hydrate.

By making the assumption that the rhombic term in the spin Hamiltonian is small so that the prevailing symmetry is axial, it has been possible to find an expression for the zero field splitting parameter 2D (Kirkpatrick, 1964). By measuring g_L^{eff} at two widely differing microwave frequencies, that is, at two widely differing values of the resonance magnetic field, the zero field splitting may be obtained from

$$2D = g_L \beta \frac{2 (B_2^2 - B_1^2)^{\frac{1}{2}}}{\alpha - 1} \qquad \alpha = g_L^{eff}(1)/g_L^{eff}(2)$$

$$\delta = (B_1/B_2)^2$$

where $$g_L = g_L^{eff}(1) \cdot \frac{1}{3} \cdot \frac{\alpha - \delta}{1-\delta}$$

and g_L^{eff} is set equal to $\frac{1}{2}(g_x + g_y)$ since it is defined as the average g value in the haem plane.

Inserting the values of g_L^{eff} and the magnetic field for the two microwave frequencies as below

35 GHz: $g_L^{eff} = 5.91$ $B_1 = 397.8$ mT

70 GHz: $g_L^{eff} = 5.89$ $B_2 = 835.7$ mT

gives

$$g_L = 1.97(2)$$

$$2D = 16.5 \pm 2.5 \text{ cm}^{-1}$$

The accuracy of this measurement is dependent upon the accuracy of the magnetic field measurements (which also determines the g value accuracy in this case.)

Fig. 4.6.

Comparison of values of 2D.

Derivative	Method	$2D\ cm^{-1}$	Reference
HbF	Far IR	12.6 ± •24	Brackett, 1970
MbH_2O	Far IR	19 ± 3	Brackett, 1970
MbF	Far IR	11.88 ± •16	Brackett, 1970
MbH_2O	Susceptibility	24	Morimoto, 1965
MbF	Susceptibility	14	Tasaki, 1968
MbH_2O	EPR	8•76 ± •12	Eisenberger, 1966
HbF	Mossbauer	14	Lang, 1966
MbF	Susceptibility	28	George, 1964
MbN_3	Susceptibility	5.8	Kotani, 1963
HbF	EPR	5	Kotani, 1964
Heme Cl^-	Far IR	13.9	Feher, 1966
HbH_2O	Far IR	21 • 5	Brackett, 1970*
MbH_2O	EPR	8.4 ± 0.6	Slade, 1968
MbH_2O	Spin-lattice relaxation	18.28 ± •36	Scholes, 1971

*Note: reported as a preliminary result only.

Where an experimental error is not estimated in the reference it is not conjectured in this table.

This value of the zero field splitting may be compared with values determined by other methods and for myoglobin. These results are tabulated in Fig. 4.6. The general pattern which emerges from this table is that (a) for myoglobin hydrate, $2D = 21.5 \pm 3\ cm^{-1}$ but with various EPR measurements agreeing at about $8.5\ cm^{-1}$ and (b) the value for MbF^- is around $13\ cm^{-1}$ but with an exceptionally high value of $28\ cm^{-1}$ obtained by a rather direct method and (c) that there are very few results for haemoglobin hydrate or fluoride which are

HbF^-	$12.6 \pm 0.24\ cm^{-1}$	(Far Infrared)
HbF^-	$14\ cm^{-1}$	(Mossbauer)
HbH_2O	$21\ cm^{-1}$	(Far Infrared)
HbH_2O	$16.5 \pm 2.5\ cm^{-1}$	(This work)

In interpreting the results of other workers it is crucially important to bear in mind the limitations of the methods used. Although Mossbauer spectroscopy is a very informative technique in respect of certain of their properties, it indicates that haemoglobin hydrate and fluoride are rather different whereas this is not shown up in the EPR spectra (Lang, 1966). It is not clear from the published Mossbauer results what accuracy may be attached to the zero field splitting; doubts have been expressed in respect of conclusions about spin states drawn from Mossbauer spectra (Williams, 1966). Much useful information has been obtained from studies of the magnetic susceptibility of proteins but the technique examines the molecule as a whole. Unfortunately it is necessary to fit the magnetic susceptibility to a rather flat curve of $n_{average}$ against D/kT (Kotani, 1961) and this may result in a substantial error on the parameter D/kT. Far Infrared spectroscopy is an extremely direct method of measuring the zero field splitting and considerable reliance must be placed on

its results.

From a knowledge of the value of 2D it is possible to calculate the smaller rhombic parameter E.

In the plane xy the angular variation of effective g value is given by

$$g_{eff} = 3\, g_o \left(1 - \frac{4E}{D} \cos 2\phi\right)$$

where ϕ is an angle in the plane xy measured from g_x, and g_o is the true g value in the spin Hamiltonian ($g_o \doteq 2$). In the xy plane the effective g value will vary between

$$g_{x,y} = 3\, g_o \left(1 \mp 4E/D\right)$$

From the values of g_x and g_y obtained experimentally at 70GHz it is possible to calculate E for the hydrate.

$$\underline{E = 0.016 \pm 0.003 \text{ cm}^{-1}}$$

The ratio of E/D is 0.002; this value is about the same as that for myoglobin fluoride (Farrow, 1971) and hydrate (Slade, 1972). No estimates of E appear to have been made for haemoglobin hydrate.

4.5 Hamiltonian parameters for Haemoglobin Fluoride.

By measuring g_L^{eff} at 35 GHz and 70 GHz microwave frequency for paste samples of the fluoride, it was possible to calculate the spin Hamiltonian parameters D and E as in the previously described case of the hydrate. Using the average value of g_x and g_y for g_L^{eff} gives the following values:

70 GHz: $g_L^{eff} = 5.866$ B = 840.9 mT

35 GHz: $g_L^{eff} = 5.904$ B = 397.8 mT

Inserting these experimental values into the expression for the zero field splitting yields

$$g_L = 1.97(2)$$

$$2D = 11.7 \pm 2.5 \text{ cm}^{-1}$$

The rhombic parameter E may be obtained from g_x and g_y and was found to be

$$E = 0.012 \pm 0.003 \text{ cm}^{-1}$$

Comparison of these results for 2D and E shows quite good agreement with the values of 2D obtained by Mossbauer and Far Infrared spectroscopy (q.v. Fig. 4.6); agreement with the EPR result of 2D = 5 cm^{-1} is poor. It is possible that this particular result has been reported as the value for D and not 2D (Farrow, 1971). Doubling this low result would bring it into general agreement with other results. No estimate of E for HbF^- seems available; E/D for MbF^- is 0.0027 (Farrow, 1971).

4.6. Summary

The electron spin resonance spectra of haemoglobin hydrate, fluoride and formate pastes have been obtained at 35 GHz and 70 GHz; no EPR signal was observed from samples of haemoglobin cyanate.

From these measurements at two widely different microwave frequencies, Hamiltonian parameters were obtained for the hydrate and fluoride. These values were:

Hydrate:	2D	=	16.5 cm^{-1}	E	=	0.016 cm^{-1}
Fluoride:	2D	=	11.7 cm^{-1}	E	=	0.012 cm^{-1}

These results have been compared with similar reported values.

4.7 References.

Bleaney, B, Proc. Phys. Soc., A63, 407, 1950.

Bleaney, B, Proc. Phys. Soc., 75, 621, 1960.

Bloembergen, N, T.J. Rowland, Acta Met., 1, 731, 1953.

Brackett, G.C., P.L. Richards, W.S. Caughey, J. Chem. Phys., 54, 4383, 1971.

Burns, G, J. App. Phys., 32, 2048, 1961.

Dowsing, R.D., D.J.E. Ingram, J. Mag. Res., 1, 517, 1969.

Dowsing, R.D., J. Comp. Phys., 6, 326, 1970.

Eisenberger, P., P.S. Pershan, J. Chem. Phys., 45, 2832, 1966.

Feher, G., P.R. Richards, Proc. Int. Conf. Mag. Res. Biol. Systems, Stockholm, 1966.

George, P., Biopolymers Symp., 1, 45, 1964.

Ibers, J.A., J.B. Swalen, Phys. Rev., 127, 1914, 1962.

Johnston, T.S., H.G. Hecht, J. Mol. Spectr., 17, 98, 1965.

Kneubuehl, F.K., B. Natterer, Helv. Phys. Acta, 34, 710, 1961.

Kneubuehl, F.K., J. Chem. Phys., 33, 1074, 1960.

Kohin, R.P., C.P. Poole, Bull. Amer. Phys. Soc., II, 3, 8, 1958.

Kirkpatrick, E.S., K.A. Muller, R.S. Rubins, Phys. Rev., 135, 86, 1964.

Kotani, M., Prog. Theor. Phys. (Supp.), 17, 4, 1961.

Kotani, M., Rev. Mod. Phys., 35, 717, 1963.

Kotani, M., Adv. in Chem. Phys., 7, 159, 1964.

Lang, G., W.Marshall, Proc. Phys. Soc., 87, 3, 1966.

Marquardt, D.W., J. Soc. Indust. App. Math., 11, 431, 1963.

Morimoto, H., T. Iizuka, J. Otsuka, M. Kotani, J. Chem. Phys., 54, 4383, 1971.

Poole, C.P., Electron Spin Resonance, 1967.

Sands, R.H., Phys. Rev., 99, 1222, 1955.

Slade, E.F., Thesis Ph.D., University of Keele, 1968.

Slade, E.F., D.J.E. Ingram, Nat., 220, 785, 1968.

Scholes, E.P., R.A. Isaacson, G. Feher, Biochim.Biophys.Acta, 244, 206, 1971.

Swalen, J.D., H.M. Gladney, I.B.M. J. of R. & D., 8, 515, 1964.

Tasaki, A., Phys. Props. Heme Proteins, Stanford Univ. Press, 1968.

Williams, R.J.P., (in) Hemes and Hemoproteins, B.Chance, R.W. Estabrook, T. Yonetani, (Eds.), Acad. Press, 1966, p.557.

CHAPTER FIVE

EPR STUDIES OF SINGLE CRYSTALS

5.1. Introductory note.

Other workers have undertaken extensive studies of myoglobin and its derivatives at microwave frequencies up to 70 GHz using electron paramagnetic resonance techniques (q.v. 2.2.2.9). In this chapter an account is given of the extension of this work to single crystal studies of oxidised deoxyhaemoglobin. The preparation of single crystals is described and the angular variation of the g value in the principal planes of the crystal discussed. Using measurements of the g value in the ab plane at 35 GHz the zero field splitting and rhombic parameters in the spin Hamiltonian are calculated.

5.2 Preparation of single crystals.

In order to grow good single crystals of deoxyhaemoglobin it is essential to use blood taken within the previous hour from the donor and to extract the haemoglobin from the red cells expeditiously. Accordingly, the haemoglobin solution was prepared by cell haemolysis after washing the cells with saline as previously described (q.v. 3.1). The remaining 2% sodium chloride was removed using a Sephadex G25 gel column which resulted in loss of concentration. The concentration was restored by using the polyacrylamide Lyphogel to remove water.

Protein crystals grow from solution when the solubility of the protein has been suitably adjusted to render the protein almost insoluble. The solubility of proteins is a complicated

function of the pH, molarity, and the temperature. Some workers have referred to a factor known as the "state of the protein": this usually refers to possible damage in the peptide side chains (such as may occur in the freeze drying process), and to the presence of nonhaem proteins which may interfere in the crystallisation process. Protein damage usually results in a drastic size limitation on the crystals.

The method used to instigate crystallization is called "salting out"; if the concentration of an electrolyte in a protein solution is gradually increased, there is first an increase in solubility followed by a decrease as the ionic strength of the electrolyte becomes greater in the solution. The latter portion of the curve of solubility against ionic strength can be expressed by

$$\log (S) = B - K.\ I/2$$

where S is the protein solubility in gm cm^{-3} and I/2 is the ionic strength in moles cm^{-3}. K, the gradiant, is dependent upon the actual protein and salt used but is not a function of pH or temperature. B, the projected intersept, depends on pH, the protein and temperature but is less affected by the actual salt used (Green, 1931).

Values of B and K may be obtained from the solubility curves of the various haemoglobin solubility curves (Jope, 1949). These data indicate that the rate of change of solubility of deoxyhaemoglobin is not so great as in other derivatives when more salt is added. This lack of critical dependence may be a contributory factor to the relative ease with which deoxyHb crystals may be grown.

By consideration of the salting out curves it has been demonstrated that the percentage of protein salted out at a

given salt concentration depends heavily upon the initial protein concentration; in the case of HbCO, for an initial protein concentration of 30 gm cm^{-3}, the greater proportion of protein would be salted out between 58% and 65% saturation with ammonium sulphate, whereas for an original protein concentration of 3 gm cm^{-1} precipitation would only commence at 66% (Dixon, 1961). The solubility of most adult haemoglobin derivatives experiences a broad minimum at 20°C; the solubility of deoxyhaemoglobin is unusual in that it appears substantially constant between 9°C and 35°C (Jope, 1949).

Crystallization of deoxyhaemoglobin was effected by the following procedure. A six per cent solution of fresh oxyhaemoglobin was converted to deoxyhaemoglobin by the addition of a small quantity of sodium dithionite in a nitrogen filled glove box. A distinct colour change from red to purple was observed. Distilled water was deionised and shaken several times under nitrogen to remove oxygen. Nitrogen was bubbled through a saturated solution of ammonium sulphate which had been twice re-crystallized. The buffer solutions of ammonium phosphate were similarly treated to remove oxygen. One ml portions of the protein solution were placed in sterile specimen tubes; ammonium sulphate, buffered to pH 6.5, was added drop by drop until a slight turbidity was observed. The tubes were closed and stored in jars containing nitrogen gas. Good crystals appeared after about a month and grew to about 3 or 4 mm in size.

Deoxyhaemoglobin crystals contain ferrous ions and are of space group P_{2_1}; human deoxyhaemoglobin is known to crystallize in three different forms. In this case, crystals were of type I which has the planes (001), (100), and (010) as faces.

It was decided to try converting the ferrous ions in

deoxyhaemoglobin crystals to the ferric valence state using an oxidizing agent; the use of potassium ferricyanide was avoided because there was a possibility of ferric ions from the ferricyanide interfering with the intended EPR measurements and because it is known to perturb the optical absorption spectrum (Cameron, 1969). The crystals were placed in specimen tubes containing saturated ammonium sulphate buffered to a series of pH values beginning at pH 6.5 and ending at pH 5.8; at this pH value, the crystals were transfered to a specimen tube containing saturated ammonium sulphate mixed with sodium nitrite (analytical grade) to give a 1 mM solution of the latter, with sufficient buffer present to give a pH 5.8. The crystals were left in this tube for several days at room temperature; it is important to note that these operations were performed in a nitrogen-filled glove box to avoid oxygenation of the haemoglobin. The excellence of sodium nitrite in this preparation is that it does not interfere with the EPR spectroscopy and does not appear to crack the crystals.

5.3 Angular variation of the *g* value

The EPR spectrometer and cavities used in these studies were the same as those briefly described in Chapter Four. Measurements of the magnetic field were made by the same techniques. Values of the magnetic field of the superconducting magnet were obtained by measuring the magnet current and using the calibration data.

Single crystals of the protein were mounted in the microwave cavities upon sample supports machined from the ceramic Stykast Lo-K; the well-developed face of the deoxyhaemoglobin

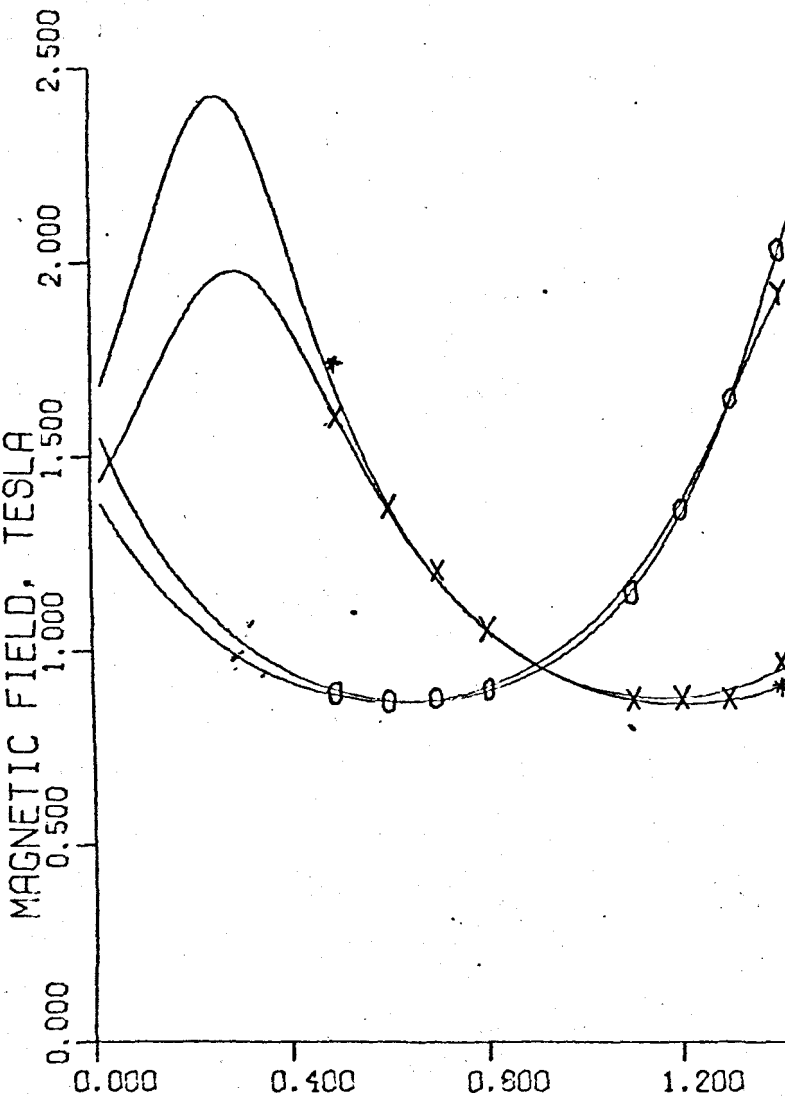

EPR LINE POSITIONS, AB

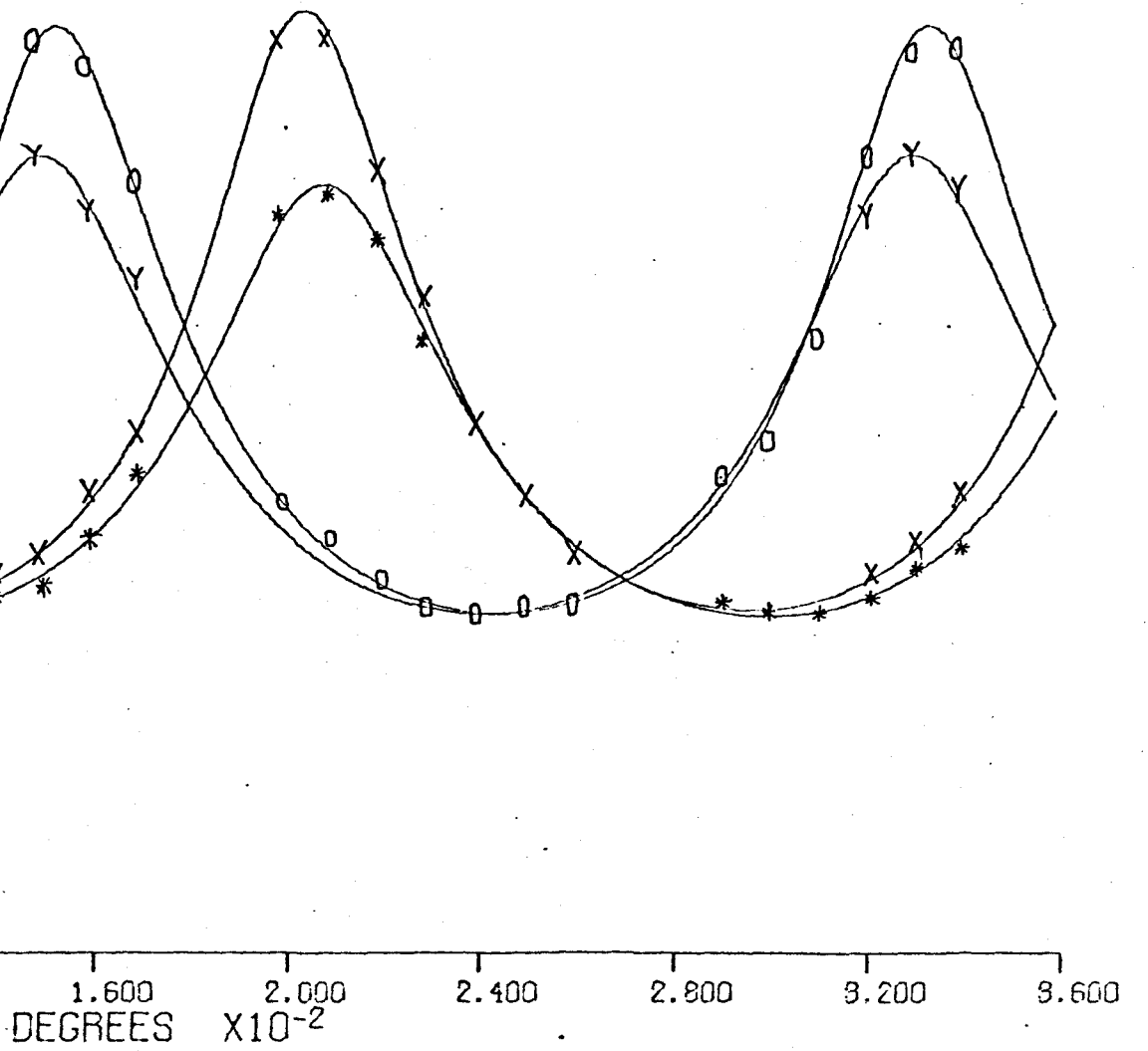

PLANE, 70 GHz, Hb-$NaNO_2$. Fig. 5.1

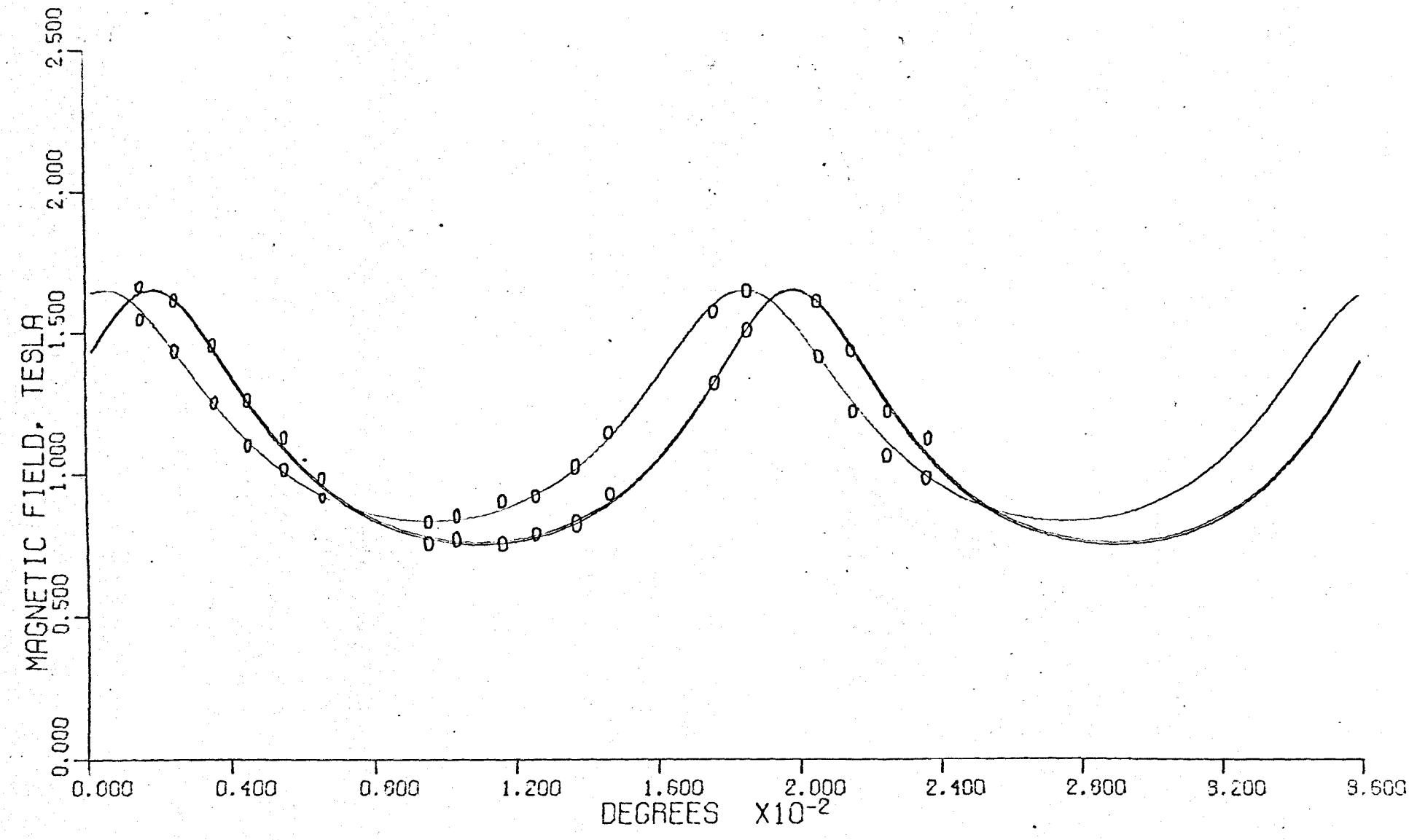

EPR LINE POSITIONS, AC PLANE, 70 GHz, Hb-$NaNO_2$. Fig. 5.2

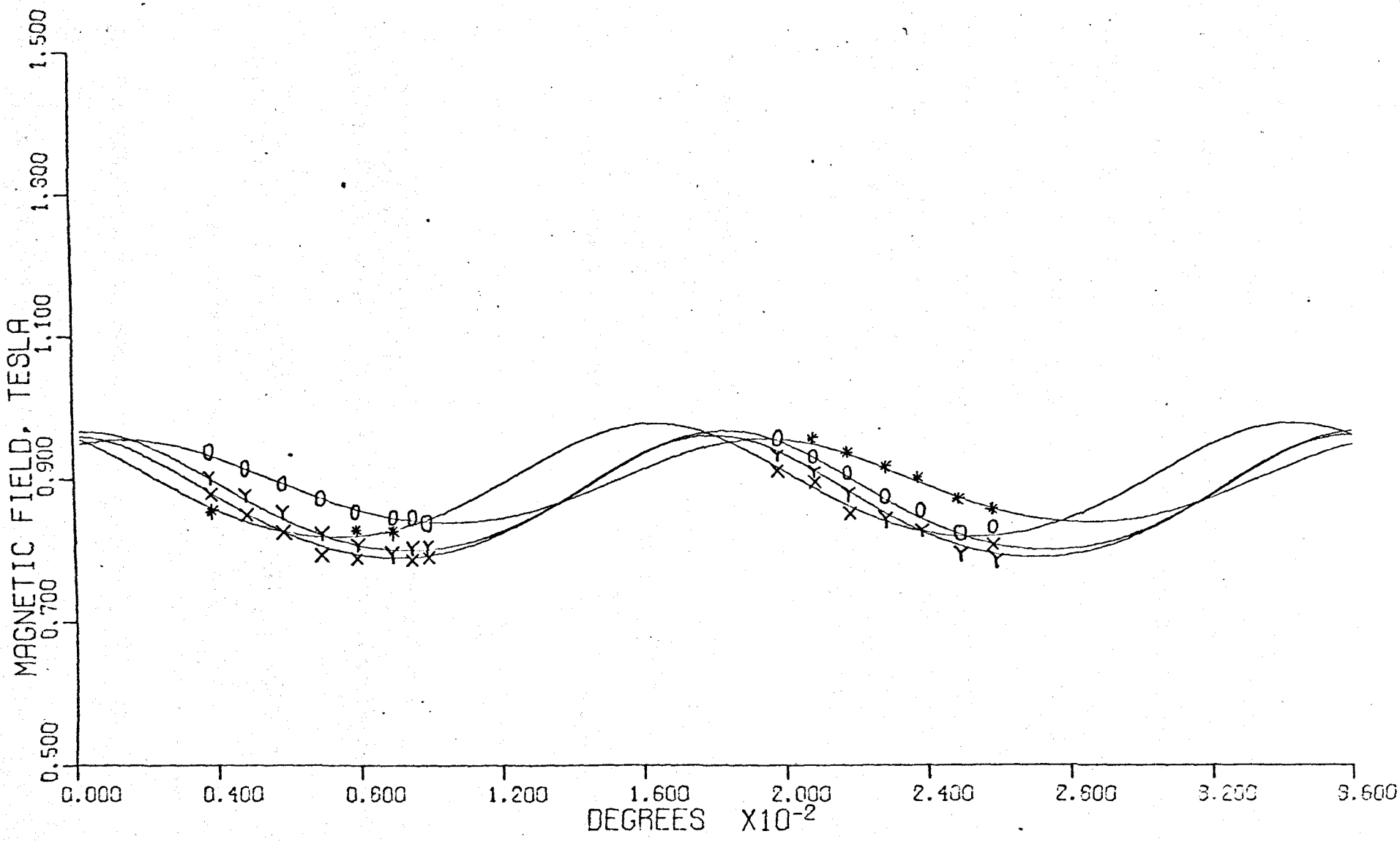

EPR LINE POSITIONS, BC PLANE, 70 GHz, Hb-$NaNO_2$. Fig. 5.3

crystal corresponds to the ab plane (001); for ab plane studies crystals were mounted horizontally on the sample holder using a tiny dab of silicone grease. For studies in either of the other two principal crystal planes (ac or bc), the crystal was mounted on a wedge support using grease so that either of these planes was horizontal; this method was desirable because only the ab face of the crystal was fully developed so as to be suitable for mounting. It is estimated that the crystals can be mounted to within 2° on most occasions. A small quantity of d.p.p.h. was added to the sample support for measurement purposes.

The angular dependence of the g value in the ab plane is shown in Fig. 5.1; near the larger g values, the curves coalesce to form two pairs. At low g values the curves separate. This indicates that the different haem groups represented in the EPR spectrum are probably inclined at different angles to the ab plane; two curves reach g values close to 2 and it is likely that the haem normals associated with these curves lie in, or close to, the ab plane if one assumes that g_z is directed along a direction near a haem normal.

The angular variation in the ac plane is given in Fig.5.2 where it may be seen that the EPR spectrum comprises almost two lines exactly; these lines perform almost identical variations between $g \approx 6$ and $g \approx 3.5$. It is apparent that these lines arise because the haem planes project symmetrically upon the ac plane.

The experimental results for the bc plane studies are given in Fig. 5.3, Because there are four lines it is evident that the four haem planes contributing to the spectrum are arranged on one side of the bc plane.

The variation of g value in these measurements will enable

determination of the g tensor and its direction cosines with respect to the principal axes of the crystal.

Similar measurements made upon horse haemoglobin enabled the orientation of the haem planes in the protein molecule to be deduced (Ingram, 1956).

In the measurements made in this work, it was noted that although eight EPR lines should have been present, only four were actually observed; some possible reasons why this may be so are given below but none is entirely satisfactory. If only half of the ionic centres in a protein molecule were converted to the ferric state, we might expect to observe only four EPR lines; however, the cooperative nature of the bonding mechanism in haemoglobin strongly indicates that this will not be the case, and if only partial conversions were made, we would anticipate that they would affect whole molecules.

Another possibility is that the actual directions of the present and absent g tensors are such that, coupled with their magnitudes, small internal molecular movements associated with bonding bring them into approximate coincidence; we have no data for this hypothesis but it would seem to be of only marginal importance.

The space group of the haemoglobin crystals actually used was considered to be $P2_1$ because the crystals closely resembled normal Type I deoxyhaemoglobin crystals; attempts to check this conclusion by x-ray techniques were unsuccessful.

The EPR observations were made at a sample temperature of $4.2^{\circ}K$; we must ask whether certain haems may have had a relaxation time too short for signals to be observed at this temperature. This question leads to a consideration of whether the ligands binds not only at the haem but also to the peptide

chains. It is known that the cyanate OCN^- and the thiocyanate SCN^- may act in this way (q.v. Sections 3.4.1,2). If the nitrite radical NO_2^- of the sodium nitrite molecule were to be attached to a particular side chain in a similar manner then it might be expected that this could affect the relaxation time of the associated haem. Furthermore, this hypothesis might suggest that two haems in a molecule are converted to ferric ions and two are not converted to the $S = 5/2$ state but that a side chain attachment brings about the small molecular movements necessary to cooperative bonding. Unfortunately, we have no data to support this idea and the situation thus remains unresolved.

5.4. Theoretical derivation of the principal *g* values.

The relationship between the magnetic and crystallographic axes of deoxyhaemoglobin treated with sodium nitrite is by no means apparent.

In order to the find the principal *g* values and their angular relationship to the crystallographic axes it was essential to measure the angular variation of the *g* value in three mutually perpendicular planes: in this case, the planes are the ab, ac and bc planes, which correspond to the (001), (010) and (100) planes.

It has been previously shown that the spin Hamiltonian which is appropriate to a high spin haem protein is given by

$$H = S \cdot g \cdot B + D\left(S_z^2 - \tfrac{1}{3}S(S+1)\right) + E\left(S_x^2 - S_y^2\right)$$

However, it would be necessary to transform from the principal axes to the crystallographic axes to find values for $\bar{g}$, D and E. This transformation is unknown.

If the simplifying assumption that D is large is made, then the EPR spectra of the lowest Kramers' doublets may be described by a spin Hamiltonian (Zeldes, 1961)

$$H = \beta \, \bar{S} \cdot \bar{g} \cdot \bar{B}$$

where an effective g value is defined by $g_{eff} = h\upsilon / \beta B$. The assumption that D is large is justified by the value obtained from the studies on pastes.

If the magnetic field has direction cosines l_i, l_j, l_k with the crystal axes then the g value is given by

$$g_{eff}^2 = \sum_{i,j=1}^{3} G_{ij} \, l_i l_j$$

The symmetric tensor G_{ij} depends on the actual reference axes chosen; the expression may be expanded using the direction cosines l_a, l_b, l_c of the magnetic field with respect to the crystal axes selected.

$$g_{eff}^2 = G_{aa} l_a^2 + G_{bb} l_b^2 + G_{cc} l_c^2 + 2 G_{ab} l_a l_b + 2 G_{bc} l_b l_c + 2 G_{ca} l_c l_a$$

where G_{mn} are components of the symmetric tensor $\bar{G} = \bar{g}^2$. Clearly, in any one plane defined by the crystal axes, g_{eff}^2 is a function of only one angle and three expressions may be obtained - one for each plane. It is comparatively straightforward to perform a least squares fit to these expressions using the experimental data from the three orthogonal planes. It is desired to find the values of G_{mn} such that the sum

of the squares of the residuals r_i is minimised. Clearly,

$$r_i^2 = \sum (G_{mm}\cos^2\theta + G_{nn}\sin^2\theta + 2\, G_{mn} \sin\theta \cos\theta - g^2)$$

The sum of r_i^2 will be minimised when all the partial derivatives with respect to G_{aa}, G_{bb}, G_{cc} are zero. This results in three simultaneous equations for each plane

$$\begin{aligned} AG_{aa} + BG_{bb} + 2CG_{ab} - D &= 0 \\ BG_{aa} + EG_{bb} + 2FG_{ab} - H &= 0 \\ CG_{aa} + FG_{bb} + 2DG_{ab} - K &= 0 \end{aligned}$$

and similarly for the ac and bc planes; the coefficients A to K are sums of trigonometric functions. The solutions of these nine simultaneous equations are the elements of the g tensor $\overline{G}$.

Alternatively, if full use of the experimental data is not desired, the tensor elements may be determined from selected points on the curves of g variation in the three planes (Schonland, 1959). The principal g values and the magnetic principal axes are found by diagonalising the matrix $\overline{G}$. The principal values are the square roots of the roots λ_1, λ_2, λ_3 of the secular equation

$$\det\ (A - \lambda\, I) = 0$$

where I is the unit matrix; the equation

$$G_{ij}\, l_{kj} = \lambda_k\, l_{ki}$$

is satisfied by the direction cosines k_{kj} $(j = 1,2,3)$ corresponding to the solution λ_k. Consequently, in diagonalising the matrix of the G tensor to give the principal values, the transforming matrix contains the direction cosines of the principal axes with the crystallographic axes, thus

Fig. 5.5: G tensor components and directions of principal axes for the four paramagnetic sites observed in deoxyhaemoglobin after treatment with sodium nitrite.

Site A G_{xx} = 12.75 G_{yy} = 26.76 G_{zz} = 39.63

G_{xy} = -11.51 G_{yz} = 0.13 G_{xz} = 10.62

Directions of principal axes.

	a	b	c
PX	88	115	28
PY	61	34	64
PZ	32	121	78

Site B G_{xx} = 12.20 G_{yy} = 26.42 G_{zz} = 38.58

G_{xy} = 11.44 G_{yz} = -0.60 G_{xz} = -9.73

Directions of principal axes.

	a	b	c
PX	87	63	27
PY	121	33	116
PZ	31	58	79

Site C G_{xx} = 9.40 G_{yy} = 26.82 G_{zz} = 35.87

G_{xy} = -10.89 G_{zx} = -3.17 G_{yz} = 3.15

Directions of principal axes.

	a	b	c
PX	91	120	27
PY	62	34	65
PZ	33	122	89

Fig. 5.5: continued.

Site D $G_{xx} = 9.53$ $G_{yy} = 27.49$ $G_{zz} = 36.64$

$G_{xy} = 10.99$ $G_{yz} = -1.90$ $G_{xz} = -1.76$

Directions of principal axes.

	a	b	c
PX	92	64	29
PY	120	35	114
PZ	32	57	90

The diagonalisation of these matrices, where $G_{xy} = G_{yx}$, $G_{xz} = G_{zx}$, $G_{yz} = G_{zy}$, yields the following average values of the principal g values. The estimated error in obtaining g values is ± 0.005.

$g_x = 5.822$

$g_y = 5.954$

$g_z = 2.004$

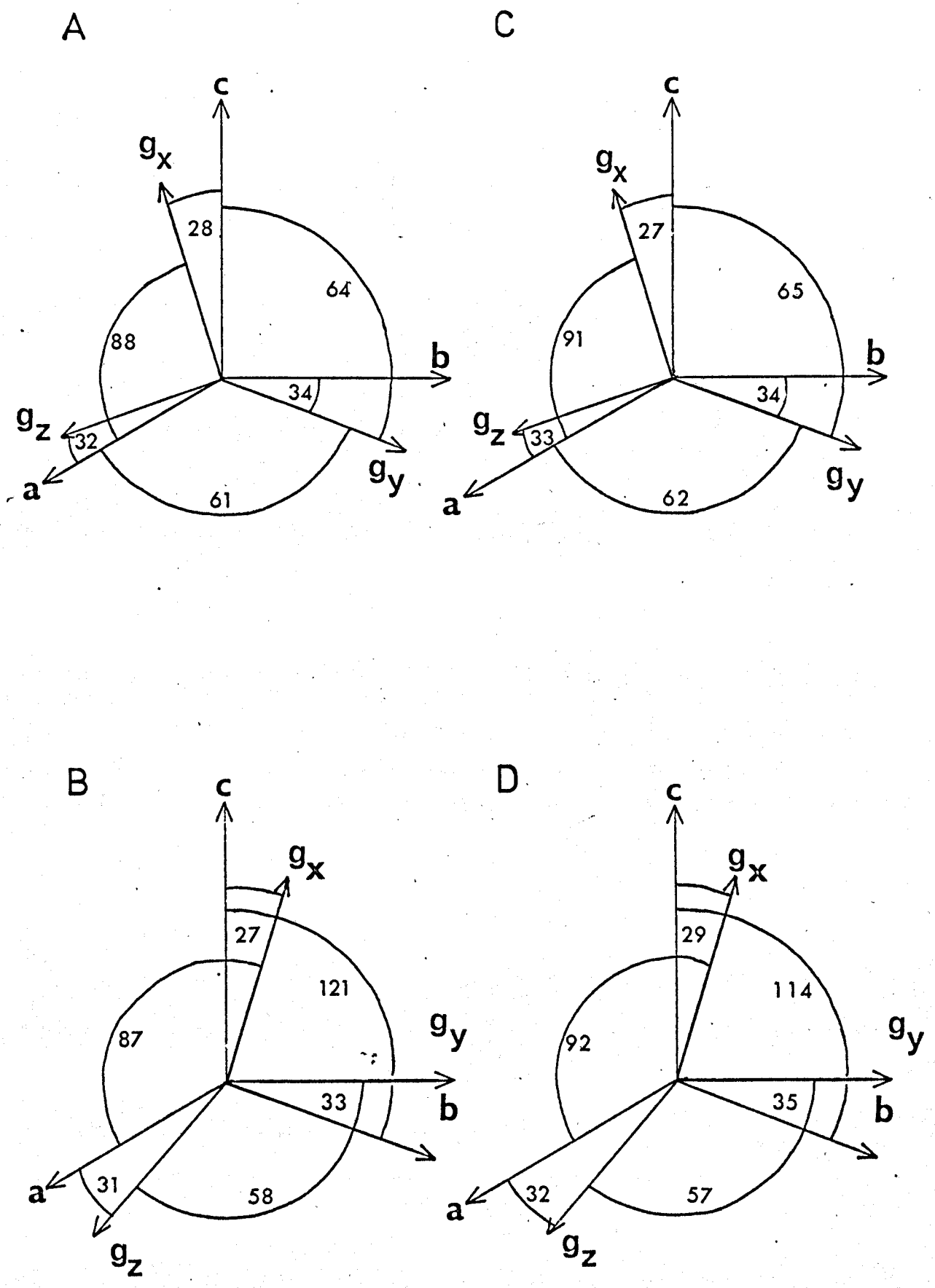

DIRECTIONS OF PRINCIPAL AXES

Fig. 5.5 cont.

$$\bar{\bar{R}}\ \bar{\bar{g}}^2\ \bar{\bar{R}} = \begin{bmatrix} g_x^2 & 0 & 0 \\ 0 & g_y^2 & 0 \\ 0 & 0 & g_z^2 \end{bmatrix}$$

where $\bar{\bar{R}}$ is the transpose of $\bar{\bar{R}}$ and

$$\bar{\bar{R}} = \begin{bmatrix} \cos\theta_{ax} & \cos\theta_{ay} & \cos\theta_{az} \\ \cos\theta_{bx} & \cos\theta_{by} & \cos\theta_{bz} \\ \cos\theta_{cx} & \cos\theta_{cy} & \cos\theta_{cz} \end{bmatrix}$$

The same transform diagonalises $\bar{\bar{g}}$ since

$$\bar{\bar{R}}\ \bar{\bar{g}}^2\ \bar{\bar{R}} = \bar{\bar{R}}\ \bar{\bar{g}}\ \bar{\bar{R}}\ \bar{\bar{R}}\ \bar{\bar{g}}\ \bar{\bar{R}}$$

whence

$$\bar{\bar{R}}\ \bar{\bar{g}}\ \bar{\bar{R}} = \begin{bmatrix} g_x & 0 & 0 \\ 0 & g_y & 0 \\ 0 & 0 & g_z \end{bmatrix}$$

The values of the G tensor, the direction cosines, and the principal values are given in Fig. 5. 5 for each paramagnetic centre.

5.5. Hamiltonian Parameters D, E.

In a similar fashion to that described in Chapter Four, it is possible to calculate the zero field splitting parameter 2D by making measurements at two well separated microwave frequencies. Use has been made of the 70 GHz measurements previously noted and a further experimental study was made of g value variation in the ab plane at 35 GHz.

In this case some difficulty was experienced in mounting the crystal and the data obtained from the ab plane is used to find the principal g values. (Farrow, 1971).

In polar coordinates the effective g value is given by

$$g_{eff}^2 = g_x^2 \cos^2\phi \sin^2\theta + g_y^2 \sin^2\phi \cos^2\theta + g_z^2 \cos^2\theta$$

where ϕ, θ are the polar angles of the magnetic field with respect to the principal axes. It is necessary to assume that $g_z = 2$ and that it is directed along the haem normal: this assumption is justified by the 70 GHz measurements. In the haem plane (the xy plane) the g value is then

$$g_{xy}^2 = g_x^2 \cos^2\phi + g_y^2 \sin^2\phi$$

The directions of g_x, g_y in the haem plane are unknown but let e be the angle between the g vectors and the projection of the a axis onto the haem plane then

$$g_{xy}^2 = g_x^2 \cos^2(\phi + e) + g_y^2 \sin^2(\phi + e)$$

which may be expanded (Slade, 1972) as

$$g_{xy}^2 = (g_x^2\cos^2 e + g_y^2\sin^2 e)\cos^2\phi + (g_x^2\sin^2 e + g_y^2\cos^2 e)\sin^2\phi + 2(g_x^2 - g_y^2)\sin e \cos e \sin\phi \cos\phi$$

If a least squares fit is undertaken in the same manner as before, the values of g_{xy}^2 can be fitted to an equation

$$g_{xy}^2 = G_1 \cos^2\phi + G_2 \sin^2\phi + G_3 \sin\phi \cos\phi$$

By equating coefficients, g_x and g_y may be found in terms of G_1, G_2, and G_3. This gives a value of $g_L^{eff} = (g_x + g_y)/2$, which may be used with the 70 GHz result to find 2D.

From the EPR measurements on single crystals of deoxy-haemoglobin treated with sodium nitrite at 35 GHz and 70 GHz, these Hamiltonian parameters were calculated as detailed in Chapter Four and are:

$$2D = 13.5 \pm 2.5 \text{ cm}^{-1}$$

$$E = 0.02 \pm 0.004 \text{ cm}^{-1}$$

We must note that there may be a further error in calculating 2D introduced when obtaining g_x and g_y by assuming g_z.

The values of E from the hydrate paste and deoxyHb/$NaNO_2$ single crystals are similar in value; the value of 2D is somewhat reduced in the latter case. However, it is gratifying to observe that the g values and Hamiltonian parameters found for ferric ions in hydrate pastes and treated deoxyhaemoglobin crystals do not differ too widely and this, in part, supports the discovery that the protein structure of haemoglobin in aqueous solution inferred from x-ray and small angle neutron scattering experiments (Conrad, 1969, Schneider, 1969) agrees well with the atomic coordinates found by x-ray diffraction analysis of hydrate single crystals (Perutz, 1968).

We may make use of the Hamiltonian parameters obtained from the hydrate pastes and also from the treated deoxyHb crystals to extend the calculations of the energies of the components of the first excited state.

It has been shown that when the symmetry of the crystalline electric field is sufficiently low then the first excited state $^4T_1$ is split into three components (because of its three-fold orbital degeneracy) labelled $^4T_{1x}$, $^4T_{1y}$, $^4T_{1z}$ and their energies above the ground state $^6A_1$ are related to 2D

and E by (Kotani, 1963)

$$D = \frac{\lambda^2}{10}\left(\frac{2}{E_z} - \frac{1}{E_x} - \frac{1}{E_y}\right)$$

$$E = \frac{\lambda^2}{10}\left(\frac{1}{E_x} - \frac{1}{E_y}\right)$$

where λ = 435 cm^{-1} is the spin-orbit coupling coefficient; the value quoted is for the free ion and the actual value in the protein will probably be reduced (Kotani, 1961). Defining $dE' = E_x - E_z$ and $dE'' = E_y - E_z$, we may obtain

$$\frac{1}{dE'} = \frac{0.2\lambda^2}{E_z^2(D-E)} - \frac{1}{E_z}$$

$$\frac{1}{dE''} = \frac{0.2\lambda^2}{E_z^2(D-E)} - \frac{1}{E_z}$$

By assuming that the values of dE' and dE'' are the same in the low spin and high spin derivatives of haemoglobin, Kotani was able to predict that 2D = 3.8 cm^{-1} in high spin derivatives using data from the azide derivative; the rather low estimate of 2D is probably due to this being a poor assumption. Using the same assumption that $E_z \approx 2000$ cm^{-1} (Kotani, 1963), the experimentally obtained values of 2D and E may be used to calculate E_x and E_y.

For the hydrate, the paste spectra indicate that $^4T_{1x}$ lies 3539 cm^{-1} above $^6A_1$ and that $^4T_{1y}$ lies 3553 cm^{-1} above $^6A_1$. The results from the single crystal studies of deoxyhaemoglobin treated with sodium nitrite suggest that $^4T_{1x}$ lies 3103 cm^{-1} above $^6A_1$ and that $^4T_{1y}$ lies 3117 cm^{-1} above $^6A_1$. Despite the assumption that $E_z \approx 2000$ cm^{-1}, it is evident in both cases

that $^4T_{1x}$ and $^4T_{1y}$ are very close together in energy but are well separated from $^4T_{1z}$.

5.6. Deoxy(ferrous)haemoglobin.

Single crystals of deoxyhaemoglobin, which contains ferrous ions, were mounted in the 70 GHz microwave cavity on the end-plate in a nitrogen-filled cabinet; the nitrogen was subsequently displaced from the waveguide and cavity by helium gas. Observations were made at 4.2°K using each crystal face in turn; the magnetic field was varied up to 5 Tesla.

No electron spin resonance signals were seen from these samples. This result agrees with the negative result from the paste samples. It is possible that the spin-lattice relaxation time is too short for the signals to be observed at 4.2°K or that the zero field splitting is larger than the microwave quantum; this latter suggestion would put an approximate lower limit on the splitting of 2.5 cm^{-1}. Since deoxyhaemoglobin has a total spin S = 2, it has non-Kramers' ions and there can be no Zeeman splittings of the lowest energy level.

Second order perturbation theory has been used to calculate the energy levels for an S = 2 ion in a weak crystal field with a strong axial component and a rhombic contribution (Abragam, 1970). Although the transition for the $S_z = \pm 1$ doublet is allowed, the low population of these levels would imply a considerably reduced signal intensity and the use of a signal averaging technique might be of assistance (Klein, 1963, Allen, 1963).

5.7 Angular variation of the EPR linewidth.

The linewidths of the first derivative EPR signals observed from samples of $NaNO_2$- deoxyHb crystals at 70 GHz are shown in Figs. 5.6 and 5.7; it will be noted that in the ab plane the width fluctuates between 23 mT and 180 mT and that in the ac plane the width fluctuates between 20 mT and 110 mT. These measurements of peak to peak width are subject to an error of approximately 10%. The variation in linewidth is fairly smooth and the smaller widths occur at orientations giving rise to larger g values. Furthermore, the curves of linewidth variation cross over at orientations corresponding to the crystallographic axes of the hydrate.

There are three aspects of the width of the EPR signal which require comment. These are: the minimum linewidth observed in certain directions, the orientation dependence of the linewidth, and the correlation between microwave frequency and the linewidth.

The common sources of line broadening do not provide adequate contributions to make up the exceptionally broad resonance lines found in haemoglobin. It has been estimated that the maximum contribution from spin-spin interactions cannot exceed 1.4 mT (Helcke, 1968). It is assumed that spin-lattice broadening is absent because the linewidth is unchanged on cooling from 77°K to liquid helium temperatures. Unresolved hyperfine structure due to the ligand or the nitrogen nuclei in the haem plane has been shown to be absent by measurements at 9 GHz on myoglobin hydrate and azide; it is likely that the hyperfine structure is concealed by the line broadening (Ohne, 1962). Exchange interactions will be negligible in haemoglobin since the paramagnetic ions are approximately 35 Å apart (q.v. Fig. 2.4).

LINEWIDTH DEPENDENCE ON ANGLE IN AB PLANE.

Fig. 5.6

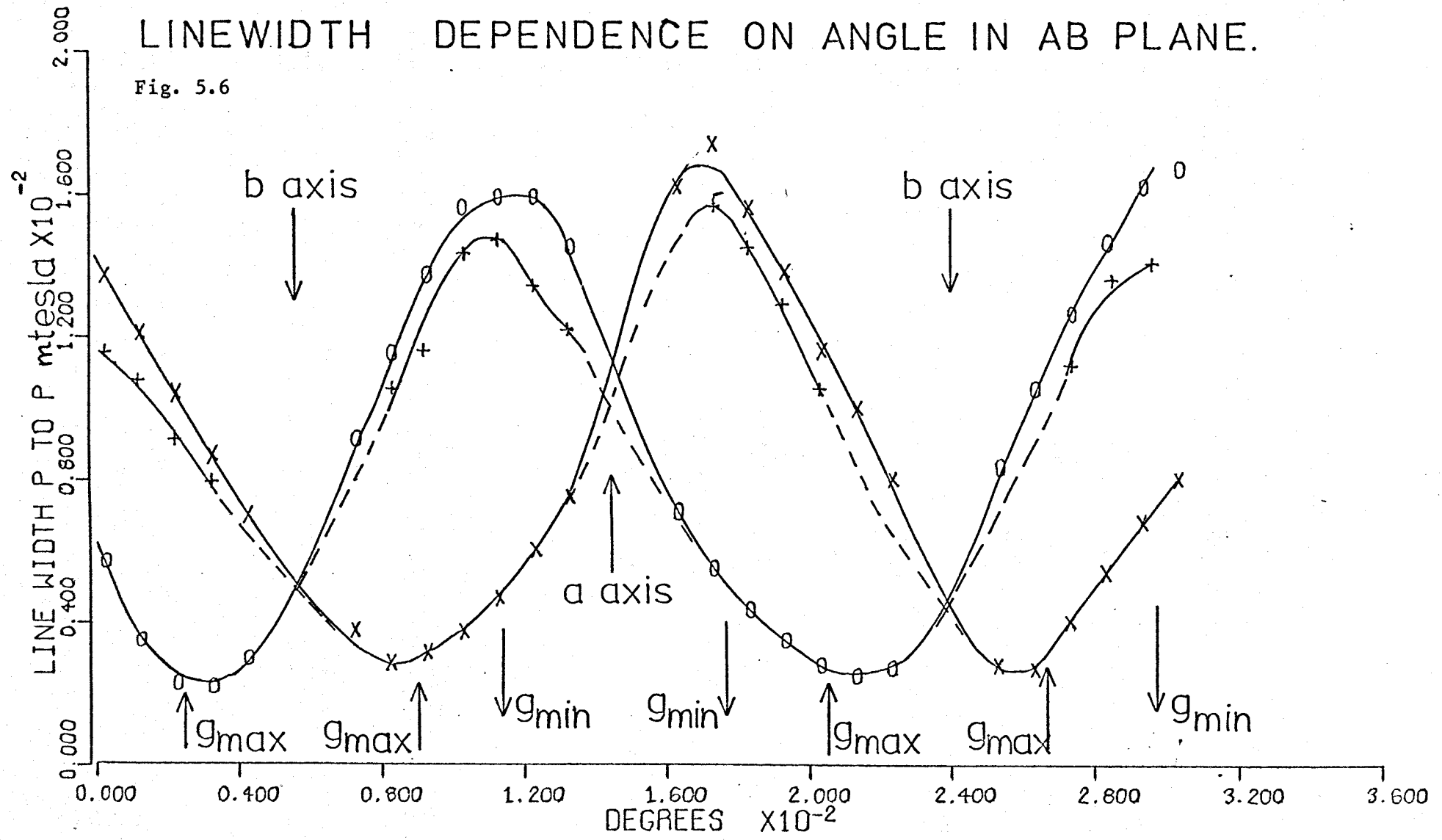

VARIATION IN LINEWIDTH IN THE AC PLANE (70 GHz)

Fig. 5.7

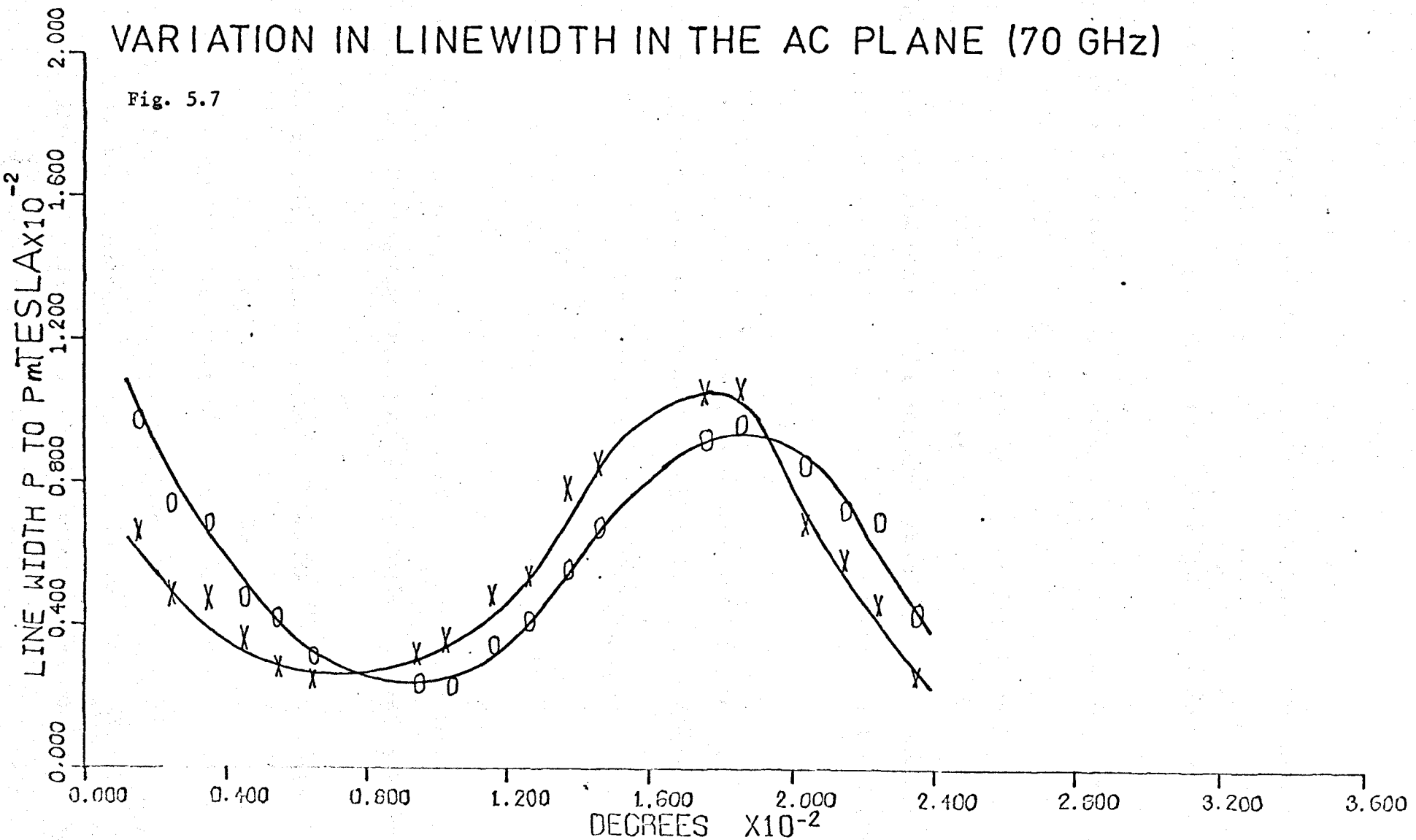

The effect of inhomogeneous broadening mechanisms other than the hyperfine interaction should also be considered; an inhomogeneous magnetic field may give rise to broadening of the absorption line. If the magnetic field is not uniform over the sample volume, then resonance will occur at different values of the field in different parts of the sample; each ion may give a sharp absorption but the overall linewidth will be determined by the field homogeneity. However, it has already been noted that the magnetic field is homogeneous to at least one part in 10^6 so the linewidth contribution due to this mechanism must be small.

Crystalline imperfections would produce inhomogeneous broadening; these imperfections are of two kinds, a mosaic structure and defects or impurities which introduce strains.

A mosaic structure may arise from the combination of many small crystallites to form a larger, apparently single, crystal. Because of small misorientations of the crystallites, the conditions for resonance in each crystallite would be identical but since the occurrence of transitions depends on the angle made by the crystallite axes and the magnetic field, the line is the sum of many lines and the line is thereby inhomogeneously broadened. Along the principal axes, the dependence of the resonance line position in the EPR spectrum upon the small angle enclosed becomes negligible and so the broadening is then minimal.

At 35 GHz microwave frequency, scatter in the azimuthal angle and a small variation in g_L was used to explain the linewidth variation in myoglobin hydrate and azide very successfully (Helcke, 1968, Slade, 1968); however, at a microwave frequency of 70 GHz, it was found that the misorientation effect could not satisfactorily explain the linewidth variation in the ab plane unless angular variations of some 50° between crystallites were assumed; the misorientation required at 35 GHz was only about 1.5° (Slade, 1968).

It was further noted that the minimum linewidth did not coincide with the maximum g value and that the residual linewidth appeared to have increased in direct proportion to the microwave frequency. It is evident that the misorientation effect is able to account for the linewidths observed at 35 GHz but does not account for the residual linewidth of approximately 20 mT at 70 GHz in the ab plane, nor does it explain the apparent frequency dependence.

Impurities and defects in a single crystal may introduce strains which alter the symmetry at the paramagnetic site and this may lead to changes in the spin Hamiltonian parameters. It has been observed that lattice defects commonly occur in haemoglobin crystals (Perutz, 1968); in pastes frozen to low temperatures, it might be expected that some modification of the Hamiltonian parameters would result from cooling-induced strains. It has been suggested that strain could introduce an additional term into the spin Hamiltonian of the form (Wenzel, 1965)

$$H' = \sum_{i,j} D_{ij} S_i S_j = \sum_{i,j} \sum_{l,m} G_{ijlm} e_{lm} S_i S_j$$

where G_{ijlm} is a magnetoelastic tensor and e_{lm} the strain; if a distribution of the tensor elements is represented by d_{ij} then the strain broadening would be

$$\Delta B^2 = \sum_{i,j} d_{ij}^2 \left(\langle a | S_i S_j | b \rangle - \langle b | S_i S_j | b \rangle \right)^2$$

where $|a\rangle = |-\tfrac{1}{2}\rangle$ and $|b\rangle = |+\tfrac{1}{2}\rangle$.

Unfortunately, in the case of $|\pm\tfrac{1}{2}\rangle$ the matrix elements vanish; but if the ligand field has a rhombic component ($E \neq 0$) then the three doublets of the $^6A_1$ ground state will no longer be pure eigenstates of S_z (Weissbluth, 1967). In this case there may be a strain contribution to the linewidth which will depend upon

the degree of rhombic symmetry, the spread in the values of D_{ij} and the magnetoelastic tensor. Since changes in D due to strain reflect variations in the crystal field splitting, it is possible that changes in the optical absorption spectrum of haemoglobin crystals might ensue if they were stressed; this might prove a suitable test of the strain broadening hypothesis.

Apart from the hypothesised strain induced fluctuations in D, there may be a statistical fluctuation in the crystal field at individual paramagnetic centres; it has been suggested that previous processing of haemproteins may damage the peptide chain (Slade,1968). This may lead to small conformational changes which would be likely to modify the geometry at the haem plane. It is possible to estimate the fluctuation in D giving rise to a linewidth contribution; assuming that the contribution due to this effect were 10 mT and that the microwave frequency were 70 GHz, the range of g_L^{eff} corresponding to this linewidth is 0.078.

It has been shown that (Eisenberger, 1966)

$$g_L = 2.002 - k D^2$$

where k depends on the separation between the ground state and the first excited state and the spin-orbit coupling. Differentiation yields

$$dg_L = - 2 k D \, dD$$

Using the values of 2D and g_L obtained from the paste spectrum for the hydrate, the value of k may be found. Differentiation of the expression for 2D (q.v. 4.4) gives

$$dg_L^{eff} = 3 \, dg_L$$

where terms which are small if $2D \simeq 15 \text{ cm}^{-1}$ and $B \simeq 1T$ have been neglected.

The value of dD may be thus be found; the hydrate paste results yield $dD = 2.9\ cm^{-1}$. A similar calculation for the treated deoxyhaemoglobin crystals gives $dD = 3.08\ cm^{-1}$.

It is concluded that a variation of $3\ cm^{-1}$ is necessary to explain a residual linewidth of 10 mT at 70 GHz; this is equivalent to a 30% fluctuation in the value of 2D between different paramagnetic centres in a given derivative. It is difficult to believe that such a large fluctuation could arise. Furthermore, fluctuations in D or E do not give rise to frequency dependence of the linewidth (Abragam, 1970).

A satisfactory explanation of the frequency dependence of the residual linewidth is yet to be found; it is tentatively suggested that the magnetoelastic tensor has a magnetic field dependent component which becomes significant at the higher fields employed at 70 GHz to observe resonance. This would yield a greater D_{ij} contribution thus increasing the linewidth through the strain broadening mechanism.

5.8 References.

Abragam, A., B. Bleaney, EPR of Transition Ions, O.U.P., 1970.

Allen, L.C., L.F. Johnson, J. Amer. Chem. Soc., 85, 2668, 1963.

Bennett, J.E., J.F. Gibson, D.J.E. Ingram, Proc. Roy. Soc., A240, 67, 1957.

Conrad, H., A. Mayer, H.P. Thomas, H. Vogel, J.Mol.Biol., 41, 225, 1969.

Dixon, M., E.C. Webb, Adv. Protein Chem., 16, 197, 1961.

Eisenberger, P., P.S. Pershan, J. Chem. Phys., 45, 2832, 1966.

Farrow, R.H., Ph.D. Thesis, University of Keele, 1969.

Green, A.A., J. Biol. Chem., 93, 495, 1931.

Helcke, G.A., D.J.E. Ingram, E.F. Slade, Proc. Roy. Soc., B169, 225, 1968.

Ingram, D.J.E., J.F. Gibson, M.F. Perutz, Nat., 178, 906, 1956.

Jope, H.M., J.R.P. O'Brien, (in) Haemoglobin, (Eds.), F.J.W. Roughton, J.C.Kendrew, Butterworth, 1949.

Klein, M.P., G.W. Barton, Rev. Sci. Instr., 34, 754, 1963.

Kotani, M., Prog. Theoret. Phys., (Suppl.), 17, 4, 1961.

Kotani, M., Rev. Mod. Phys., 35, 717, 1963.

Kotani, M., H. Morimoto, Magnetic Resonance in Biol. Systems, Pergamon, 1967.

Ohne, K., Y. Tanabe, F. Sasaki, Proc. Conf. on Quantum Chem., Stockholm, 1962.

Perutz, M.F., Proc. Roy. Soc., A225, 264, 1954.

Perutz, M.F., J. Cryst. Growth, 2, 54, 1968.

Perutz, M.F., Nat., 219, 29 & 131, 1968.

Pryce, M.H.L., Proc. Phys. Soc., A63, 25, 1950.

Schneider, R., J. Mol. Biol., 41, 231, 1969.

Schonland, D.S., Proc. Phys. Soc., 73, 788, 1959.

Slade, E.F., D.J.E. Ingram, Nat., 220, 785, 1968.

Slade, E.F., R.H. Farrow, Biochim. Biophys. Acta, 278, 450, 1972.

Weil, J.A., J.H. Anderson, J. Chem. Phys., 28, 864, 1958.

Weissbluth, M., Struc. Bond., 2, 1, 1967.

Wenzel, R.F., Y.W. Kim, Phys. Rev., 140A, 1592, 1965.

Zeldes, H., R. Livingstone, J. Chem. Phys., 34, 247, 1961.

CHAPTER SIX

CONCLUSIONS

6.1 Optical absorption measurements at room temperature.

The preparation of solutions of various haemoglobin derivatives and measurements of their optical absorption spectra have been described in 3.1 and 3.2; the movement of the Soret band in hydrate/hydroxide mixtures is shown in Fig. 2.5 and a similar effect has been observed for fluoride samples (q.v. Fig. 3.5). It is thought that neither the chloride nor bromide ions attach to the protein at the haem plane since their absorption spectra were identical with those of the hydrate.

Although the use of a lyophillic material was satisfactory in concentrating the protein solutions, it is suggested that attention should be paid to the use of dialysis under pressure because the latter process is quicker and the risk of chemical reaction is substantially reduced.

The extinction coefficients of the organic monobasic acid derivatives, haemoglobin formate, acetate, propionate, n-butyrate, and iso-butyrate are given in Table 3.0; it is suggested that the n-butyrate ion is too large to be bound in the haem pocket but that the isomeric ion, iso-butyrate, is able to bond to the haem iron. It is thought that this effect may be caused by steric hindrance, possibly due to the proximity of the histidine residue and that this comparison parallels the case of tert-butyl-iso-cyanide and ethyl iso-cyanide; in this latter example, the larger tert-butyl-iso-cyanide is unable to bond in the haem pocket. It is suggested that the monobasic acid derivatives be studied by EPR to determine the spin state of the iron and to find out

whether small conformational changes result as radicals later in the series are bound.

Both haemoglobin cyanate and thiocyanate have been studied; their absorption spectra are reported (q.v. Fig. 3.8). It is to be noted that haemoglobin thiocyanate is soluble, unlike myoglobin thiocyanate, and efforts were made to detect precipitation but none was observed. No EPR signals were observed from either derivative at 9 GHz and 35 GHz; at the latter frequency, the samples were at a temperature of 4.2°K. This result may indicate a rapid spin lattice relaxation; it is known that OCN^- ions may attach at the peptide chain termini but no such knowledge is available in respect of the SCN^- ion. Bonding of the OCN^- to the peptide chains may bring about small conformational changes and this might explain an unfavourable spin lattice relaxation.

It was known that the SCN^- ion is ambidentate and infrared studies were made to determine its mode of bonding at the haem. Measurement of the stretching and flexing frequencies of the ion indicate that it is likely to bond through the sulphur terminal (q.v. Table 3.1).

It is possible that the use of neutron diffraction techniques could confirm the bonding mode in SCN^- and $HbSCN^-$ should be examined using EPR spectroscopy at temperatures below 4.2°K.

6.2 Cryogenic optical absorption studies.

Measurements of optical absorption at low temperatures were undertaken to gain more understanding of the magnetic properties of certain derivatives of haemoglobin, especially those thought to be thermal equilibrium mixtures of spin states.

The construction of the sample Dewar and cell has been described and the problems of macroscopic sample movements, Mie

scattering, cylindrical cuvettes, and the shifting of the light beam on the detector photocathode have been discussed. The absorption spectra of haemoglobin hydrate, hydroxide, formate, azide, and fluoride have been reported in 3.5.3.1. et seq; a specimen of haemoglobin hydrate with isonitolhexaphosphate attached was also studied. The optical absorption at low temperatures of oxy(ferrous) haemoglobin is discussed.

It was found that the hydrate was anomalous and that it may comprise two components, one always in the high spin state and the other being a thermal equilibrium mixture with a low spin ground state. The hydroxide was found to display a good correlation between absorption in the 540 nm band and magnetic susceptibility (q.v. Fig. 3.20). Examination of the fluoride and the hydrate-IHP complex showed that they were in only one spin state. The absorption spectrum of the azide suggests that it has a low spin ground state and that there is an increasing propotion of the high spin state as the temperature is increased. It is tentatively suggested that the formate derivative may comprise two parallel equilibria: first, two different modes of ligation of the formate radical at the haem plane and second, that one mode has a solely high spin character and the other is a thermal equilibrium mixture with a low spin ground state.

The observed temperature dependence of the optical absorption of oxyhaemoglobin has been discussed in 3.5.3.8.

This work at low temperatures could be extended to single crystals and studies could also be made of deoxyhaemoglobin in solution.

6.3. EPR measurements on haemoglobin solutions.

Using a superconducting magnet calibrated in the laboratory, EPR spectra were obtained for samples of haemoglobin hydrate, fluoride and formate at 4.2°K using 70 GHz radiation; EPR spectra were also obtained for these derivatives at 35 GHz.

No spectra were observed from samples of haemoglobin cyanate or deoxyhaemoglobin at either frequency.

The hydrate and fluoride spectra were analysed to obtain values for g_x, g_y, g_z and the linewidth. The formate was not analysed because of the small splitting observed; it is possible that this is due to the formate having two bonding modes and hence two g tensors for each similar paramagnetic site. An attempt was made to fit an anisotropic linewidth tensor to the hydrate spectrum at 70 GHz.

Using the g values obtained, the Hamiltonian parameters 2D and E were calculated; for the hydrate these were

$$2D = 16.5 \pm 2.5 \text{ cm}^{-1}$$
$$E = 0.016 \pm 0.003 \text{ cm}^{-1}$$

The only result available for direct comparison is $2D = 21 \text{ cm}^{-1}$ from Far Infra-Red measurements; results for similar complexes are given in 4.4 but no other estimate of E is available. However, the value of E/D is comparable with that for myoglobon hydrate.

6.4. EPR measurements on single crystals.

The preparation of single crystals of human deoxyhaemoglobin and their treatment with sodium nitrite to give ferric ions has been described; angular variation studies were made at 70 GHz

and 4.2°K in three mutually perpendicular planes and in the ab plane at 35 GHz.

The accuracy of mounting crystals in the microwave cavity was approximately 2°. The G tensor obtained from the measurements at 70 GHz is given in Fig. 5.5 and 5.8.

By assuming $g_z = 2$ it was possible to find g_x and g_y from the results in the ab plane at 35 GHz.

The values of the Hamiltonian parameters 2D and E were thus obtained from measurements on single crystals of deoxyhaemoglobin treated with sodium nitrite and are:

$$2D = 13.5 \pm 2.5 \text{ cm}^{-1}$$
$$E = 0.02 \pm 0.004 \text{ cm}^{-1}$$

It may be noted that this is a similar result to that found from the paste spectra of haemoglobin hydrate; further, the values of g_x and g_y are not widely different between the hydrate pastes and the converted deoxyhaemoglobin crystals. We therefore conclude that the EPR spectra of the deoxyhaemoglobin crystals treated with $NaNO_2$ arise from ferric ions to which water molecules have become attached.

No signals were obtained from crystals of deoxyhaemoglobin at 4.2°K at 70 GHz frequency and magnetic fields up to 5 Tesla. This suggests that the microwave quantum is too small to excite a transition, being about 2.5 cm^{-1}, or that there is a rapid spin-lattice relaxation, an effect common in ferrous compounds. It is suggested that signal averaging could be employed to observe the $S_z = \pm 1$ transition.

It is suggested that single crystal EPR studies should be made of the hydrate and fluoride; this work could then be extended to further derivatives such as the formate and azide.

Further, it would be worthwhile to examine deoxyhaemoglobin at 70 GHz at lower temperatures - a method successful with other ferrous compounds - or to perform EPR experiments at higher microwave frequencies.

6.5. EPR linewidths.

The linewidth variation in the single crystal spectra in the ab and ac planes is shown in Fig.5.6,7. The minimum linewidth in the ab plane is 23 mT and in the ac plane is 20 mT.

This residual linewidth does not relate well to the usual line broadening mechanisms. The misorientation of crystallites is inadequate to explain the angular variation at 70 GHz and it does not provide an explanation of the frequency dependence observed in the paste linewidths.

Statistical fluctuations in 2D would have to be approximately 30% to account for a residual linewidth of 10 mT at 70 GHz. Such a large variation must be regarded with suspicion. In rhombic crystalline fields, strain broadening may contribute to the linewidth but the contribution would only increase at higher microwave frequencies if the magnetoelastic tensor contained field dependent terms.

Further information might be obtained by observing the optical absorption spectra of single crystals (treated deoxyHb, hydrate, or other derivative) under stress since the ligand field splitting might thereby be altered; however, the fragility of protein crystals makes this very difficult.

6.6. Summary.

This thesis is an account of spectroscopic research carried

out with various samples of human haemoglobin derivatives. Particular attention has been paid to optical spectroscopy at low temperatures and to electron paramagnetic resonance at 70 GHz. It is hoped that both aspects of this work will be extended; in particular, cryogenic optical absorption in proteins should be put on a sound theoretical footing to take account of Mie scattering and EPR studies should be made of other haemoglobin derivatives.